THE STUDY OF THE INTERACTION OF INTENSE PICOSECOND LIGHT PULSE WITH MATERIALS: MULTI-PHOTON CONDUCTIVITY IN SEMICONDUCTORS AND MEASUREMENT OF PICOSECOND PULSE WIDTH

Chi H. Lee, et al

Maryland University

Prepared for:

Army Research Office-Durham
Advanced Research Projects Agency

1 April 1973

TECHNICAL RESEARCH REPORT

AD 760560

THE STUDY OF THE INTERACTION OF INTENSE PICOSECOND LIGHT PULSE WITH MATERIALS

QUARTERLY TECHNICAL REPORT
(TR - 013)

SUBMITTED TO

THE U.S. ARMY RESEARCH OFFICE

PERIOD
December 22, 1972 to March 21, 1973

REPORTED BY

CHI H. LEE
and
S. Jayaraman

Approved for Public Release
Distributions Unlimited.

DEPARTMENT OF ELECTRICAL ENGINEERING
UNIVERSITY OF MARYLAND
COLLEGE PARK, MARYLAND 20742

DOCUMENT CONTROL DATA - R & D
(Security classification of title, body of abstract and indexing annotation must be entered when the overall report is classified)

1. ORIGINATING ACTIVITY (Corporate author)

Department of Electrical Engineering
University of Maryland
College Park, Maryland 20740

2a. REPORT SECURITY CLASSIFICATION
Unclassified

2b. GROUP

3. REPORT TITLE

The Study of the Interaction of Intense Picosecond Light-Pulse with Materials: Multi-photon Conductivity in Semiconductors and Measurement of picosecond pulse width.

4. DESCRIPTIVE NOTES (Type of report and inclusive dates)

A quarterly technical report, December 22, 1972 to March 21, 1973

5. AUTHOR(S) (First name, middle initial, last name)

Chi H. Lee and S. Jayaraman

6. REPORT DATE
April 1, 1973

7a. TOTAL NO. OF PAGES
~~145~~ 161

7b. NO. OF REFS
75

8a. CONTRACT OR GRANT NO.
DA-ARO-D-31-124-72-G82

b. PROJECT NO.
ARPA Order No. 675 Am. 9

c.
Program Code No. 9E20

d.

9a. ORIGINATOR'S REPORT NUMBER(S)
TR-013

9b. OTHER REPORT NO(S) (Any other numbers that may be assigned this report)

10. DISTRIBUTION STATEMENT

Reproduction in whole or in part is permitted for any purpose of the United States Government.

11. SUPPLEMENTARY NOTES

12. SPONSORING MILITARY ACTIVITY
ARPA and U.S. Army Research Office

13. ABSTRACT

The two-photon conductivity in GaAs and $CdS_{.5} - Se_{.5}$ and the three-photon conductivity in CdS were investigated with the use of Mode-locked Nd:glass laser as the exciting source. The square law dependence of the two-photon conducitivity and the cubic law dependence of the three-photon conducitivity on the excitation intensity were subsequently utilized to measure the autocorrelation of the intensity in second and third order of the picosecond pulses from the mode-locked Nd:glass laser. The absorption coefficients estimated from the photoconductivity measurement were found to agree in order of magnitude with the theoretically calculated values from time dependent perturbation theory and the band structure of the semiconductor.

14 KEY WORDS	LINK A		LINK B		LINK C	
	ROLE	WT	ROLE	WT	ROLE	WT
Two-photon absorption						
Three-photon absorption						
Semiconductors						
CdS						
GaAs						
$CdS_{.5} - Se_{.5}$						
Photoconductivity						
Picosecond pulses						
Mode-locked Lasers						

Quarterly Techinical Report

for

Period December 22, 1972 to March 21, 1973

Submitted to the U.S. Army Research Office

ARPA:	675, Am 9
Program Code Number.	9E 20
Name of Grantee:	University Of Maryland
Effective Date of Grant:	March 22, 1972
Grant Expiration Date:	March 21, 1973
Principle Investigator and Phone Number:	Dr. Chi H. Lee (301) 454-2443
Grant Number:	DA-ARO-D-31-124-71-G82
Research Assistants:	Mr. S. Jayaraman Mr. V. Bhanthumnavin Mr. S. Mak
Short Title of Work:	"The Study of the Interaction of Intense Picosecond Light Pulses with Materials"
Report by:	Chi-hsing Lee Chi H. Lee

APPROVAL SHEET

Title of Thesis: Multi-Photon Conductivity in Semiconductors and Measurement of Picosecond Pulsewidth

Name of Candidate: Subramania Jayaraman
Doctor of Philosophy, 1972

Thesis and Abstract Approved: Chi-hung Lee

Dr. C.H.Lee
Associate Professor
Department of
Electrical Engineering

Date Approved: 12 - 20 - 1972

ABSTRACT

Title of Thesis: Multi-Photon Conductivity in Semiconductors and Measurement of Picosecond Pulse Width

Subramania Jayaraman, Doctor of Philosophy, 1972

Thesis directed by: Dr. C.H.Lee, Associate Professor of Electrical Engineering Department

With the advent of intense sources of coherent optical radiation, in the form of Q-switched and mode-locked lasers, the multi-photon conductivity in semiconductors is experimentally feasible to study. In this thesis, we investigated the two-photon conductivity in GaAs, $CdS_{.5}$-$Se_{.5}$ and three-photon conductivity in CdS using Q-switched and mode-locked Nd:glass laser pulses with a view to examine their suitability to measure picosecond pulse width. The two-photon conductivity in GaAs (low resistivity and high resistivity samples) was studied with Q-switched and mode-locked Nd:glass laser pulses. The two-photon conductivity in GaAs was found to exhibit a square law dependence on intensity over a very narrow region of laser intensity and this was found consistent with the thickness of the crystal and the measured two-photon absorption coefficient in GaAs. Then the square law region was used to measure the picosecond pulse width and the two-photon conductivity correlation pattern gave a contrast ratio of $\sim$1.8 and a half width of $\sim$ 8 - 10 psecs. Two-photon conductivity in $CdS_{.5}$-$Se_{.5}$ with the use of mode-locked Nd:glass laser pulses displayed a square law

region over a more dynamic range of incident laser intensities and the photoconductivity correlation gave a contrast ratio of $\sim$ 2.4 and a half width of $\sim$ 8 - 10 psecs. This larger contrast ratio was attributed to the smaller two-photon absorption coefficient and thickness of $CdS_{.5}Se_{.5}$ (resulting in longer square law region and improved resolution). Finally, we measured the three-photon conductivity in polycrystalline and single crystal CdS and used it to measure the third order auto correlation function of the intensity of the picosecond pulses and hence estimate the pulse width.

The estimated two and three-photon absorption coefficients in $CdS_{.5}Se_{.5}$ and CdS from the measured photoconductivity agreed well within an order of magnitude with the theoretically calculated values from the known band structure and time dependent perturbation theory.

VITA

Name: SUBRAMANIA JAYARAMAN

Permanent Address: Kambarasampettai, Tiruchy-2, Tamil Nadu, India.

Local Address: 4302, Knox Road, College Park, MD-20740.

Degree and Date to be conferred: Ph.D., 1972.

Date of birth: October 22, 1937.

Place of birth: Tiruchy, India.

Secondary Education: E.R.High School, Tiruchy-2, June, 1953.

Collegiate Institutions Attended	Dates	Degree	Date of Degree
University of Maryland	9/69-12/72	Ph.D.	1972
Dalhousie University(Canada)	10/67-8/69	M.Sc.	1969
Madras University(India)	6/55-6/60	B.Sc.	1960

Major: Electrical Engineering

Minor: Physics

Publications:

1. ' Photovoltaic Cell X-ray Exposure rate meter ', Vol.10, pp 323-330, ' Health Physics ', Pergamon Press, 1964.
2. ' Vortex Induced Vibrations of a Mechanical Compliant System ', Master's Thesis, Dalhousie University, Halifax, Canada, 1969.
3. ' Observation of Two-Photon Conductivity in GaAs By a Giant Pulse Nd:glass Laser ', Bull. Am. Phys. Soc., Series II, Vol.16, No:4, p653, 1971.
4. ' Observation of Two-Photon Conductivity in GaAs Using Nanosecond and Picosecond Nd:Glass Laser Pulses ', Appl. Phys. Letters, 20, 392, 1972.
5. ' Observation of Three-Photon Conductivity in Single and Polycrystalline CdS ', to be presented in the Annual Meeting of the American Physical Society, New York, Jan. 29, 1973.

Positions Held: Scientific Officer, Bhabha Atomic Research Centre, Trombay, Bombay, India 10/60-6/67.

Teaching Assistant, Physics Department, Dalhousie University, Halifax, Canada 9/67-9/69.

Research Assistant, Solid State Laser Laboratory, Department of Electrical Engineering, University of Maryland, College Park, MD-20742 9/69-12/72.

Membership in Professional Societies: Member, IEEE.

Member, American Physical Society.

MULTI-PHOTON CONDUCTIVITY IN SEMICONDUCTORS

AND

MEASUREMENT OF PICOSECOND PULSEWIDTH

By

Subramania Jayaraman

Thesis submitted to the Faculty of the Graduate School
of the University of Maryland in partial fulfillment
of the requirements for the degree of
Doctor of Philosophy
1972

IX

Acknowledgements

I am greatly indebted to my research supervisor Dr.C.H.Lee. I wish to thank him for his constant encouragement, advice and assistance during the conduct of this project. I also wish to thank Dr. Urs Hochuli and Dr.A.G.Lieberman for many helpful discussions.

I am grateful to Dr. H.C.Lin for permitting me to use the Integrated Circuit Laboratory facilities to prepare the ohmic contacts to the crystals.

I also wish to thank Mr. V.Rinker for the design of necessary mechanical equipment. I thank Mr. R.Sumner for his help in diagnosing and curing the many electronic ills, the project suffered during the period of my stay.

The financial support for this research given by the Advanced Research Projects Agency and monitored by U.S.Army Research Office under Grant No: DA-ARO-D-31-124-71-G82 is gratefully acknowledged.

I thank my colleagues Mr. V.Bhanthumnavin, Mr. Y.H.Park, Mr. P.Mak and Dr. M.Kim for many helpful discussions.

Finally, I wish to thank my friend Mr. K.R.Choudhary who induced me to stay long hours in the department which consequently resulted in the following thesis.

TABLE OF CONTENTS

List of Tables

List of Figures

Figure

CHAPTER I

A. INTRODUCTION:

The development of powerful sources of electromagnetic radiation by means of Q-switched and mode-locked lasers had made it possible to observe a number of intensity dependent optical interactions in matter which involve two or more photons. The multi-photon absorption in condensed media with the use of intense optical masers can, in principle, be investigated either by photo-conductivity measurements or by observing fluorescence. The measurement of photoconductivity is a more sensitive method and so it can be used to study the multi-photon absorption in semi-conductors and other crystalline media.

Any intrinsic semiconductor normally does not exhibit any optical absorption capable of producing electron-hole pairs for photon energies less than the forbidden energy gap. This is true for the light intensities normally employed in conventional optical absorption experiments. However, at high incident light intensities, multi-photon absorption of light in semiconductors leading to the creation of non-equilibrium charge carriers can in principle occur. This corresponds to the production of electron-hole pairs with simultaneous absorption of several photons. Semiconductors are a convenient medium for the investigation of such non-linear absorption processes at optical wavelengths, since the forbidden gap is of the order of a few electron volts as compared to the electronic states of the atom which are separated from the ground state

by several electron volts. This facilitates the experimental investigation of the multiphoton processes with a fewer number of quanta.

It is well known that a semiconductor shows appreciable optical absorption for photon energies greater than the forbidden gap E_g. This process is one-photon absorption and can be described time dependent first order perturbation theory in quantum mechanics. If $\hbar\omega < E_g$ but $2\hbar\omega > E_g$, the semiconductor will show some optical absorption because of two-photon absorption and this process can be calculated by second order perturbation theory. Similarly if $(n-1)\hbar\omega < E_g$ but $n\hbar\omega > E_g$, then there will be n-photon absorption in the semiconductor which will be weaker and weaker as n increases and can be predicted by n-th order terms in perturbation theory. The two-photon absorption process in a semiconductor can be described as follows; An electron is excited from an initial state 'i' (Valence band) to a final state 'f' (Conduction band) via a virtual intermediate state 'n' by absorbing two photons. In the case of Three-photon absorption, the electron goes to the conduction band via two intermediate virtual states. The mathematical description of these processes will be given in the second chapter.

Multi-photon absorption processes exhibit several interesting features as compared to one-photon process. These characteristic features make multi-photon absorption processes worthy of use in a number of applications.

1. In the case of one-photon absorption, the absorption coefficient $K^{(1)}$ is a constant.

$K^{(2)} \propto I$ for two-photon absorption

$K^{(n)}\ I^{n-1}$ for n-photon absorption.

2. The absorbed intensity $\propto I$, for one-photon absorption

$\propto I^n$, for n-photon absorption.

This power dependence can be used to identify the order of the absorption process. These non-linear dependences could be very useful in optical electronics. The square law of two-photon absorption can be used to measure the second order intensity correlation of the laser pulses and thus provide one of the non-linear optical methods of measuring the width of picosecond pulses. Similarly the higher order processes can be used to mesure the higher order intensity correlations.

3. In the case of one-photon absorption, the light intensity decreases very rapidly in the direction of propagation. This is because of the large one-photon absorption coefficient and also the intensity distribution inside the crystal follows an exponential law. Therefore the large portion of the absorption occurs near the surface. In the case of two-photon absorption, the light intensity changes much less rapidly, so the surface conditions are not important. As a result, the 2-photon measurement reveals the properties of the bulk semiconductor. This advantage of two photon absorption is used in the optical pumping of semiconductor lasers resulting in increased volume of coherent emission.

4. In atomic media, the one-photon absorption occurs only between states of opposite parity, whereas the two-photon absorption is allowed only between the states of same parity. This allows one

to probe excited states of the same parity as the ground state by two-photon absorption. In the conventional optical absorption spectroscopy, two-photon absorption complements one-photon absorption. But in the case of semiconductors, except at k=0 all states are of mixed parity and so it is possible to produce one-photon and two-photon processes by properly selecting the energy of the photon. At k = 0, the initial and final states are usually of opposite parity and normally two-photon absorption is forbidden.

So a study of multiphoton absorption in solids is richly rewarding. Following is a brief review of what has been done before.

B. REVIEW OF PREVIOUS WORK:

In the early days of quantum mechanics, Maria Goeppert-Mayer[1] calculated the two-photon transition probability in atomic media using second order time dependent perturbation theory. Her prediction awaited the development of lasers and in 1961, was first demonstrated by Kaiser and Garret.[2] They focussed a Ruby laser in Europium doped CaF_2, and observed a strong blue fluorescence around 4250 A. The Eu^{++} ion makes a transition from the 4f ground state to an excited vibrational 5d state. This is followed by a non-radiative transition to a metastable state. Then fluorescence occurs in the transition from this to the ground state. Its intensity was found to be proportional to the square of the laser intensity.

Abella[3] has observed two-photon absorption from a Ruby laser beam in Cesium vapour. The $6S_{\frac{1}{2}}$-$9D_{\frac{1}{2}}$ transition occurs between states

of same parity and is not observed in the linear absorption spectrum. The two-photon excited photocurrent was studied extensively by Hasegawa and Yoshimura[4] in anthracene crystals using a ruby laser.

R.Braunstein[5] and Braunstein and Ockmann[6] studied for the first time two-photon absorption in a semiconductor , CdS. The two-photon excited emission in CdS using a ruby laser was intensively investigated by them. Cadmium Sulphide has an energy gap (E_g= 2.5eV) and the ruby laser has a photon energy $\hbar w$ = 1.78 eV. They excited electrons from the valence band to the conduction band by two-photon absorption and subsequently studied the recombination radiation from the exciton and impurity levels as a function of laser intensity and compared to the emission excited by single quanta absorption for photons of energy $\hbar w > E_g$. It was found that the intensity of recombination radiation was proportional to I_0^n for single quanta excita tion and I_0^{2n} for two-quanta excitation where I_0 is the excitation intensity and n is a constant which differs for different groups of emission lines. They also developed a theory based on 2nd order time dependent perturbation theory and band structure of CdS. The two-photon absorption coefficient was 2. $10^{-4}cm^{-1}$ for the laser flux of 6 . 10^{22} photons/cm^2/sec.

N.G.Basov et. al.[7],[8] reported the observation of laser action in GaAs and other semiconductors at 77°K as a result of two-photon excitation by a Nd;glass laser beam. S.Wang and C.C.Chang[9] reported the emission at room temperature of coherent radiation from ZnS excited by a Q-switched ruby laser through the two-photon absorption process.

V.S.Dneprovskii et.al.[10] investigated the two-photon conductivity of ZnS, CdS and CdS_x-Se_{1-x} crystals using a ruby laser. B.V.Zubov et.al.[11] studied the two-photon absorption in Germanium using a Q-switched CaF_2: Dy^{2+} laser by observing the recombination radiation. B.M.Ashkinadze et.al.[12] observed the two-photon conductivity in CdS excited by giant pulses from a ruby laser and determined the cross section for two-photon absorption. N.A.Goryunova et.al.[13] investigated two-photon conductivity in a crystal $CdSnP_2$ at 77 K using a Nd:glass laser. Two-photon conductivity in ZnS and CdS were studied by A.Gingolani[14] and by S.Rafi Ahmad and D.Walsh.[15]

Two-photon absorption had been investigated by many more authors in various crystals like GaSe[16],[17], CdS_x-Se_{1-x}[18]. Most of these studies indicated a square law dependence on the excitation intensity. Two-photon absorption was usefully employed to shape the Q-switched pulses. R.K.Chang et.al.[19,20] and Lisitsyn[21] inserted two-photon absorbing semiconductors in the cavity of a Q-switched laser to obtain shaped elongated pulses. They demonstrated that laser pulses of controllable duration could be got by using non-linear absorbers inside the cavity.

The three-photon absorption in CdS was studied with the use of Nd:glass laser only recently. B.M.Ashkinadze et.al.[22] detected the luminescence emitted by CdS at 77° K excited by a Nd:glass laser. They detected the recombination radiation at 5200° A after three-photon absorption and found that the luminescent intensity depended on the excitation intensity as $I_{lum} = I_{excit}^{3.4}$.

They used a focussed Q-switched laser beam to get higher intensities. Arsenev et.al.[23] used the three-photon absorption process in CdS using a mo de locked Nd:glass laser to estimate the picosecond pulsewidth from a measurement of the decay of the luminescence along the length of the crystal.

Higher order absorption processes have been investigated in some of the alkali halide crystals.[24] I.M.Catalano et.al.[25] reported four-photon conductivity in KI, five-photon conductivity in KCl and NaCl using a Q-switched ruby laser.

Most of these experimental investigations were done with Q-switched pulses. With the availability of mode-locked Nd:glass lasers, it is possible to produce upto a few gegawatts/cm^2 without focussing. The pulsewidths are of the order of a few picoseconds and so the measurement of photoconductivity is a transient one and one can estimate the number of non-equilibrium carriers produced exactly. All the recombination times are slow compared to the generation time. Such a study of the interaction of picosecond pulses with semiconductors will throw more light on the behaviour of the non-equilibrium charge carriers in a very short time scale. The multi-photon processes can be studied with ease because of the high peak power associated with these ultra short pulses. Another advantage of using these short pulses is the higher damage threshold because of their short time duration.

C. AIM OF THE PRESENT EXPERIMENT:

In the present study, we chose to investigate the multi-photon conductivity in semiconductors using a Nd:glass laser with a view to examine their suitability to measure picosecond pulsewidth. Since two-photon conductivity in GaAs, CdS_x-Se_{1-x} and three-photon conductivity in CdS were not extensively studied before, we undertook to investigate these processes using Q-switched and mode-locke Nd:glass laser pulses. In the following thesis, we present an investigation of two-photon conductivity in GaAs, $CdS_{.5}$-$Se_{.5}$ crystals and three-photon conductivity in CdS and the use of these processes to measure intensity correlations of second and third order of the picosecond pulses of the Nd:glass laser and hence estimate the pulsewidth.

The theory for multi-photon absorption and multi-photon conductivity in semiconductors is given in Chapter 2 and will be compared in a later chapter with our experimental investigation. A brief account of picosecond pulsewidth estimation using second and third order intensity correlations is also given. The design of experiments and the description of the laser used are given in Chapter 3. Chapter 4 gives a detailed discussion of the results obtained in the current investigation.

CHAPTER 2

THEORY

INTRODUCTION:

Gallium Arsenide is a direct band gap semiconductor whose forbidden energy gap is 1.41 ev at room temperature. The photon energy of the Nd:glass laser is 1.17 ev. So it is possible to excite the electrons from the valence band to the conduction band by the absorption of two photons simultaneously. CdS_x-Se_{1-x} is a II-VI semiconductor with a fobidden energy gap at k =0. The magnitude of the energy gap varies with the composition x. For x =0.5, the energy gap corresponds to $\gtrsim$2ev. As such one can study the non-equilibrium charge carriers produced by simultaneous absorption of two photons. In a single photon absorption process, the absorption coefficient is independent of the intensity of light. For the case where the charge carriers are generated by the two-photon absorption, the absorption coefficient is linearly dependent on the light intensity. For Cadmium Sulphide (CdS), the band gap occurs at k=0 and $\simeq$ 2.42ev. The absorption coefficient in such process will be proportional to the square of the intensity of light as we shall see presently. The two and three-photon absorption coefficients can be calculated using time dependent perturbation theory and the appropriate band structure for these crystals.

In this chapter, we will outline the derivation of two and three-photon absorption coefficients. These expressions will be used to calculate the generation rate of non-equilibrium

carriers and subsequently a formula for multi-photon conductivity will be derived. These theoretical expressions will be used to compare with our experimental observations. Finally, the theory of picosecond pulse width measurement using two-photon and three-photon absorption is given.

TWO-PHOTON ABSORPTION COEFFICIENT:

Maria Goppert Mayer[1] first used second order time dependent perturbation theory to calculate the two-photon transition rate in atomic media. Braunstein and Ockmann[6] gave a similar calculation for semiconductors. They derived an expression for the transition rate for two-photon absorption using an initial valence band, a final conduction band and an intermediate virtual conduction band different from the final one. They did not include the initial valence band and the final conduction band as intermediate states. Obviously their derivation is not applicable to semiconductors for the following reason. The conduction band and valence band at k =0 are having definite parity as s and p levels of the atom. So two-photon absorption is forbidden at k = 0. However at k different from zero, the energy levels are of mixed parity and so the dipole matrix elements between these levels are non-vanishing. Basov et al.[8] derived the two-photon transition probability taking into account the contributions made by considering the valence band and the conduction band as intermediate states. We will give only an outline of the derivation and the details are relegated to the appendix 1.

The Hamiltonian for an electromagnetic field interacting with the valence electrons in a semiconductor is given by

$$\mathcal{H} = \frac{p^2}{2m} + V(r) + \frac{e}{mc}\,\hat{p}\cdot\hat{A}$$

where $\frac{p^2}{2m} + V(r)$ is the unperturbed Hamiltonian in the absence of e.m.field and $\frac{e}{mc}\,\hat{p}\cdot\hat{A}$ is the interaction Hamiltonian and can be considered as a perturbation. The solution of the unperturbed Hamiltonian gives the band structure of the material. We will assume that the bands are parabolic and that the two-photon transition occurs near k = 0 so that we can use the band structure derived from Kane's theory.[26] The transition rate per unit volume for two-photon absorption is given by (see appendix 1)

$$\frac{W_i}{V} = \frac{2\pi}{\hbar}\,\frac{1}{(2\pi)^3}\int d^3k\left[\sum_n \frac{H_{fn}\,H_{ni}}{E_n - (E_i + \hbar\omega)}\right]^2 \delta(E_f - E_i - 2\hbar\omega)$$

where $H_{fn} = \langle f|\frac{e}{mc}\,\hat{p}\cdot\hat{A}|n\rangle$

We will consider the valence band and the conduction band as the initial and final states (i,f). The intermediate state n can be either the final conduction band or the initial valence band. The higher conduction bands and the deeper valence bands are far away and the square of the energy denominator correspondingly increases and so the contributions from these bands can be neglected. The band structure of GaAs is shown in Figure 1.

$$\therefore \frac{W_i}{V} = \frac{2\pi}{\hbar}\,\frac{1}{(2\pi)^3}\int d^3k\left[\frac{H_{cc}\,H_{cv_i}}{\hbar\omega} + \frac{H_{cv_i}\,H_{v_i}}{-\hbar\omega}\right]^2 \delta(E_c - E_v - 2\hbar\omega)$$

i = 1,2,3 for three valence bands.

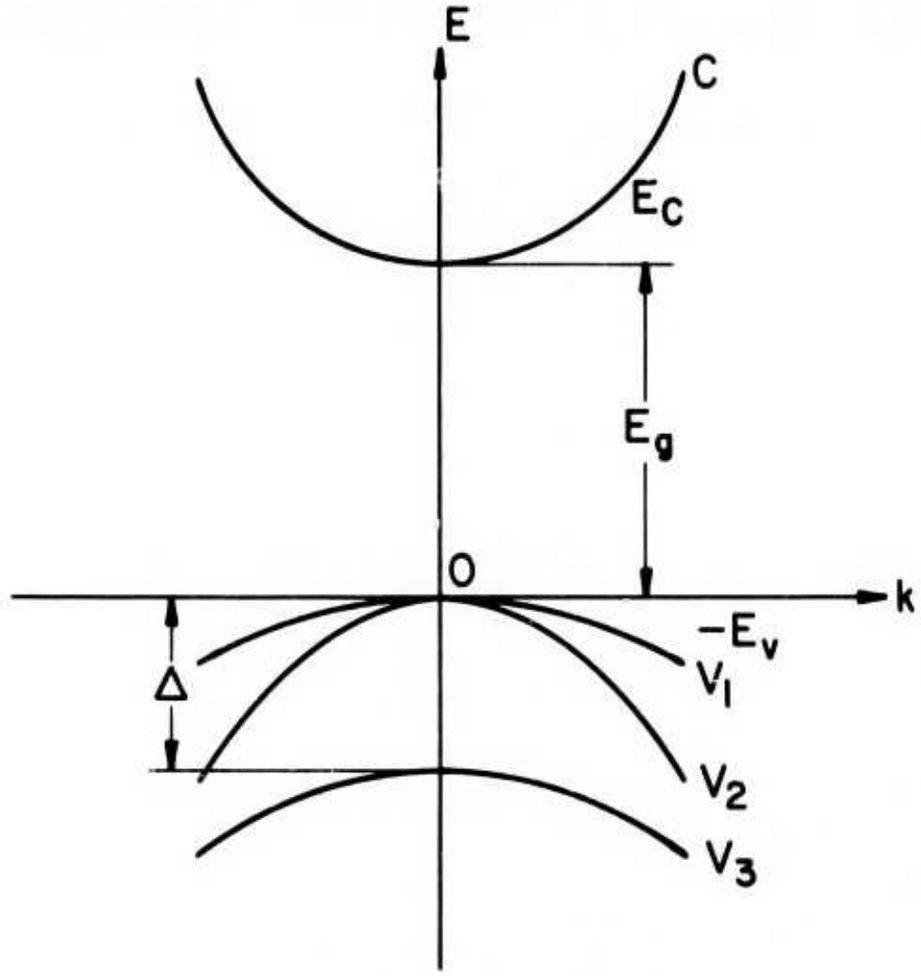

BAND STRUCTURE OF Ga As

C - conduction band ; $V_{1,2,3}$ - valence bands.

E_g - forbidden gap ; Δ - split off band width.

Energy measured w.r.t. the top of valence bands V_1 and V_2.

$E_g = 1.41$ ev ; $\Delta = 0.33$ ev (at 300 °k) ;

Effective masses m_c^*, $m_{V_1}^*$, $m_{V_2}^*$, $m_{V_3}^* = 0.72\, m_o$,

$0.68\, m_o$, $0.085\, m_o$, $0.25\, m_o$; m_o - electron rest mass.

FIGURE 1

The matrix elements can be evaluated using the Bloch wave functions

$$\psi_{c,k} = \frac{1}{(2\pi)^{3/2}} u_{ck}(r)\ e^{i\vec{k}\cdot\vec{r}}$$

Where c is the band index

k is the momentum vector.

$$H_{cv} = \frac{eA}{mc} (\hat{p}\cdot\vec{\alpha})_{cv}\ \delta(\vec{k}_c - \vec{k}_v)$$

$$H_{cc} = \frac{eA}{m_c^* c} (\hbar\vec{k}_c\cdot\vec{\alpha})\ \delta(\vec{k}_c - \vec{k}_{c'})$$

$$H_{vv} = -\frac{eA}{m_v^* c} (\hbar\vec{k}_v\cdot\vec{\alpha})\ \delta(\vec{k}_v - \vec{k}_{v'})$$

$\vec{A} = A\vec{\alpha}$, where A is the magnitude of the vector potential of the e.m.field and $\vec{\alpha}$ is the polarisation vector.

$$\frac{1}{m^*_{cv_i}} = \frac{1}{m_c^*} + \frac{1}{m^*_{v_i}} \quad , \quad E_c - E_{v_i} = E_g + \frac{\hbar k^2}{2m^*_{cv_i}}$$

and the intensity $I = \dfrac{\omega^2 \epsilon^{1/2} A^2}{8\pi c}$

Putting all these expressions into Eq.(3) and integrating , we get

$$\left(\frac{W_i}{V}\right) = \frac{2^{\frac{15}{2}}\ \pi e^4}{\epsilon c^2 (\hbar\omega)^6} \frac{\left|(\vec{\alpha}\cdot\vec{P})_{cv_i}\right|^2}{m^2}\ m^{*1/2}_{cv_i}\ (2\hbar\omega - E_g)^{3/2} I^2$$

The two-photon absorption coefficient $K_i^{(2)}$ Is defined as

$$K_i^{(2)} = 2\hbar w \left(\frac{W_i}{V}\right) / I$$

Taking into account the degeneracy of the bands due to spin, we get

$$K_i^{(2)} = \frac{2^{\frac{19}{2}} \pi e^4}{\epsilon c^2 (\hbar w)^5} \frac{\left|(\vec{\alpha}\cdot\vec{p})_{cv_i}\right|^2}{m^2} m_{cv_i}^{*1/2} (2\hbar w - E_g)^{3/2} I \quad \text{----- (1)}$$

where i = 1,2,3 for three valence bands.

The two-photon absorption coefficient is thus seen to be proportional to the first power of the intensity. Now knowing the band structure and the values of the effective masses, we can calculate the absorption coefficient. The two-photon absorption coefficient for GaAs and $CdS_{.5}$-$Se_{.5}$ was calculated using this formula and is shown in Appendix 2 and 3.

THEORY OF THREE-PHOTON ABSORPTION:

For CdS, we require an expression for the three-photon absorption coefficient. We have to use the third order time dependent perturbation theory. We use the same two band model as we used in the derivation of $K^{(2)}$. The Hamiltonian $\mathcal{H}$ is given by

$$\mathcal{H} = H_0 + H' + H''$$

where

$$H_0 = \frac{p^2}{2m} + V(r)$$

$$H' = \frac{e}{mc} \vec{p}\cdot\vec{A} \quad \text{and} \quad H'' = \frac{e^2}{2mc^2} \vec{A}\cdot\vec{A}$$

In the previous derivation, we omitted H'' since H'' contributes to two-photon process as a first order term and the matrix element vanishes because of orthogonality of the wave functions of the initial and the final states. But in the third order process, H'' contributes through a second order term.

We get for the transition probability per unit volume as shown in appendix 4 ,

$$\frac{W_t}{V} = \frac{2\pi}{\hbar}\frac{1}{(2\pi)^3}\int d^3k\Big[\sum_n \frac{H'_{fn}H''_{ni}}{E_{ni}-2\hbar\omega} + \sum_n \frac{H''_{fn}H'_{ni}}{E_{ni}-\hbar\omega} + \sum_n\sum_m \frac{H'_{fn}H'_{nm}H'_{mi}}{(E_{ni}-2\hbar\omega)(E_{mi}-\hbar\omega)}\Big]^2 \delta(E_f-E_i-3\hbar\omega)$$

Using Bloch wave functions we can write the matrix elements. The dipole matrix elements are the same as before.

$$H''_{nf} = \left\langle n \left| \frac{e^2}{2mc^2}\,\vec{A}\cdot\vec{A} \right| f \right\rangle$$

$$H''_{(c_n,k_s)(c_m,k_t)} = \left\langle c_n, k_s \left| \frac{e^2}{2mc^2}\,\vec{A}\cdot\vec{A} \right| c_m, k_t \right\rangle \simeq \delta_{k_s,k_t}\,\delta_{c_n,c_m}\frac{1}{2m}\left(\frac{e}{c}\right)^2 \vec{A}\cdot\vec{A}$$

Omitting the photon momentum to be small as before and taking the initial valence band and the final conduction band as virtual intermediate states, we get

$$\frac{W_i}{V} = \frac{2\pi}{\hbar}\frac{1}{(2\pi)^3}\int d^3k\;\delta(E_c-E_{vi}-3\hbar\omega)\;|W_{cv}|^2$$

Where

$$W_{cv} = \frac{H'_{cv} H''_{vv}}{-2\hbar\omega} + \frac{H''_{cc} H'_{cv}}{2\hbar\omega} + \frac{H'_{cv} H'_{cc} H'_{cv}}{(E_{cv}-2\hbar\omega)(E_{cv}-\hbar\omega)}$$

$$+ \frac{H'_{cv} H'_{vv} H'_{vv}}{(-2\hbar\omega)(-\hbar\omega)} + \frac{H'_{cv} H'_{vc} H'_{cv}}{(-2\hbar\omega)(E_{cv}-\hbar\omega)} + \frac{H'_{cc} H'_{cv} H'_{vv}}{(E_{cv}-2\hbar\omega)(-\hbar\omega)}$$

Substituting the matrix elements in W_{cv}, we find the first two terms to cancel out to zero and we are left with the four terms containing the dipole matrix elements.

$$E_{cv} = 3\hbar\omega \simeq E_g + \frac{\hbar^2 k^2}{2\mu}$$

where $$\frac{1}{\mu} = \frac{1}{m_c^*} + \frac{1}{m_v^*}$$

After integration (see appendix 4), we get an expression for $\frac{W_t}{V}$ as

$$\frac{W_t}{V} = 2^{15/2} \pi^2 \hbar^2 \frac{1}{(\hbar\omega)^{10}} \left(\frac{e^2}{c\epsilon^{1/2}}\right)^3 \left(\frac{1}{\mu}\right)^{1/2} \frac{B_0^2}{m^2} \quad I^3$$

$$\times \left[\frac{4}{5}(3\hbar\omega - E_g)^{5/2} - \frac{2}{3} B_0^2 \frac{\mu}{m^2} (3\hbar\omega - E_g)^{3/2} + \frac{1}{4} \frac{B_0^2}{m^4} \mu^2 (3\hbar\omega - E_g)^{1/2}\right]$$

where $B_0 = \langle \vec{\alpha} \cdot \vec{P} \rangle_{cv}$

Taking into account spin degeneracy and the definition of three-photon absorption coefficient as

$$K^{(3)} = \frac{3\hbar\omega (W_t/V)}{I^3},$$

we get

$$K^{(3)} = 3 \times 2^{17/2} \pi^2 \hbar^2 \frac{1}{(\hbar\omega)^9} \left[\frac{e^2}{c\epsilon^{1/2}}\right]^3 \left(\frac{1}{\mu}\right)^{1/2} \frac{B_0^2}{m^2} \quad I^2$$

$$\times \left[\frac{4}{5}(3\hbar\omega - E_g)^{5/2} - \frac{2}{3} \frac{B_0^2}{m^2} \mu (3\hbar\omega - E_g)^{3/2} + \frac{1}{4} \frac{B_0^4}{m^4} \mu^2 (3\hbar\omega - E_g)^{1/2}\right] \quad \text{--(2)}$$

The calculation of the absorption coefficient in the case of CdS is shown in Appendix 5.

Theory of Multi-photon Conductivity:

Once we know the absorption coefficient, we can calculate the generation rate of carriers in the crystal. The intensity distribution along the length of the crystal for multi-photon absorption follows a differential equation

$$\frac{dI}{dx} = -\beta_n I^n$$

where n denotes the order of absorption and

$$\beta_n I^{n-1} = K^{(n)} \sim \text{absorption coefficient.}$$

Integrating, we get

$$I_x = \frac{I_0}{\left[1 + (n-1)\beta_n I_0^{n-1} x\right]^{\frac{1}{n-1}}} \qquad \text{---- (3)}$$

The generation rate of non-equilibrium charge carriers F(x) is given by

$$F(x) = \frac{\beta_n I_x^n}{n\hbar\omega}$$

$$= \frac{\beta_n}{n\hbar\omega} \frac{I_0^n}{\left[1 + (n-1)\beta_n I_0^{n-1} x\right]^{\frac{n}{n-1}}} \qquad \text{----- (4)}$$

The concentration of the generated carriers under steady state conditions obey the following differential equation.

$$D_p \frac{\partial^2 p}{\partial x^2} - \frac{p}{\tau} = -F(x)$$

where p is the concentration of non-equilibrium charge carriers and D_p is the diffusion constant and τ is the life time of the

carrier. Jick H.Yee [29,30,31] solved this equation by the method of variation of parameters (see Appendix 6) and used the solution to calculate the photoconductivity ΔG as

$$\Delta G = \int_0^L \int_0^{\frac{a}{c}} q \left(\mu_p + \mu_e\right) p(x)\, dy\, dx \qquad \text{.....(5)}$$

The final formula for steady state n-photon conductivity is as follows

$$\Delta G^{(n)} = \alpha \tau \frac{I_0}{n\hbar\omega} \left[1 - \frac{1}{\left[1+(n-1)\beta_n I_0^{n-1} L\right]^{\frac{1}{n-1}}}\right]$$

$$- \frac{\alpha \tau \beta_n I_0^n}{n\hbar\omega} \cdot \frac{V_s\, e^{-\lambda L/2}}{\left[(\lambda+V_s)-(\lambda-V_s)e^{-\lambda L}\right]} \cdot \int_0^L \frac{\cosh \lambda\left(\frac{L}{2}-x\right)}{\left[1+(n-1)\beta_n I_0^{n-1} x\right]^{\frac{n}{n-1}}} dx \qquad \text{....(6)}$$

where $\alpha = q \frac{a}{c}\left(\mu_p + \mu_e\right)$, $D_p \lambda^2 = \frac{1}{\tau}$

In the case of GaAs, the diffusion length $(1/\lambda)$ is very short of the order of 10^{-4}cm and $\lambda L \gg 1$, ($10^4 \times .03 = 300$) , the formula for two-photon conductivity becomes for n=2,

$$\Delta G^{(2)} = \alpha \frac{\tau}{2\hbar\omega} \cdot \frac{\beta_2 I_0^2 L}{1 + \beta_2 I_0 L} \qquad \text{.....(7)}$$

This expression holds good for steady state conductivity and in an experiment with Q-switched laser pulses, the pulses are long compared to the steady state life time of the carriers and so we are in short measuring the steady state photoconductivity. This happened to be the case with GaAs since the photo-conductivity life time was found to be short compared to the Q-switched pulse duration. For $\beta_2 I_0 L < 1$, $\Delta G^{(2)} \propto I_0^2$

indicating the two-photon nature of the absorption process.

In the case of mode-locked pulse excitation, non-equilibrium charge carriers are produced within an interval determined by the pulsewidth and normally the lifetime of the carriers is long compared to the picosecond pulsewidth and so we are measuring the transient photoconductivity. In the case of crystals like $CdS_{.5}$-$Se_{.5}$ and CdS, the electron life time is of the order of a few microseconds or more and so we will be measuring the transient photoconductivity whether we use Q-switched or mode-locked pulse excitation. So we will presently calculate the multi-photon conductivity for a transient process.

Multi-photon conductivity for short pulse excitation:

If a short pulse is incident on the crystal, the concentration of carriers generated at a point 'x' due to multi-photon absorption is given by

$$P(x) = F(x)\, t_i$$

$$= \frac{\beta_n}{n\hbar\omega} \frac{I_0^n}{\left[1+(n-1)\beta_n I_0^{n-1} x\right]^{\frac{n}{n-1}}} \cdot t_i$$

where t_i is the pulse width.

Then $\Delta G^{(n)}$ can be calculated using the expression (5)

$$\Delta G^{(n)} = \frac{a}{c} \eta (\mu_p + \mu_e) \frac{\beta_n I_0^n}{n\hbar\omega} t_i \int_0^L \frac{dx}{\left[1+(n-1)\beta_n I_0^{n-1} x\right]^{\frac{n}{n-1}}}$$

$$\therefore \Delta G^{(n)} = \frac{a}{c} q (\mu_p + \mu_e) \; t_i \frac{I_0}{n\hbar\omega} \left[1 - \frac{1}{\{1 + (n-1)\beta_n I_0^{n-1} L\}^{\frac{1}{n-1}}} \right] \quad \cdots (8)$$

This agrees with the Jick Yee's formula if we neglect the second term and replace γ the electron life time by the pulse width t_i . As before for a two-photon process,

$$\Delta G^{(2)} = \frac{a}{c} q (\mu_e + \mu_p) \frac{\beta_2 I_0^2 L}{1 + \beta_2 I_0 L} \frac{t_i}{2\hbar\omega} \quad \cdots\cdots (9)$$

For a three-photon process,

$$\Delta G^{(3)} = \frac{a}{c} q (\mu_e + \mu_p) \frac{t_i}{3\hbar\omega} I_0 \left[1 - \frac{1}{(1 + 2\beta_3 I_0^2 L)^{1/2}} \right] \quad \cdots (10)$$

When $\beta_3 I_0^2 L \ll 1$,

$$\Delta G^{(3)} = \frac{a}{c} q (\mu_e + \mu_p) \frac{t_i}{3\hbar\omega} \beta_3 I_0^3 L \quad \cdots\cdots (11)$$

$\Delta G^{(3)} \propto I_0^3$ indicating the three-photon nature of the absorption process. The formula for $\Delta G^{(2)}$ and $\Delta G^{(3)}$ will be used in a later chapter to estimate the values of the two-photon and three-photon absorption coefficients from the measured photoconductivity.

Theory of picosecond pulsewidth measurement:[32]

The square law and cube law dependence of photoconductivity can be used to measure the second and third order intensity correlation of the picosecond pulses and hence to estimate the pulsewidth. So far only fluorescence[33,34,67] and harmonic measurements[36,68] have been done. From a multi-photon photoconductor, the output we get is an electronic signal and so if the photoconductivity method is successful, we could construct an electronic detector for the measurement of picosecond pulsewidth. The theory behind higher order intensity correlation measurement is given below.

Second order correlation:

The typical arrangement for the two-photon technique for the display of picosecond pulses is shown in Fig. 2. Carriers are produced in the crystal by simultaneously absorbing two photons at the fundamental laser frequency from the resulting light field of the superposition of the two beams. The resulting light beam is represented by a field $E_r(t)$ given by

$$E_r(t) = E(t) + E(t+\tau)$$

where $E(t)$ is the incident light field in one direction and $\tau = 2nZ/c$ is the delay time between the two signals, and 2z is the path difference between the two beams. The output from the crystal can be measured and is an average value of $\langle \Delta G \rangle$ of the photoconductivity, averaged in time and space over several optical wavelengths. Now,

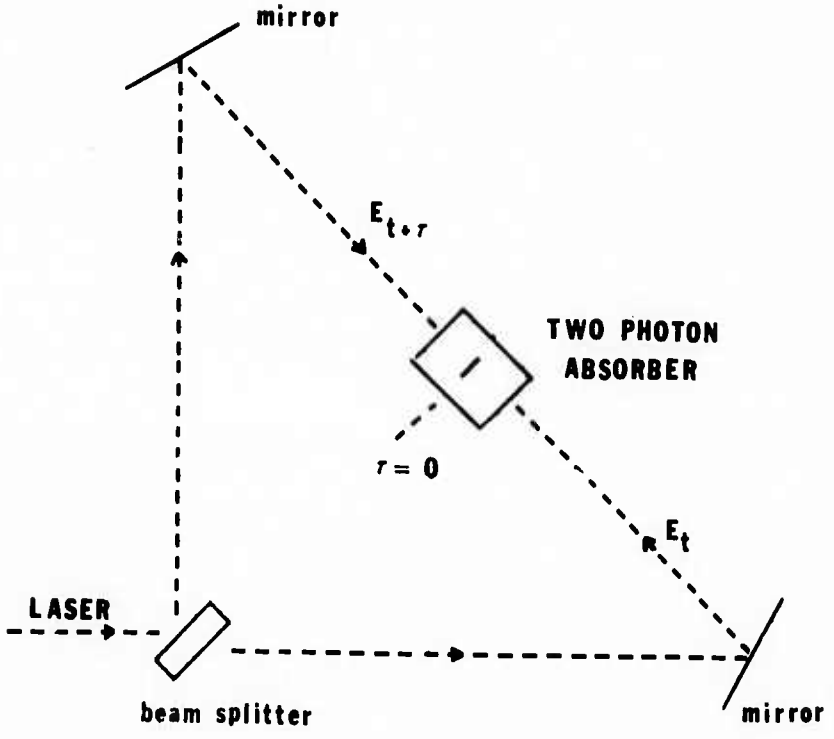

FIGURE 2: ARRANGEMENT FOR TWO-PHOTON CORRELATION

$$\langle \Delta G \rangle \simeq \langle V_r(t)\, V_r(t)\, V_r^*(t)\, V_r^*(t) \rangle \qquad \text{-----(12)}$$

where $V_r(t)$ is the analytic signal associated with the real field $E_r(t)$. The quantum mechanical probability 'P' for Two-photon absorption is given by

$$P \simeq \mathrm{Tr}\,(\rho\, a^\dagger a^\dagger a\, a) \qquad \text{------(13)}$$

where ρ is the density matrix describing the light field. In the classical limit, $V(t)$ corresponds to the creation operator $a^\dagger$ and $V^*(t)$ to the annihilation operator a. (12) is proportional to (13) in the classical limit.

$$V_r(t) = V(t) + V(t+\tau)$$

Let $V = V(t)$ and $V_\tau = V(t+\tau)$.

Then the observed conductivity at a certain position is expressed as,

$$\langle \Delta G \rangle(\tau) = \langle (V+V_\tau)(V+V_\tau)(V^*+V_\tau^*)(V^*+V_\tau^*) \rangle$$

$$= 2\langle VV\,V^*V^* \rangle + 4\langle V\,V_\tau\,V^*V_\tau^* \rangle$$

$$+ 2\langle (VV^* + V_\tau V_\tau^*)(VV_\tau^* + V^*V_\tau) \rangle$$

$$+ \langle VV_\tau^*\,VV_\tau^* + V^*V_\tau\,V^*V_\tau \rangle$$

The first two terms are proportional to the intensity correlation functions $G^{(2)}$, also known as Glauber's[37] second order correlation functions. The last two terms describe interference effects

giving spatial variations proportional to $\cos(\omega_0 \tau)$ and $\cos(2\omega_0 \tau)$, where ω_0 is the mean center frequency of the light field. Due to the slow response of the crystal, these variations are averaged out to zero. The normalised photoconductivity is now expressed by the intensity correlation function $G^2(\tau)$ of the field.

$$\langle \Delta G \rangle(\tau) = \frac{2\,G^2(0) + 4\,G^2(\tau)}{G^2(0)}$$

$$G^2(\tau) = \frac{\langle V(t)\, V(t+\tau)\, V^*(t)\, V^*(t+\tau) \rangle}{\langle V(t)\, V^*(t)\, V(t+\tau)\, V^*(t+\tau) \rangle}$$

$\langle\ \rangle$ refers to a time average or an ensemble average. If only a time averaging is considered, then

$$I(t) = V V^*$$

$$G^2(\tau) = (\bar{I})^{-2} \int_{-\infty}^{\infty} I(t)\, I(t+\tau)\, dt$$

where $\bar{I}$ is the mean intensity.

At the peak of the pulse, $\tau = 0$,

$$\langle \Delta G \rangle_{\text{peak}} = \frac{2\,G^2(0) + 4\,G^2(0)}{G^2(0)} = 6$$

$$\langle \Delta G \rangle_{\text{background}} = \frac{2\,G^2(0) + 4\,G^2(\tau)}{G^2(0)}$$

$$\text{Contrast Ratio 'R'} = \frac{\langle \Delta G \rangle_{\text{peak}}}{\langle \Delta G \rangle_{\text{background}}} = \frac{3\,G^2(0)}{G^2(0) + 2\,G^2(\tau)}$$

For a bandwidth limited short pulse ($T = \Delta\gamma^{-1}$) i.e. in the case of a perfectly mode-locked beam,

$$\langle \Delta G \rangle_p = 6$$

$G^2(0) = 0$ at delay times $\tau \gg \Delta\gamma^{-1}$ due to the vanishing intensity.

$$\therefore \langle \Delta G \rangle_b = 2.$$

Contrast Ratio = 3.

If we scan the region near the perfect overlap of the pulses, we can map the correlation function as a function of τ. The two-photon conductivity can be measured as a function of τ. This should give a peak at the overlap point ($\tau=0$) and this peak must be, according to theory, three times higher than the background. The halfwidth of the correlation curve gives a measure of the pulsewidth. Similar structure of the correlation curve is exhibited by Q-switched or a free running laser but with a reduced contrast ratio of 1.5 . Care must be exercised to interpret the results of these measurements. However if one observes the mode-locking of the laser beam in a fast oscilloscope, one can easily eliminate the possibility of reduced contrast ratio due to Q-switching or free running of the laser.

Third Order Correlation:

If we use a three-photon absorber instead of the two-photon absorber, we can measure the autocorrelation function of third order. As before, the three-photon conductivity can be

measured as a function of τ. Then the observed photoconductivity at certain position is expressed as

$$\langle \Delta G^{(3)} \rangle (\tau) \simeq \langle (V+V_\tau)(V+V_\tau)(V+V_\tau)(V^*+V^*_\tau)(V^*+V^*_\tau)(V^*+V^*_\tau)$$

This corresponds to the three-photon absorption probability

$$P^{(3)} \simeq Tr\,(\rho a^\dagger a^\dagger a^\dagger a\, a\, a)$$

As before, we can express the normalised photoconductivity in terms of Glauber's[37] third order correlation functions. After a straight forward algebraic simplification,

$$\langle \Delta G^{(3)} \rangle (\tau) \simeq \frac{2\,G^3_0(0) + 9\,G^3_1(\tau) + 9\,G^3_2(\tau)}{G^3_0(0)}$$

Where $$G^N_n(\tau) = \left(\bar{I}\right)^{-3} \int_{-\infty}^{\infty} I^n(t)\; I^{N-n}(t+\tau)\; dt$$

where $\bar{I}$ is the mean intensity.

At the peak of the pulse, $\tau = 0$, so $\langle \Delta G^{(3)} \rangle_{peak} = 20$

At a point far away from the overlap (ie) $\tau >> 1/\Delta\gamma$, $G^3(\tau) = 0$, so $\langle \Delta G^{(3)} \rangle_{background} = 2$.

Therefore, Contrast Ratio $= \dfrac{\langle \Delta G^{(3)} \rangle_p}{\langle \Delta G^{(3)} \rangle_b} = 10$

Therefore the third order correlation measurement will give a larger contrast ratio and so it can be easily measured. Q-switched or free running laser should give a contrast ratio of 2.5[40] and so in a measurement of picosecond pulsewidth using the third order process one can easily differentiate the Q-switched pulse from the mode-locked pulse since there is a factor of 4 in contrast

ratios unlike a factor of 1.5 in the case of measurement with a two-photon process.

In chapter 4, we will be discussing the correlation measurements using two-photon conductivity in GaAs and $CdS_{.5}$-$Se_{.5}$ and using the three-photon conductivity in CdS. Once we demonstrate in principle the picosecond pulsewidth measurement using multi-photon conductivity in semiconductors, the construction of an electronic multichannel detector using a layered thin film semiconductor structure may become feasible in the near future.

CHAPTER 3

Design of Experiments:

In this thesis, we present an experimental investigation of two-photon conductivity in GaAs using Q-switched and mode-locked Nd:glass laser. We also studied two-photon conductivity in $CdS_{.5}$-$Se_{.5}$ and three-photon conductivity in CdS using only mode-locked laser . The present chapter gives a brief account of the laser used and the design of experiments. To facilitate understanding of the correlation measurements using these non-linear photoconductors, we will give a brief account of the mode-locking the laser.

The Neodymium Glass Laser:

In the Neodymium glass laser, the Nd^{3+} ion is present as an impurity atom in glass. The energy levels involved in the laser transition in a typical glass are shown in Fig. 3. The glass rod is usually pumped by a coaxial Xenon flash lamp. The Nd:glass has a wide absorption band in the ultraviolet and in the visible region. After absorption of the wide band light from the flash lamp, the system relaxes to the excited state (upper lasing level) $4F_{\frac{3}{2}}$. The laser emission occurs at a wavelength of 1.059 μm and the lower level is 1950 cm^{-1} above the ground state. We have here a four level laser, since the thermal population of the lower laser level is negligible. The fluorescent linewidth is around 100 cm^{-1}[41]. This rather large inhomogeneous linewidth

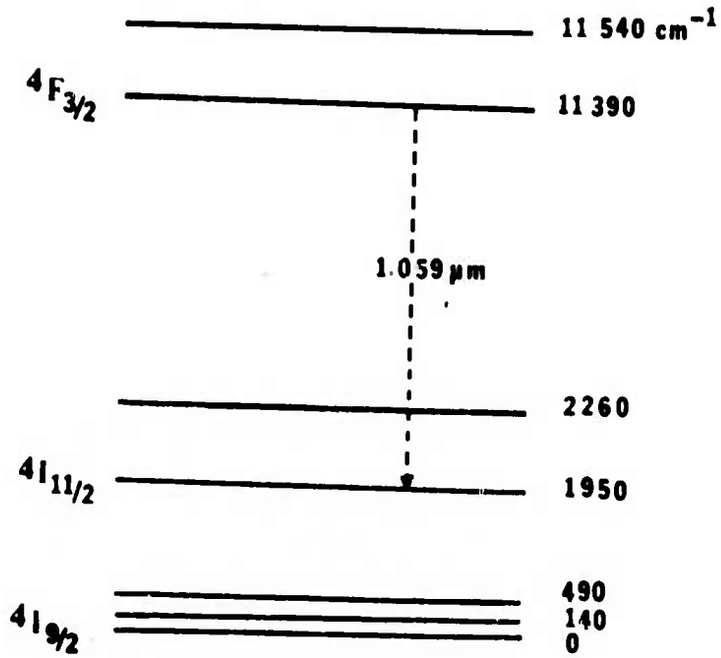

ENERGY LEVEL DIAGRAM FOR Nd^{3+} ION IN GLASS

FIGURE 3

is due to the amorphous structure of glass, which causes different Nd^{3+} ions to see slightly different surroundings. Different ions consequently radiate at slightly different frequencies, causing a broadening of the spontaneous emission spectrum. This large linewidth is advantageously utilised in the mode-locking of lasers as we shall see presently.

The laser used in the present investigation was a Korad KI-system with a Nd:glass rod having a Brewster-Brewster configuration to avoid reflection losses. The laser rod was of diameter 0.5" and length 8" . Two dielectric mirrors (99.9 % and 65% reflectivities) formed the laser cavity. The useful beam came out of the partially transparent mirror.

Q-switching the Nd:glass laser was done by introducing a cell containing Kodak 9860 dye solution in dichloroethane inside the cavity. Since the same configuration was used to mode-lock the laser, it was sometimes difficult to get neat Q-switched pulses. For this purpose, we introduced an interferometric flat inside the cavity to avoid mode-locking.

Mode-locking the Laser:- (42,43)

Let us consider a laser as a resonant Fabry-Perot cavity whose dimensions are large compared to the wavelength. Then we note that many axial interferometric modes within the inhomogeneous linewidth can oscillate more or less independently of each other. In the Q-switched case, these modes are, in general, uncoupled and

have no fixed phase relationship with one another. The resultant electric field

$$E_R = \sum_n E_n$$

where E_n is the electric field of the n-th mode.

Intensity $I_{uncoupled} = E_R \cdot E_R^* = N.E_0^2$ for 'N' modes, since $\langle E_{n1} | E_{n2} \rangle$ vanishes for uncorrelated fields.and $E_n = E_0.\mathrm{Exp}(i\phi_n)$ where ϕ_n is at random and E_0 is the mode amplitude (assumed to be equal).

Now consider the case where there is a fixed relationship between the phases of the different modes which are equally spaced at

$$\omega_q - \omega_{q-1} = 2\pi \times \frac{c}{2\ell} = \omega$$

where ℓ is the length of the cavity. Let us assume for simplicity the phases to be zero. Then the resultant electric field is given by

$$E_R = \sum_{-(N-1)/2}^{(N-1)/2} E_0 \, e^{i(\omega_0 + n\omega)t}$$

where ω_0 is the center frequency of the laser

$$E_R = E_0 \, e^{i\omega_0 t} \, \frac{\mathrm{Sin}\,(N\omega t/2)}{\mathrm{Sin}\,(\omega t/2)}$$

Now when the modes are locked in phase, the laser intensity is given by

$$I_{\text{mode-locked}} = E_0^2 \, \frac{\mathrm{Sin}^2\,(N\omega t/2)}{\mathrm{Sin}^2\,(\omega t/2)}$$

Therefore we see that the intensity of the mode-locked laser is in the form of a train of pulses with a period $T = \frac{2\pi}{\omega}$

and $I_{peak}(\text{mode-locked}) = N^2E_0^2 = N\, I_{\text{unmode-locked}}$. We see that the intensity is increased by the number of participating modes. The pulsewidth is defined as the time from the peak to the first zero and is equal to $\frac{2\pi}{N\omega} \simeq \frac{1}{\Delta\gamma}$ where $\Delta\gamma$ is the inhomogeneous line width.

Thus we see that when the modes are locked in phase, we get a train of pulses of greater intensity and lower width which is approximately the inverse of the gain line width. As we have seen, the inhomogeneous line width of the laser is $3X10^{12}$ Hz ($\Delta\gamma$) and we should expect pulses of 0.33 psecs duration theoretically.

To generate these ultra short pulses, we must couple together all the laser modes falling within the line width by putting an active or passive modulator in the cavity. Normally we use passive mode-locking with the help of saturable dye solution. Despite its wide use, passive mode-locking is not well understood. However the mode-locking using a saturable absorber can easily be explained on a qualitative basis in the time domain as follows:

The saturable absorber has a non-linear transmission characteristic. Viewing the laser as a quantum mechanical oscillator building up from spontaneous emission noise, the low amplitude portions of the amplified fluctuating spontaneous emission noise are discriminated against the high amplitude portions because of the non-linear transmission of

the dye solution. At low light intensities only a small fraction of the laser light is transmitted through the absorber. At high light intensities, the absorber becomes transparent. The lower intensity portion of the pulse is cut off by the saturable absorber and the absorber is bleached during the peak of the pulse. By the time the pulse is reflected back, the absorber relaxes to ground state and once again the pulse is amplified and narrowed. Within a few cycles (return cavity round trip times), the pulse is narrowed to its limit namely, the inverse of the oscillating bandwidth of the laser system.

The block diagram of a mode-locked laser is shown in figure 4 . The saturable absorber used in mode-locking the Nd:glass laser was Kodak 9860 dye solution in dichloroethane. Mode-locking was done for a number of other lasers such as Ruby, Nd:Yag, He-Ne. Because of the narrower line widths of the latter media, production picosecond pulses of higher intensity is really limited to Nd^{3+}:glass medium.

Calibration of the output intensity:

The experimental set-up is shown in figure 4. The Nd:glass laser was Q-switched using the dye cell containing Kodak 9860 dye in dichloroethane and an interferometric flat wich served to prevent any mode-locking. The output through the partially reflecting mirror was sent through a flash lamp filter. The photo diodes measured the intensity of the light reflected from ordinary glass beam splitters. The energy of

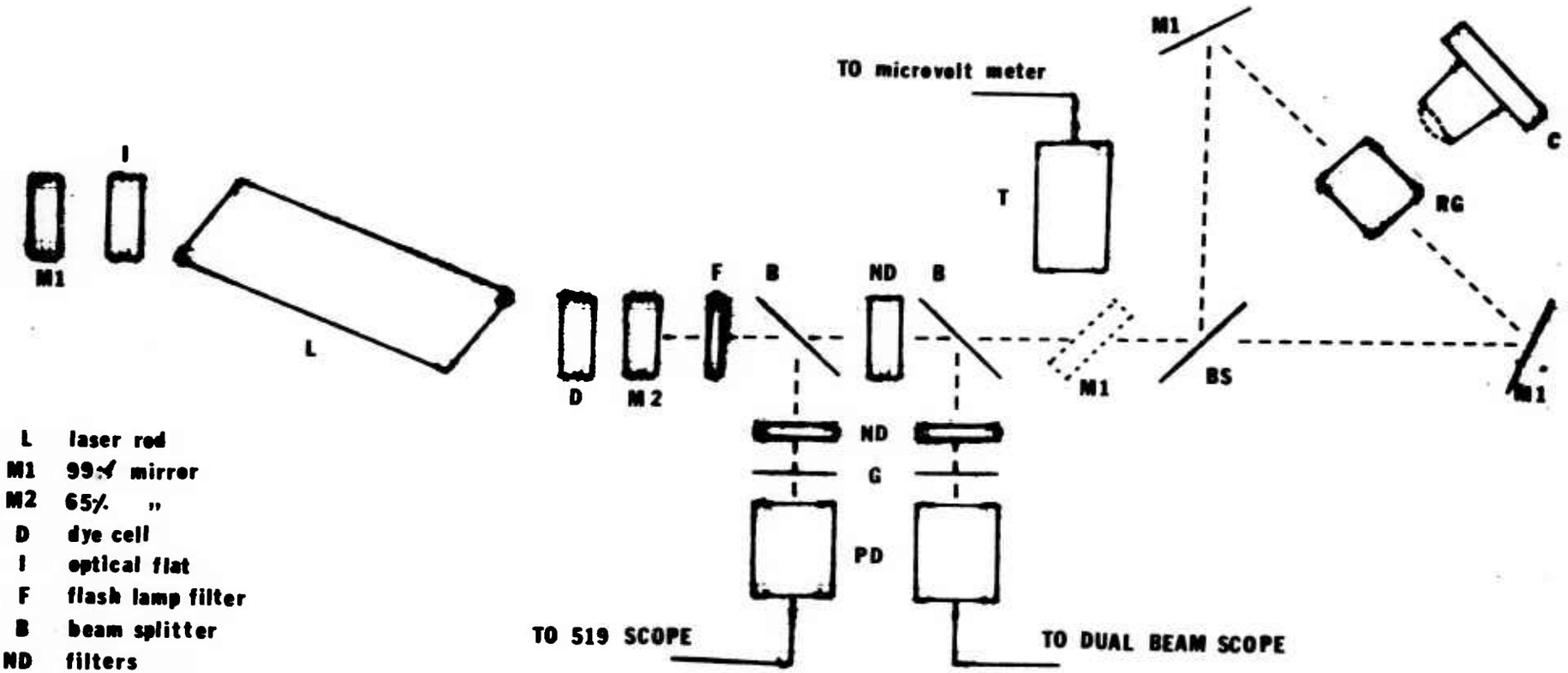

L	laser rod
M1	99% mirror
M2	65% „
D	dye cell
I	optical flat
F	flash lamp filter
B	beam splitter
ND	filters
G	ground glass
PD	Photo diodes
T	calorimeter
BS	beam splitter
RG	rhodamine 6G
C	camera

FIGURE 4 : EXPERIMENTAL SET UP – Nd:GLASS LASER

the beam was measured by a calibrated thermopile calorimeter the output of which was connected to a microvoltmeter. The output from one of the photo diodes (ITT coaxial photo tube) was connected to a fast 519 oscilloscope. This combination had a rise time of 0.7 nsecs. The measurement on this was used to determine the pulsewidth and also the Q-switching of the pulse could be checked. The other photo diode was connected to a Tektronix dual beam scope and the pulse height was taken as a measure of the intensity of the pulse. For the intensity calibration, every laser pulse was simultaneously recorded on both the oscilloscopes and the energy in Joules was determined from the calorimeter output. Knowing the pulsewidth, we calibrated the pulse height in the dual beam oscilloscope with the intensity calculated from the energy and cross-section of the beam. The linearity of the photo diode was checked for two decades of intensity. So the photo diode was set to read intensity in Mw/cm^2.

In the case of mode-locked pulses, emission occurred only during short intervals of the order of picoseconds. So to measure peak intensity, we should measure the pulsewidth. We removed the optical flat from the cavity and used a contact dye cell with the 99% mirror. The dye cell was very thin and could hold approximately 2ccs at 2mms thickness and 5 cms diameter. This thin contact dye cell was found extremely useful in getting neat mode-locked pulse trains well over 80 % of the times we fired laser. The mode-locking was

checked by one of the photo diodes (ITT) connected to a 519 scope. This combination had a risetime of a fraction of a nanosecond (.7 nsecs). The pulse energy was determined as before by a calibrated thermopile detector. In a separate measurement, the pulsewidth was determined by the Two-Photon fluorescence technique (TPF). The laser beam intensity was divided into two equal parts by a 50%-50% beam splitter as shown in figure 4. Then the two beams were totally reflected by mirrors to cross at a long cell containing 10^{-3} molar solution of Rhodhamine 6G in ethanol which exhibits two-photon absorption of Nd:glass laser photons and subsequently emits near the second harmonic of Nd:glass laser. This fluorescent intensity due to the overlap of the two split beams was photographed using a polaroid camera. A typical picture of the mode-locked pulse train and the TPF trace of the same pulse train is given in figure 5 . We could count the total number of pulses in the half width of the pulse train and determine the energy per pulse (peak energy) . In the TPF trace, we see an enhanced intensity in the region of overlap and the width of this bright spot 'w' approximately gives the pulsewidth ($\tau \approx \frac{w n}{c}$ where $\frac{c}{n}$ is the velocity of light in ethanol, $n \simeq 1.44$). This TPF trace should give a contrast ratio of 3 according to the theory developed in chapter 2 . We did not measure the contrast ratio and so our measurement is only an approximate one. Since we observed a neat mode-locked pulse train in the 519 scope, we could safely estimate the pulse width without measuring contrast

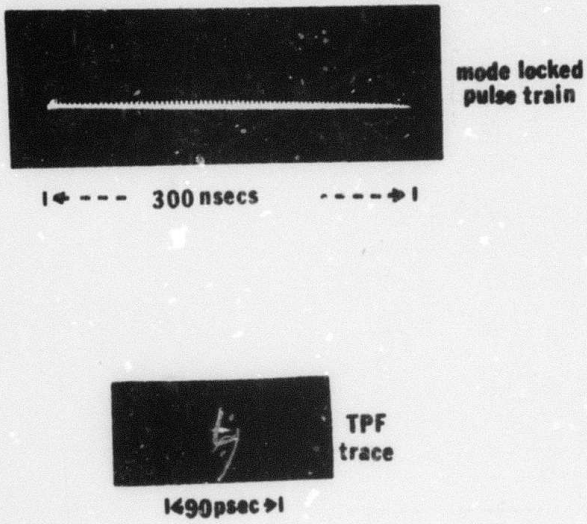

FIGURE 5

ratio. Over several exposures, we got a value for the pulse width to be 3 - 9 psecs . We could easily produce a peak energy of a few millijoules which corresponded to an average power of a few gega watts (10^9 watts). This rather high peak power facilitated the investigation of muti-photon conductivity in semiconductors.

Measurement of Photoconductivity:

Almost all the crystals used in the present experiment were cut from single crystalline wafers. Ohmic contacts were made to both ends of the crystal by alloying indium at an inert atmosphere (under nitrogen flow). The low resistivity crystals were checked on a transistor curve tracer for the non-rectifying contacts. All the crystals were connected to a low voltage battery V through a resistance R (either 50 or 125Ω). When the crystals were illuminated with laser pulses, the change in voltage 'v' across the resistance R because of the conductivity change was measured directly on the oscilloscope. When the battery was short circuited, the crystals were investigated for any photovoltaic effect. In all the crystals, the photovoltaic effect was barely observable (much less than 1% of the photoconductivity signal). This confirmed the ohmic nature of the contacts.

The change in conductivity ΔG due to the laser pulses could be computed from the voltage change v across the resistance R[44]. Let r_0 be the dark resistance of the

crystal. Let the change of the crystal resistance on illumination be Δr. We shall denote the dark current by i_d and the current during illumination by i_i. Then,

$$v = (i_i - i_d) R$$

where $$i_i = \frac{V}{R + r_0 - \Delta r} \quad , \quad i_d = \frac{V}{R + r_0}$$

$$\therefore \quad v = VR \frac{\Delta r}{(R + r_0 - \Delta r)(R + r_0)}$$

$$\Delta r = \frac{v (R + r_0)^2}{VR + v (R + r_0)} \qquad \text{------ (1)}$$

$$\Delta G = G_i - G_0 = \frac{1}{r_0 - \Delta r} - \frac{1}{r_0} = \frac{\Delta r}{r_0 (r_0 - \Delta r)}$$

Hence $$\Delta r = \frac{r_0^2 \Delta G}{1 + r_0 \Delta G} \qquad \text{- - - - - (2)}$$

Equating (1) and (2) we get,

$$\Delta G = \frac{v (R + r_0)^2}{r_0^2 VR - v r_0 R (r_0 + R)} \qquad \text{- - - - - (3)}$$

Thus in general the relationship between the signal v and the photoconductance ΔG is seen to be non-linear. To estimate ΔG, we have to know the dark resistance of the crystal r_0 in addition to V and R. This formula (3) was used to estimate the photoconductivity of low resistivity samples.

In the case of high resistivity compensated semiconductors, r_o is large of the order of several megohms and R is usually small and so the dark current can be neglected. Then Eq.(3) becomes

$$\Delta G = \frac{\vartheta}{R\left[\frac{V r_o^2}{(R+r_o)^2} - \frac{\vartheta\, r_o}{(R+r_o)}\right]}$$

$$\Delta G = \frac{\vartheta}{(V-\vartheta)R} \qquad \text{- - - - - - - -} \quad (4)$$

since $\frac{r_o}{R+r_o} = 1$.

The above results will be used to calculate the photoconductivity of low and high resistivity semiconducting crystals in the next chapter.

CHAPTER 4

EXPERIMENTAL RESULTS AND DISCUSSION:

Introduction:

In this chapter, we present the results of an investigation of two-photon conductivity in GaAs (both low resistivity and high resistivity type) using Q-switched and mode-locked Nd;glass laser pulses. The two-photon conductivity in GaAs was then used to measure the second order intensity correlation of the mode-locked pulse train and estimate the picosecond pulse width. We also investigated the two-photon conductivity in $CdS_{.5}-Se_{.5}$ and the three-photon conductivity in CdS using mode-locked pulse excitation and the use of these effects in measuring the pulse width.

A. Two-photon conductivity in GaAs using Q-switched Nd:Laser:

The particular crystal used in the present investigation was an n-type GaAs crystal of thickness 0.28 mms doped with Oxygen (concentration $3X10^{14}/cm^3$) and having a resistivity of 2.4 cm. The crystal was exposed to Q-switched Nd:glass laser pulses of duration 60-80 nsecs and the maximum intensity was 10 MW/cm^2 . The experimental setup is shown in figure 6 . A dye Q-switched Nd:glass laser was used. The Q-switched laser pulse entered a pair of beam splitters through a flash lamp filter, an aperture and calibrated neutral density filters (to vary the intensity of radiation) .

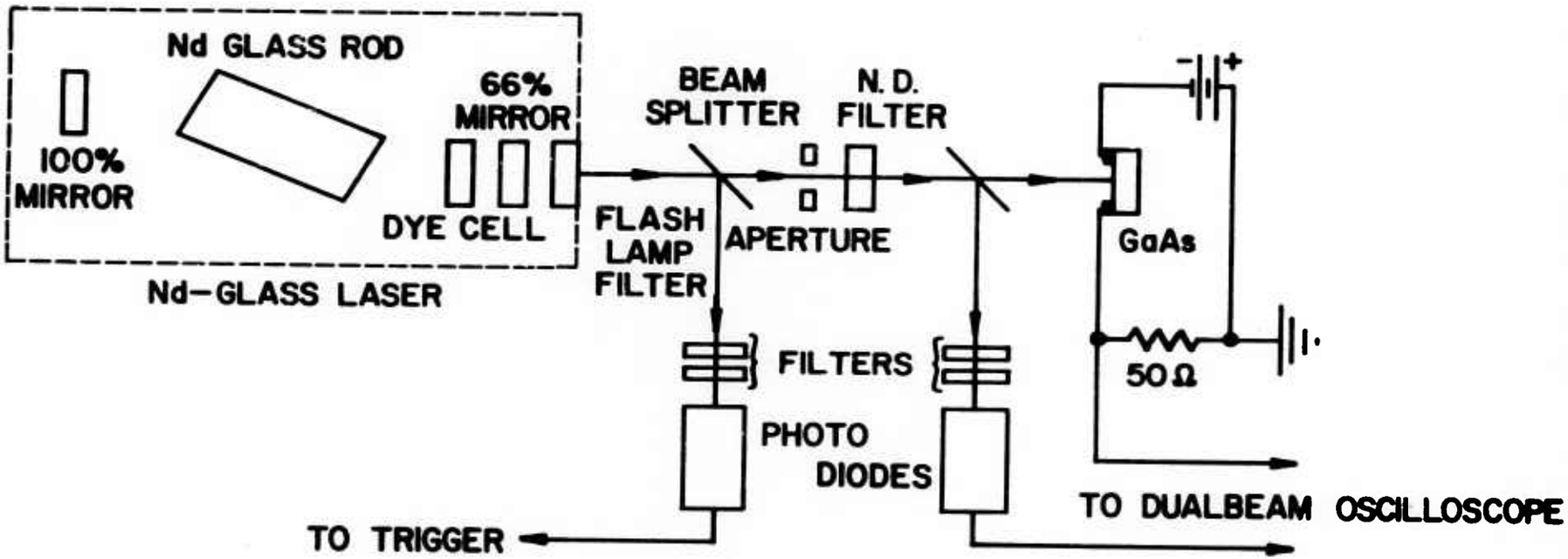
Nd GLASS ROD
100% MIRROR
66% MIRROR
DYE CELL
Nd-GLASS LASER
BEAM SPLITTER
N.D. FILTER
FLASH LAMP FILTER
APERTURE
GaAs
50 Ω
FILTERS
PHOTO DIODES
TO TRIGGER
TO DUALBEAM OSCILLOSCOPE

figure 6

Two photo diodes were used, one to trigger and the other to measure the intensity falling on the crystal. The GaAs crystal was connected in series with a 50Ω resistance to a battery. The change in voltage across the 50Ω resistance was fed to a dual beam oscilloscope along with the laser pulse from the photo diode. Polaroid camera was used to photograph the dual beam traces. The photoconductivity was computed from the change in voltage across the 50Ω resistance using Eq.(3) of chapter 3.

The measured photoconductivity ΔG in millimhos against laser intensity in Mw/cm^2 is shown in figure 7 in a log-log graph. The photoconductivity was measured over three decades of laser intensity .01 to 10 MW/cm^2. The result of two independent runs gave concordant results. In figure 7, we observe a break-in-slope between 1 and 2MW/cm^2 and this could be explained by the magnitudes of the one and two-photon absorption coefficients.

The one and two-photon absorption coefficients in the same crystal were determined by transmission measurements. We investigated the dependence of the intensity I_x of the light transmitted through the crystal on the intensity I_0 of the laser beam incident on the crystal. The intensity of light I_x at a depth 'x' of the crystal is written as

$$\frac{dI_x}{dx} = -\alpha I_x - \beta I_x^2$$

where α is the one-photon absorption coefficient in cm^{-1} and β is the two-photon absorption coefficient in cm/MW .

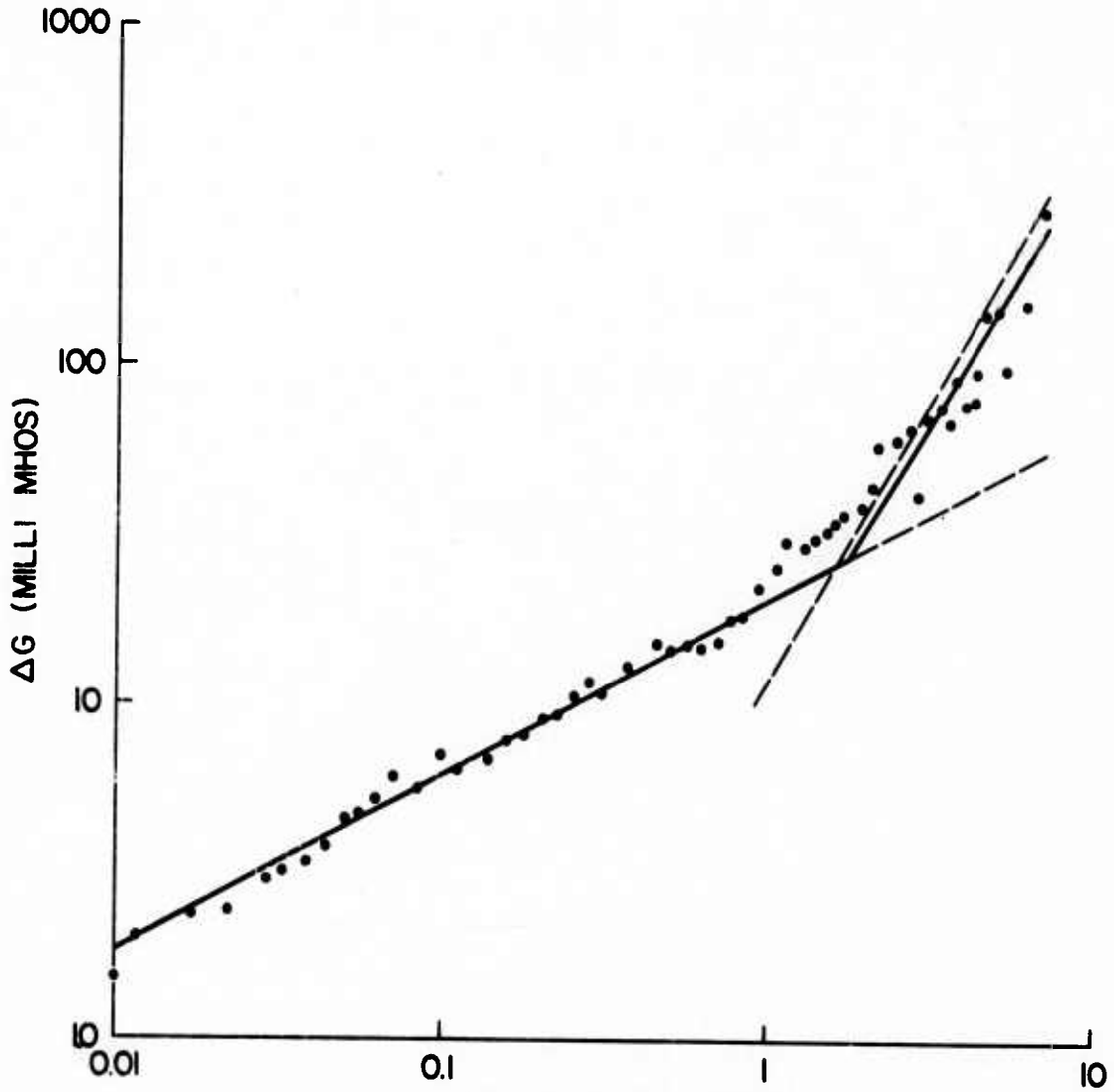

Q-SWITCHED PULSE EXCITATION
•—• EXPERIMENTAL
n-TYPE O_2 DOPED GaAs

FIGURE 7

The solution of this equation is of the form

$$I_x = \frac{I_s e^{-\alpha x}}{1 + \frac{\beta}{\alpha} I_s (1 - e^{-\alpha x})}$$

where I_s is the incident light intensity just inside the crystal surface. If R is the reflection coefficient for normal incidence,

$$\frac{I_o}{I_x} = \frac{e^{\alpha x}}{(1-R)^2} + \frac{(e^{\alpha x} - 1)}{1-R} \frac{\beta}{\alpha} I_o$$

The experimental arrangement is shown in figure 8 . We measured the incident intensity I_0 and the transmitted intensity I_x by calibrated photo diodes. The plot of I_o/I_x against I_0 is shown in figure 9 . A least square fit was made to the data points. Knowing the reflection coefficient R ($\simeq (n-1)^2/(n+1)^2$, n-refractive index of GaAs) and the thickness of the crystal x , we determined the value of α to be 2.5 cm^{-1} from the Y-intercept in figure 9 . From the slope of the line, the value of β was determined to be about 5.0 cm/MW. This value agrees fairly well with the computed value of 3.7 cm/Mw according to appendix 2 and Basov's [7] experimental value . The single photon absorption coefficient was also measured at 1.06 micron using a Cary Spectrometer and this gave a value of ~ 3 cm^{-1}.

EXPERIMENTAL SETUP FOR TWO PHOTON ABSORPTION COEFFICIENT MEASUREMENT

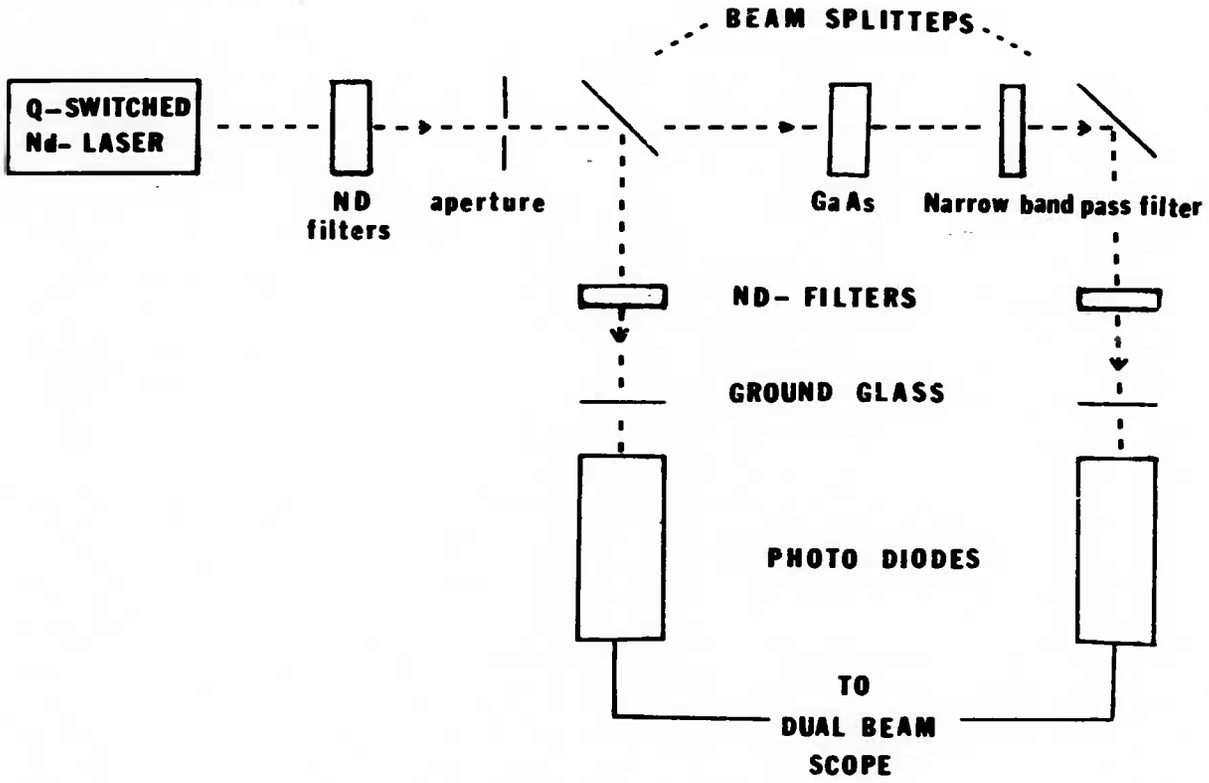

FIGURE 8

TWO PHOTON ABSORPTION COEFFICIENT MEASUREMENT

IN Ga As

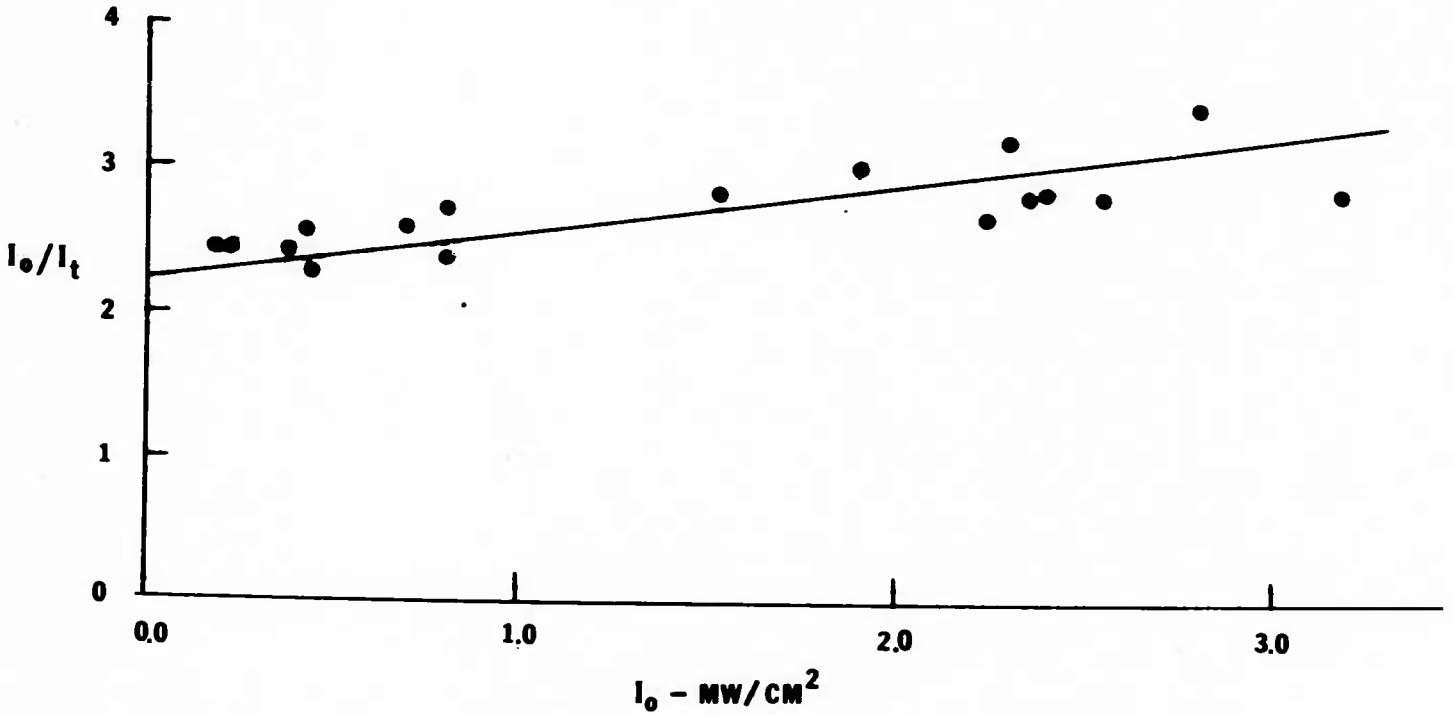

FIGURE 9

Now the break-in-slope observed between 1 and 2 MW/cm^2 could be explained. Below 1 MW/cm^2, the single photon process predominates and above 1 MW/cm^2, the two-photon absorption takes over. This agrees with the above values obtained for α and β. The two-photon absorption coefficient $K^{(2)} = \beta I_0$ (cm^{-1}) increases proportional to the intensity and is much greater than α above 1 MW/cm^2.

Below 1 MW/cm^2, the slope of the curve is less than unity and is approximately equal to 0.6 thus indicating the nature of single photon absorption, probably due to impurity levels. According to A.Rose[45], the slope of the photoconductivity curve between $\frac{1}{2}$ and 1 can possibly be explained by a continuous spectrum of levels in the forbidden band with an exponential energy dependence of the level density. As shown in Appendix 7, such a model gives an intensity dependent life time. Nearly the same slope has been observed by L.M.Blinov et al.[46] and R.H.Bube[47] in their photoconductivity experiments (one-photon absorption) with GaAs. Quite recently S.S.Li and C.I.Huang[48], in their investigation of recombination and trapping processes of photoinjected carriers in Cr-doped GaAs, found the life time of the carrier τ dependent on intensity as $\tau \approx I_0^{-\frac{2}{5}}$. This agrees with the slope 0.6 for ΔG versus I_0 in our experiment.

Above 1 MW/cm^2, the slope of the curve is more than doubled indicating the two-photon nature of the photoconductivity.

The impurity (single photon) conductivity line below 1 MW/cm^2 is extrapolated and is subtracted from the curve above 1 MW/cm^2 . The resulting photoconductivity is due to the true two-photon effect and the log-log plot against intensity is shown in figure 10 . A least square fit straight line to these points gave a slope of 1.85.

To effect a comparison of the experimentally observed two-photon conductivity with Jick Yee's theoretically calculated values, one requires the correct values of the mobility and the life time of the carriers. The mobility of the carriers is fairly well known for a given concentration. The life time τ for the calculation of steady state two-photon conductivity is estimated as follows:

The fairly longer laser pulse excitation results in reaching a steady state value of the photoconductivity. The photoconductivity decay curve gives an idea of the response time and the steady state life time of the carriers could be observed only if the laser excitation pulse width is smaller than the carrier life time. At lower intensities below 1 MW/cm^2 , the carrier life time depends on the laser intensity (continuously decreasing with increase of intensity according to A.Rose[45]; see Appendix 7) . However at high light intensities, where two-photon effects are observable, the carrier density increases rapidly because of intensity dependent absorption resulting in moving the Fermi level towards the conduction band very rapidly, and the crystal

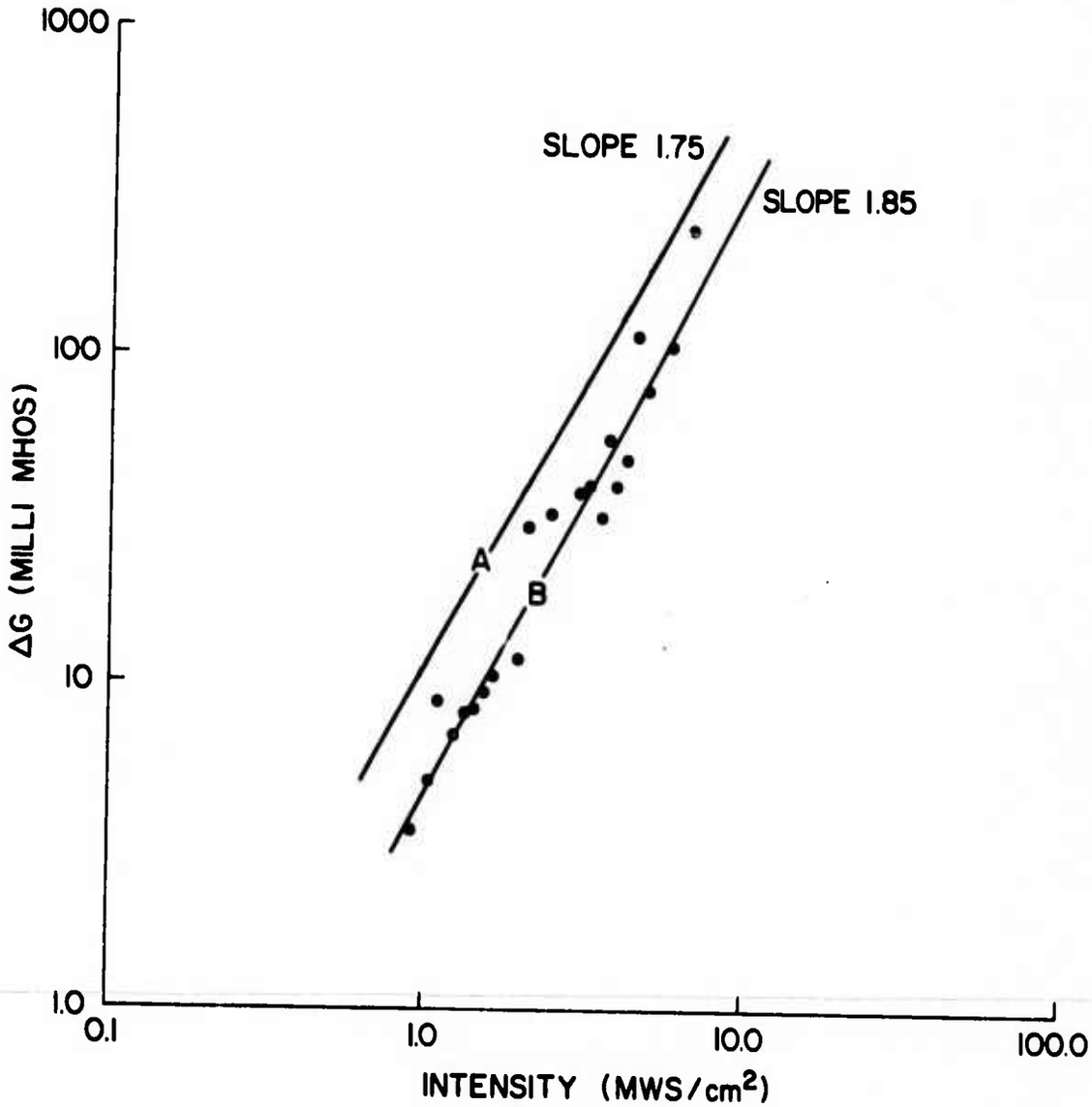

Q-SWITCHED PULSE EXCITATION
A – JICK YEE'S CURVE
B – EXPERIMENTAL CURVE
n-TYPE O_2 DOPED GaAs
CRYSTAL THICKNESS = 0.028 cm; MOBILITY = 7000 cm^2/v-sec
LIFE TIME ≈ 10^{-10} secs

FIGURE 10

behaves like a trap free semiconductor and so the life time remains essentially constant at higher intensities. To calculate the two-photon conductivity, one requires this constant life time and as an approximation the following estimation is done at 1 MW/cm^2 where two-photon effects are just observable. This estimation gives a slightly higher value of the life time resulting in an increase in the calculated value of the two-photon conductivity.

At approximately 1 MW/cm^2, where two-photon conductivity is negligible, the measured value of the single-photon conductivity is used to estimate the steady state life time of the carriers. Neglecting surface recombination, we get for single-photon conductivity

$$\Delta G = \frac{a}{c} q \mu I_0 \alpha L \tau_{st}$$

where α = single-photon absorption coefficient.

At $I_0 = 1$ MW/cm^2, $\Delta G = 0.02$ mhos

$L = 0.028$ cm, $\frac{a}{c} = \frac{1}{3}$, $\alpha L \approx 0.1$

$$\mu = 6500 \text{ cm}^2/\text{v-sec}$$

τ_{st}, the steady state life time of the carriers is estimated to give approximately 10^{-10} secs which agrees favourably with Blinov's value[46] ($\approx 5 \times 10^{-11}$ secs). Using this value of τ, the two-photon conductivity of GaAs is calculated using Jick Yee's expression (see Eq. (7) of chapter 2).

$$\Delta G = \frac{a}{c} q (\mu_e + \mu_p) \frac{\beta L I_o^2}{1 + \beta L I_o} \frac{\gamma}{2\hbar\omega}$$

$$\beta = 5 \text{ Cm/MW} \quad , \quad \mu_e + \mu_p \approx 7000 \text{ Cm}^2/\text{V-Sec}$$

$$\hbar\omega = 1.17 \text{ eV} \quad , \quad \frac{a}{c} = \frac{1}{3}$$

The theoretically calculated two-photon conductivity is also shown in figure 10 . The slopes of the experimental and theoretical lines are nearly equal thus indicating the two-photon nature of the excitation. The magnitude of the observed photoconductivity agrees well within an order of magnitude with the theoretically computed values. The observed discrepancy may be attributed to the inaccuracy involved in the estimation of life time and also to the non-uniformity of the beam distribution.

Thus we state that we have observed two-photon conductivity in GaAs and the magnitude of the same agrees within an order of magnitude with the theoretically calculated values. One may have some doubts that the same conductivity could be got by generation of non-phase matched second harmonic of Nd:glass laser radiation and subsequent single photon absorption. The following calculation precludes such a possibility.

The conversion efficiency for second harmonic generation is given by [41]

$$\eta_{SHG} = 2\left(\frac{\mu_o}{\epsilon_o}\right)^{3/2} \frac{\omega^2 d^2 \ell^2}{n^3} \frac{\sin^2(\Delta k \cdot \ell/2)}{\left(\frac{\Delta k \cdot \ell}{2}\right)^2} I_o \quad \text{---} \quad (1)$$

where $\left(\frac{\mu_o}{\epsilon_o}\right)^{1/2}$ = 377 ohms

ℓ = thickness of the crystal = 0.00028 meters

d = 12×10^{-22} mks units (non-linear susceptibility)

ω = 17.8×10^{14} radians/sec

$\hbar\omega$ = 1.17 ev

n^3 = 40

n = dielectric constant

$n^{2\omega} - n^{\omega}$ = 0.75

λ = 1.06 μm

$\frac{\Delta k \cdot \ell}{2}$ = 1250

$\Delta k = \frac{2\omega}{c}(n^{2\omega} - n^{\omega})$

For I_o = 10 MW/cm^2 , $\eta \simeq 10^{-6}$, $I_{2\omega} \simeq 1$ watt/cm^2.

$\alpha_{2\omega} \simeq 10^5$ cm^{-1}

From this we can calculate the absorption coefficient for such a process as $\beta_{2\omega} I_o \simeq 10^{-5}$ cm^{-1}. This absorption coefficient is negligible compared to the two-photon absorption coefficient we have observed above.

B. Two-photon conductivity in GaAs using mode-locked pulse Excitation:

In an actual experiment, where we may use this two-photon excitation of conductivity for picosecond pulse width measurement, the crystal has to be exposed to mode-locked laser pulses with higher individual pulse intensity. Therefore the photoconductivity with a mode-locked laser was investigated using two different types of GaAs crystals.

1. O_2-doped n-type GaAs (same as in section A)
2. Cr-doped high resistivity GaAs of thickness 0.033 cm and resistivity greater than 10^8 Ω cm.

The experimental arrangement was the same as in figure 6 except that we were using a mode-locked laser instead of a Q-switched laser. The response of the crystal (Cr-doped GaAs) to laser pulses is shown in figure 11. The upper most figure(a) was due to Q-switched pulse excitation. When the mode-locked pulse train (of picosecond pulses) was utilised as the excitation light source, the laser pulse and the photoconductivity signal as appeared on the 519 scope is shown in traces (b) and (c) of the same figure 11 . The photoconductivity signal clearly shows a similar periodic structure of the exciting pulse train. This indicates that the conductivity change responded rapidly to the excitation of an individual pulse in the train. In other words, the life time of the induced charge carriers is much less than the separation ($\frac{2L}{c}$ = 4.5 nsecs) between two adjacent pulses.

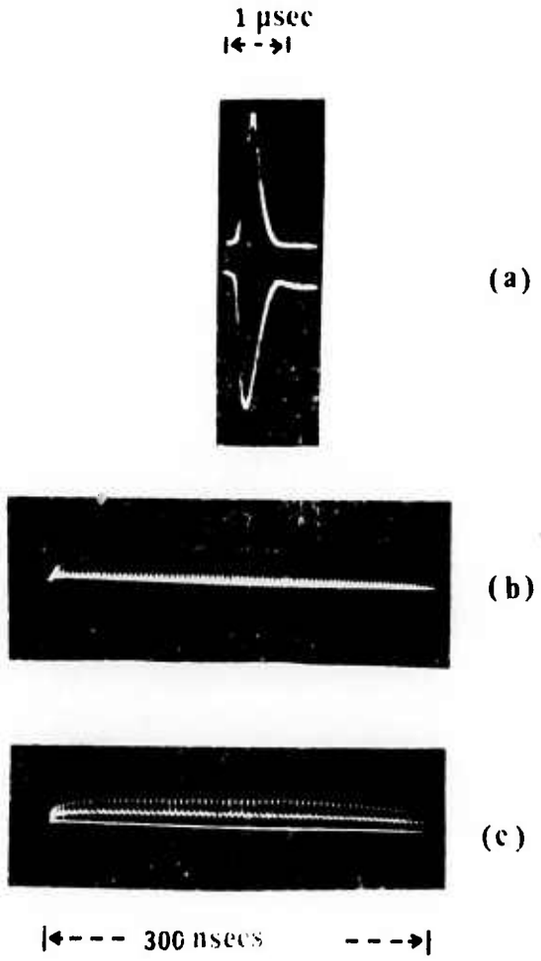

Figure 11

The estimate of the life time for the sample is of the order of 0.1 nsecs as shown in the previous section. Since the width of an individual pulse was a few picoseconds ($\sim$ 3 psecs TPF measurement), the effect shown in figure (c) should be of a transient nature. In figure 11. (c) one notices that the photoconductivity does not fall to zero between two adjacent pulses in the train. This was mainly due to the fact that the time response of the measuring circuit was not fast enough.

We concluded from this that the observed photoconductivity was in the form of spikes, each spike corresponding to single subnanosecond pulse of the mode-locked pulse train. It is evident that such a short pulse excitation produces non-equilibrium charge carriers dependent only upon the intensity of the short pulse and on the time width of the pulse. So the photoconductivity must be independent of all the recombination processes such as surface recombination, trapping etc. Since the individual pulse intensity is of the order of a few GW/cm^2, the two-photon absorption and the effect of higher order processes on the two-photon absorption could be studied at higher intensities of light. Further in the Q-switched case, We found that the GaAs crystal got the surface damaged when we exceeded 15 MW/cm^2. But in the case of mode-locked pulse train, the damage threshold is raised because of the shorter duration of the individual pulses.

The photoconductivity and the laser intensity were recorded as usual on the dual beam oscilloscope. Since the same amount of time resolution was introduced in both the channels, we could correspond the peak of the photoconductivity to the peak of the laser pulse. The photoconductivity of the two samples was investigated with mode-locked pulses in the peak intensity range of approximately a few MW/cm^2 to a few GW/cm^2 and a log-log plot of this versus relative intensity is shown in figure 12. Both curves display a slope of 2 in the low intensity region, changing to unity slope at higher intensities. If we compare the low intensity portion of the transient photoconductivity with that of figure 7 , we see a reduction in the magnitude of ΔG by a factor of approximately 100 . Since the picosecond pulses have higher peak intensity we start with a region of slope 2 . The transient two-photon conductivity, according to chapter 2 , is given by

$$\Delta G^{(2)} = \frac{a}{c} q (\mu_e + \mu_p) \frac{\beta_2 I_0^2 L}{1 + \beta_2 I_0 L} \times \frac{t_i}{2\hbar\omega} \qquad ----(2)$$

The over-all reduction in magnitude of ΔG comes from the fact that the pulse duration t_i enters in the expression for photoconductivity instead of the steady state life time of the carriers in the case of Q-switched excitation. t_i is approximately 100 times less than τ_{st}. This explains the reduction in the magnitude of ΔG in the case of mode-locked pulse excitation.

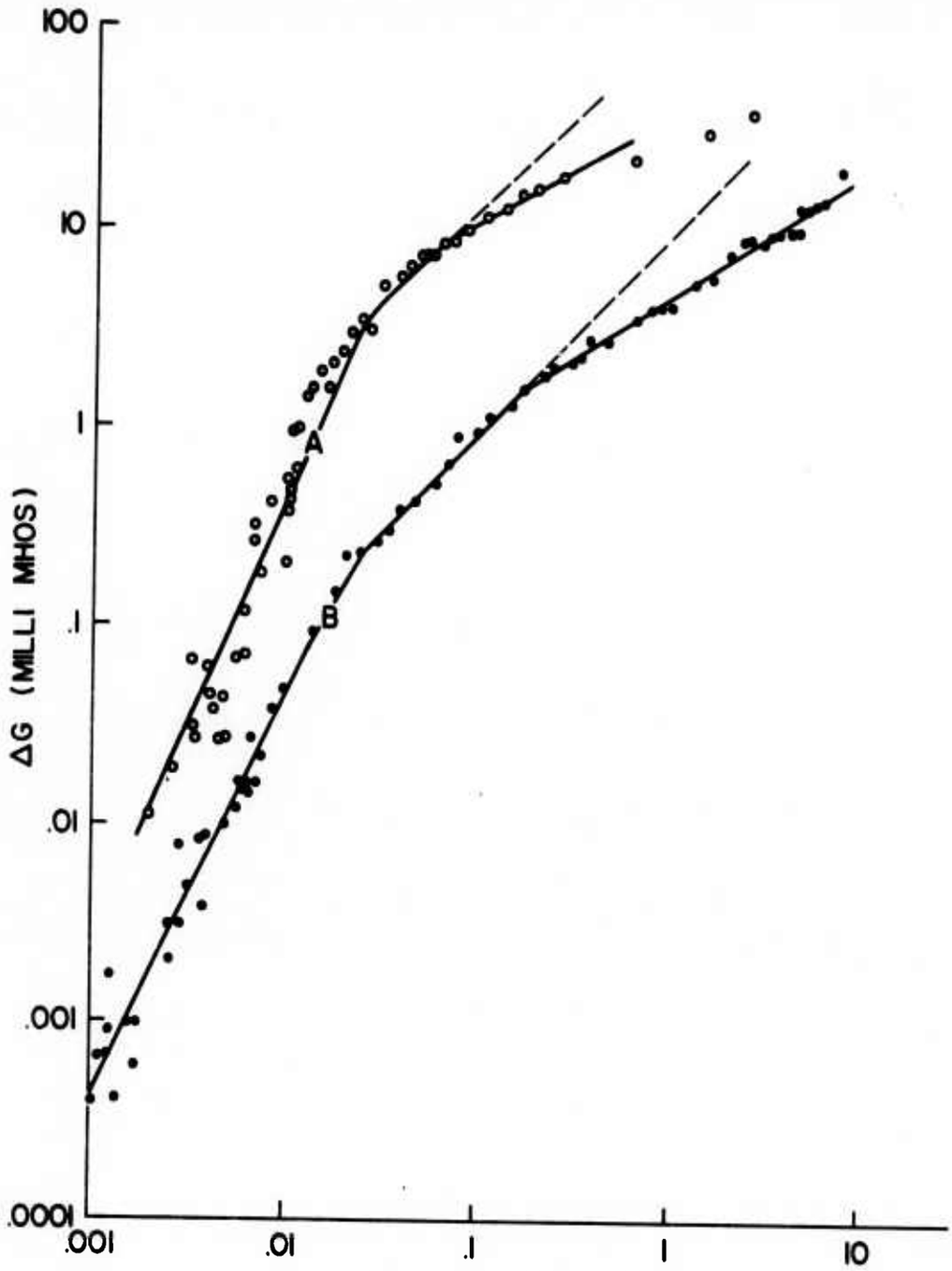

MODE LOCKED PULSE EXCITATION

EXPERIMENTAL PHOTO CONDUCTIVITY

A n-TYPE O_2 DOPED GaAs (.028cm THICK)
B Cr-DOPED SEMI INSULATING GaAs (.033cm THICK)

LIFE TIME $\tau >> t_1$ (pulse width) $\approx$ 1 p sec

FIGURE 12

The theoretical photoconductivity versus intensity is displayed on figure 13 in a log-log graph. Here also the slope is 2 at lower intensities and changing to unity at higher intensities.

$$\Delta G^{(2)} \propto \frac{\beta_2 L I_o^2}{1 + \beta_2 L I_o}$$

At lower intensities, $\beta_2 L I_o << 1$, $\Delta G^{(2)} \propto I_o^2$

At higher intensities, $\beta_2 L I_o >> 1$, $\Delta G^{(2)} \propto I_o$

As we see, the change of slope from 2 to 1 depends on the intensity I_o, β_2 and L . This also confirms the order of magnitude of the two-photon absorption coefficient $\beta_2 (\approx 5$ cm/MW) of the two samples. The low resistivity sample is of slightly lower thickness 'L' and so the change in slope occurs at a slightly higher intensity. Thus the experimental photoconductivity displays the two-photon nature of the excitation.

In the unity slope region, $\Delta G^{(2)} \propto \mu I_o$, the ratio of the conductivities in this region at a particular intensity gives the mobility ratio of the two semiconductors. The mobility ratio was found to be 30 . The mobility for the O_2-doped GaAs was 7000 cm^2/V-sec. This gives the mobility for Cr-doped GaAs 230 cm^2/V-sec. This value of the mobility was used for the calculation. Such a low mobility in Cr-doped GaAs can be explained by the compensated impurities in the high resistivity crystalas observed by Cronin and Haisty.[49] In the region of slope 2 , the conductivity ratio is proportional to the thickness ratio, β_2 ratio and the mobility ratio.

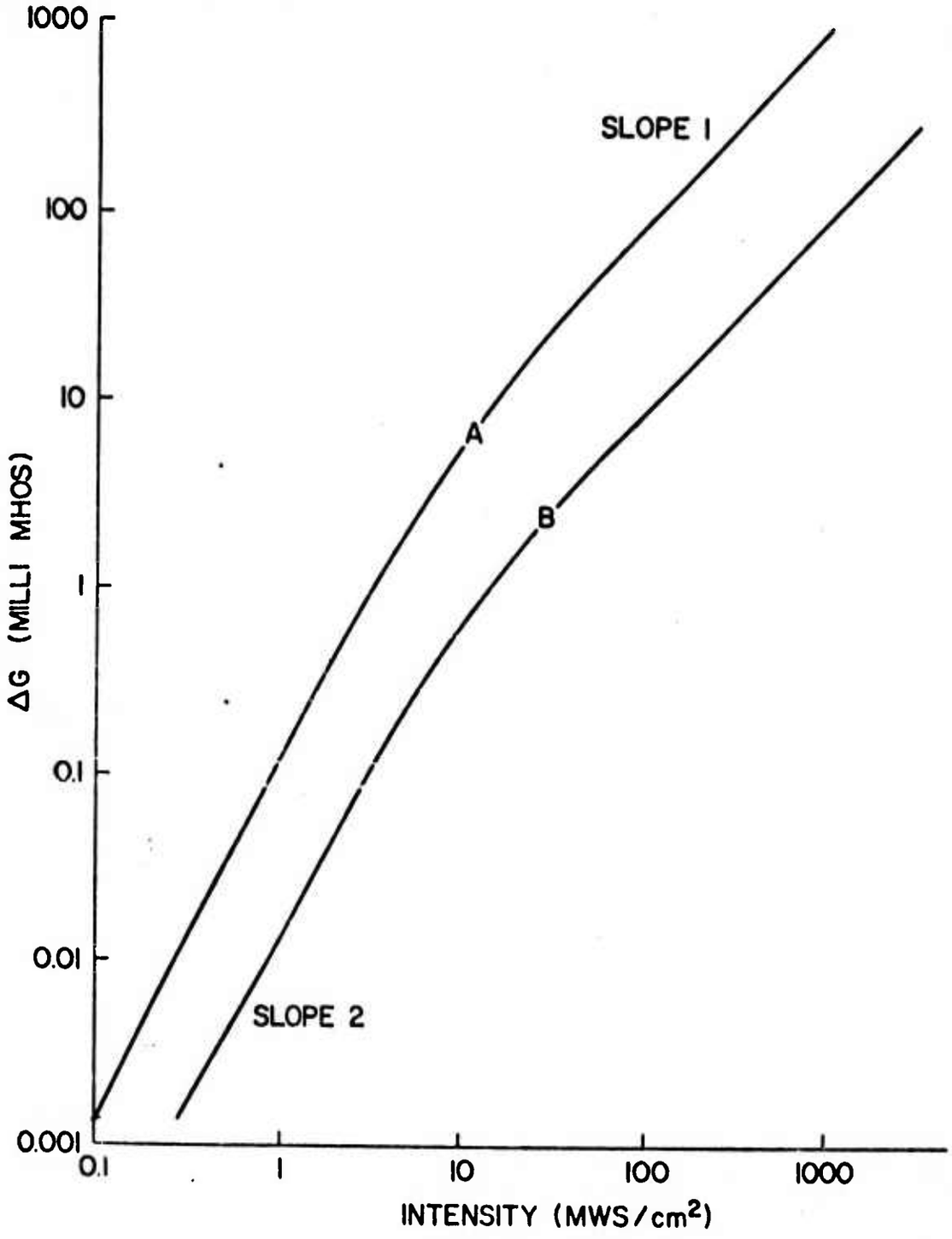

CALCULATED TWO PHOTON CONDUCTIVITY

A n–TYPE O_2 DOPED GaAs
(.028 cm THICK, $\mu_e + \mu_r = 7000$ cm²/v-sec)

B Cr–DOPED SEMI INSULATING GaAs
(.033 cm THICK, $\mu_e + \mu_r \approx 235$ cm²/v-sec)

LIFE TIME $\tau >> t_1$ (pulse width) $\approx$ 1 p sec

FIGURE 13 COMPUTED TWO PHOTON CONDUCTIVITY

Using the mobility ratio determined earlier, and the thickness ratio (0.028/0.033), the ratio of two-photon absorption coefficients in two different GaAs samples was found to be approximately unity. This gives a check on the measured β_2 values for the two samples. Since the intensity was not measured absolutely, the magnitudes of the photoconductivity could not be compared exactly.

Cr-doped GaAs crystal had a high dark resistance (10^9 ohms) and so we could measure the photoconductivity very accurately at higher intensities. At high intensities of light, the photoconductivity curve showed a sub-linear dependence as shown in figure 14 . If the conductivity is due to two-photon absorption alone, we should observe a slope of 1 at very high intensities as shown by the extrapolated linear dependence. The observed conductivity is less than the ideal extrapolated curve of slope unity. The following discussion proposes a possible mechanism for the sub-linear dependence at higher intensities.

The non-linearity is definitely not due to the surface recombination since the excitation is due to short pulse whose width is much less than the recombination times. Since conductivity is directly proportional to mobility, it was first suspected that mobility may decrease at high excitation levels because of electron-hole scattering. This decrease in mobility at high excitation levels in Si (4.2°K) was observed by A.A.Patrin et al[50]. The following discussion rules out

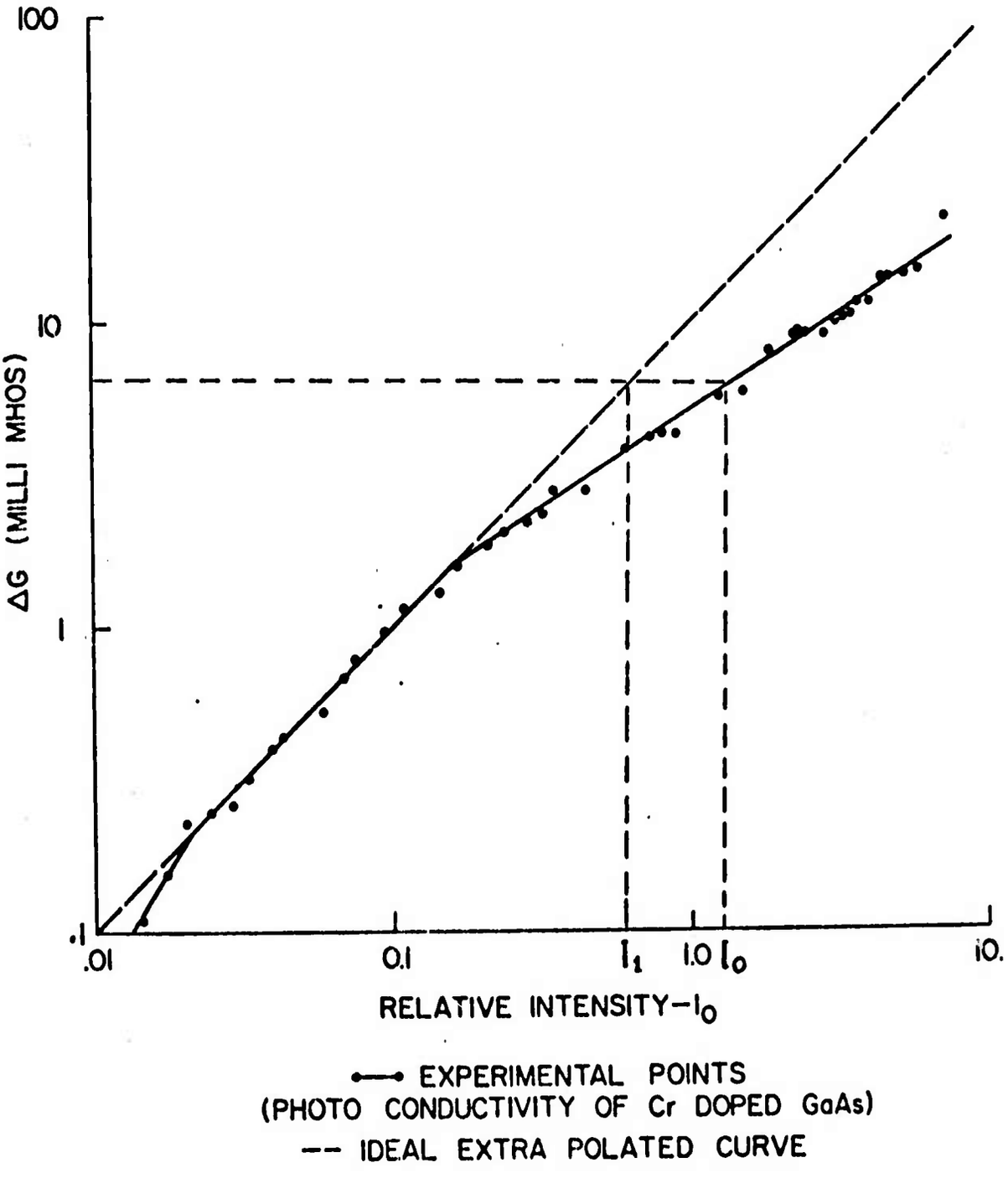

FIGURE 14: NON-LINEARITY IN THE PHOTO CONDUCTIVITY RESPONSE

this possibility in the present experiment.

At room temperature, the mobility in GaAs is determined by screened polar scattering and impurity scattering.[51] The room temperature mobility was found to be 230 cm^2/volt-sec as shown in the earlier section. When the crystal is excited by high intensity laser pulses, the density of non-equilibrium charge carriers increases. The contribution of mobility due to electron-hole scattering was calculated using the Brooks-Herring Formula.[52]

$$\mu_{e-h} = \frac{2^{7/2}\,\epsilon^2\,(kT)^{3/2}\,(m_e + m_h)^{1/2}}{\pi^{3/2}\,e^3\,(m_e m_h)^{1/2}\,(n_e n_h)^{1/2}\left[\ln(1+B) - \frac{B}{1+B}\right]} \qquad \text{---(3)}$$

Where

$$B = \frac{6\,\epsilon\,(kT)^2\,m_e\,m_h}{\pi\,\hbar^2\,e^2\,(m_e + m_h)\,(n_e n_h)^{1/2}}$$

ϵ = dielectric constant = 11.8

m_e = electron effective mass = 0.072 m

m_h = hole effective mass = 0.68 m

m = electron rest mass

e = electronic charge

k = Boltzmann's constant

T = absolute temperature

$\hbar$ = Planck's constant/ 2π

$n_e = n_h$ = carrier density (non-equilibrium)

At T = 300 K , the computed mobility μ_{e-h} at high carrier

densities of the order of 10^{18}/cc gave a value of 10^4 cm^2/V-sec. Mobilities combine approximately as

$$\frac{1}{\mu_{eff}} = \frac{1}{\mu_{normal}} + \frac{1}{\mu_{e-h}}$$

The normal mobility is low and so will not be affected by the electron-hole scattering mobility. Therefore the observed non-linearity is not due to electron-hole scattering.

The second possibility may be due to the stimulated free carrier absorption (free electron absorption) . The free electron absorption in GaAs[53] for a given concentration of 10^{17}/cc is approximately 0.03 cm^{-1} at 1 micron wavelength. So the stimulated free carrier absorption is low and the observed non-linearity is not due to this process.

The intervalley scattering of electrons to a low mobility valley is also ruled out since the scattering can occur only with the help of a phonon and the corresponding cross section must be low. The system can be considered as atwo level system and two-photon saturation can be considered. But the carrier concentration is very much low compared to the degeneracy population and so saturation of the transition is ruled out.

Another possibility is the coherent interaction of picosecond pulses with the two-photon absorbing medium.[54,55] Above a particular threshold intensity, the medium can exihibit self induced transparency[56] and because of this the pulse propagates with negligible absorption. Such self induced transparency could be observed only if the dephasing time of the population

inversion is much longer than the pulse width. This could happen only at low temperatures. Such a self induced transparency in GaAs at 77°K using Nd:glass laser pulses (of picoseconds duration) was observed recently.[57] They in fact observed negligible two-photon absorption above 50 MW/cm^2 upto 10 GW/cm^2. However at room temperature, the dephasing time is short compared to the picosecond pulse duration and they observed no self induced transparency but only regular two-photon absorption. Since our measurement is at room temperature, we could not explain this non-linearity by the above arguments.

The more likely possibility is that due to stimulated intra-valence band absorption. For III-V semiconductors, the absorption by free holes can be much larger than the free electron absorption. This is due to the presence of transitions between sub-bands V_1 and V_2 of the valence band. The intra-valence band absorption in GaAs with various p-type doping densities had been extensively studied by Braunstein[59] and Braunstein and Kane.[60] The hole absorption coefficient at 1 μm for the crystal doped with $10^{17}/cm^3$ is about 3 cm^{-1}. This absorption coefficient is due to the transitions between the light hole, heavy hole and split-off valence bands as shown in figure 1.

In the present case, at higher intensities of light, the non-equilibrium charge carriers are produced proportional to the light intensity and the associated stimulated absorption

by the non-equilibrium holes should also increase linearly with the light intensity. Referring to figure 14 , from the non-linear region, the absorption coefficient due to intra-valence band transitions was calculated as follows:

For a particular value of ΔG, the intensities I_1 and I_0 at the ideal slope 1 curve and the experimental curve are determined.

$$I_1 = I_0 e^{-\alpha L}$$

$$\alpha = \frac{1}{L} \ln \frac{I_0}{I_1}$$

L = thickness of the crystal.

α = absorption coefficient due to intraband absorption

The carrier density is proportional to I_1 and so α is plotted against I_1 in figure 15 in log-log graph. Again at lower intensities, α increases linearly with light intensity (carrier density) thereby showing that the non-linearity in the two-photon conductivity is due to stimulated intra-valence band absorption.

However at very high light intensities, α increases rather slowly. This means that part of the light intensity is being utilised in the generation of non-equilibrium charge carriers (contributing to conductivity) . The difference in absorption coefficient between the linear dependence and the sub-linear one in the α versus I_1 graph (figure 15) is plotted against relative intensity I_0 in a log-log graph in figure 16. The slope of 2 in figure 16 suggests that there is a generation mechanism whose absorption coefficient increases as the square of the light intensity. According to Eq.(2)of (of chapter 2) , for three-photon absorption the absorption

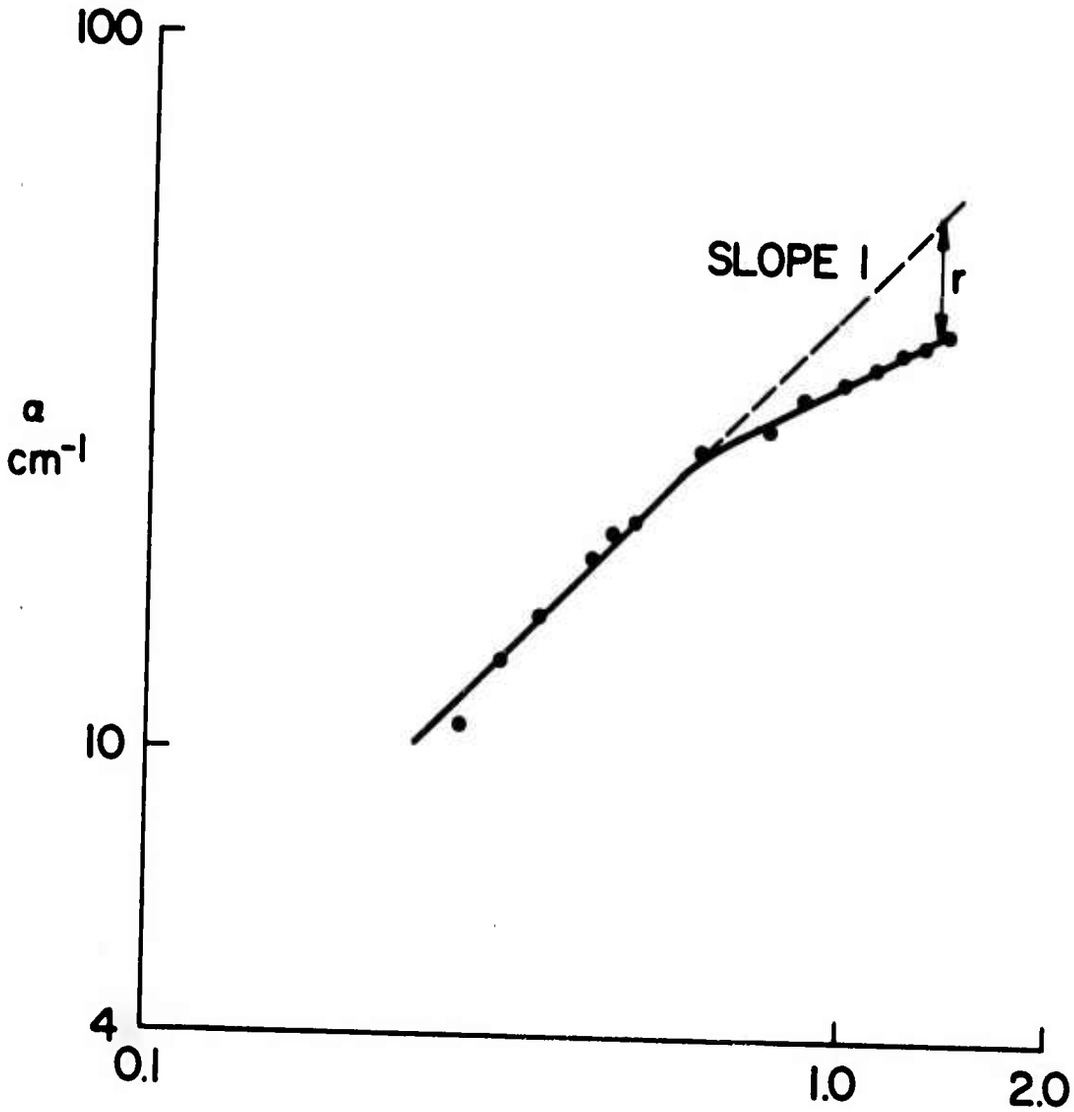

—●— EXPERIMENTAL DATA OF FREE HOLE ABSORPTION

--- EXTENSION OF LINEAR DEPENDENCE

FIGURE 15

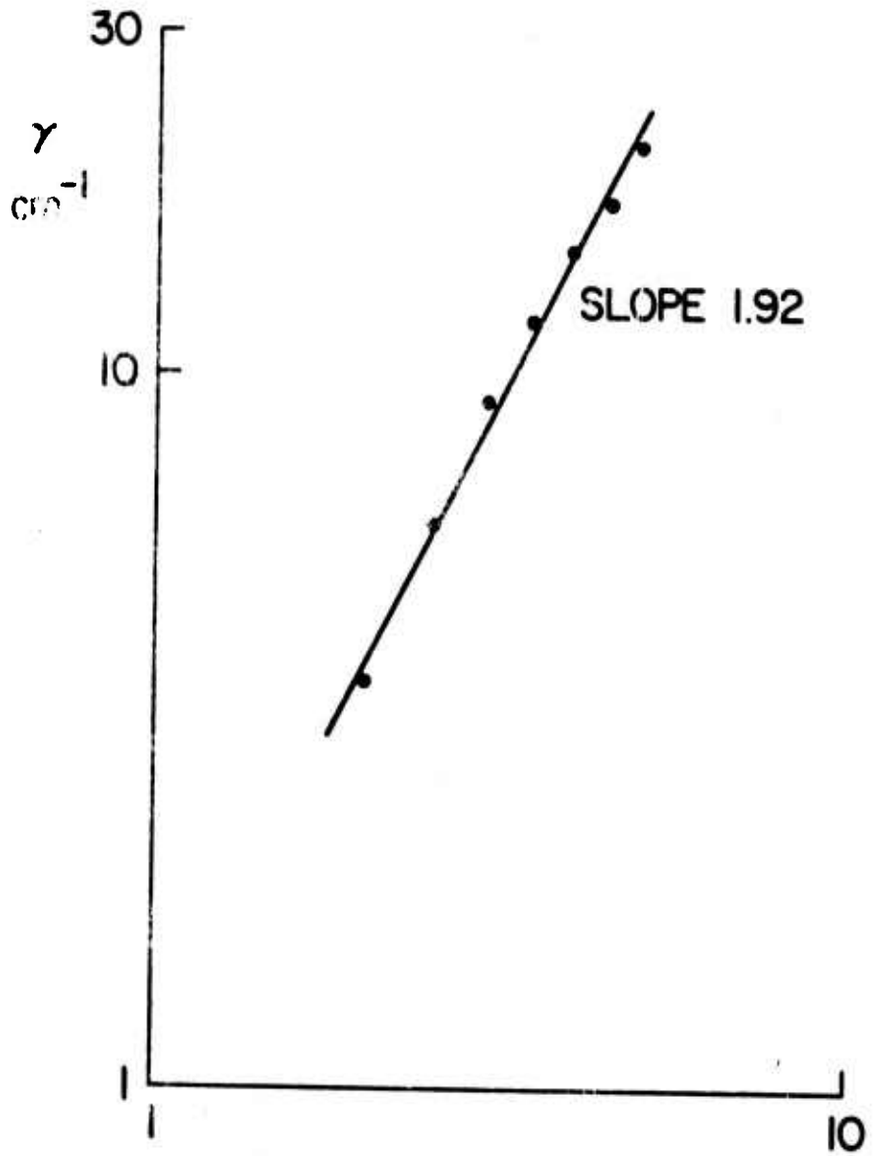
30
γ
10
SLOPE 1.92
1
1
10
RELATIVE INTENSITY–I_0
EXPERIMENTAL THREE PHOTON ABSORPTION COEFFICIENT

FIGURE 16

coefficient must be proportional to the square of the intensity of radiation. Hence we conclude that we have observed the three-photon generation of carriers in GaAs at very high intensities of light.

Referring to figure 12, the maximum intensity was approximately determined to be 5-10 GWs/cm^2 and the corresponding observed three-photon absorption coefficient was 20 cm^{-1}. Using the formula derived in chapter 2 (Eq.(2)) for three-photon band to band transitions in semiconductors and applying it to GaAs (transitions from $V_{1,2}$ to C) , we get for 5 - 10 GW/cm^2 of light intensity, a three-photon absorption coefficient as $\sim$ 14 cm^{-1} which agrees favourably with the experimentally observed values.

In conclusion, we state that we could easily observe two-photon absorption in GaAs with the use of mode-locked pulse train for excitation. Since we can go upto very high intensities, and since the two-photon absorption coefficient is large (5 cm/MW), we see that the two-photon conductivity is modified by thickness, stimulated hole absorption and three-photon absorption.

C. Measurement of Picosecond Pulse Width Using Two-photon Conductivity in GaAs:

The two-photon conductivity in GaAs (Cr-doped high-resistivity type) was investigated in the earlier section using a Nd:glass mode-locked laser. As we see from figure 12, the photoconductivity shows a square law dependence on the intensity of laser light in the lower intensity part of the graph. Such a square law could , in principle, be utilised to map the second order correlation function of the intensity of the laser pulse. This will give us a measure of the pulse width.

The experimental arrangement for the measurement of picosecond pulse width using two-photon conductivity in GaAs is shown in figure 17 . The mode-locked pulse train from a Nd:glass laser was partially reflected by a plane glass beam splitter onto an ITT photodiode the output of which was monitored on a 519 oscilloscope. Another beam splitter reflects part of the beam on a reference GaAs crystal through ND glass filters. The transmitted beam was attenuated by ND filters and then split into two equal components by a 50%-50% dielectric beam splitter. The two beams were then made to collide on a GaAs crystal using two dielectric reflectors. Both the reference and signal GaAs crystals were cleaved from a Cr-doped high resistivity GaAs wafer of thickness 0.33 mm. Indium solder was alloyed to the end faces of the crystals and ohmic contacts were thus established. Both the crystals were

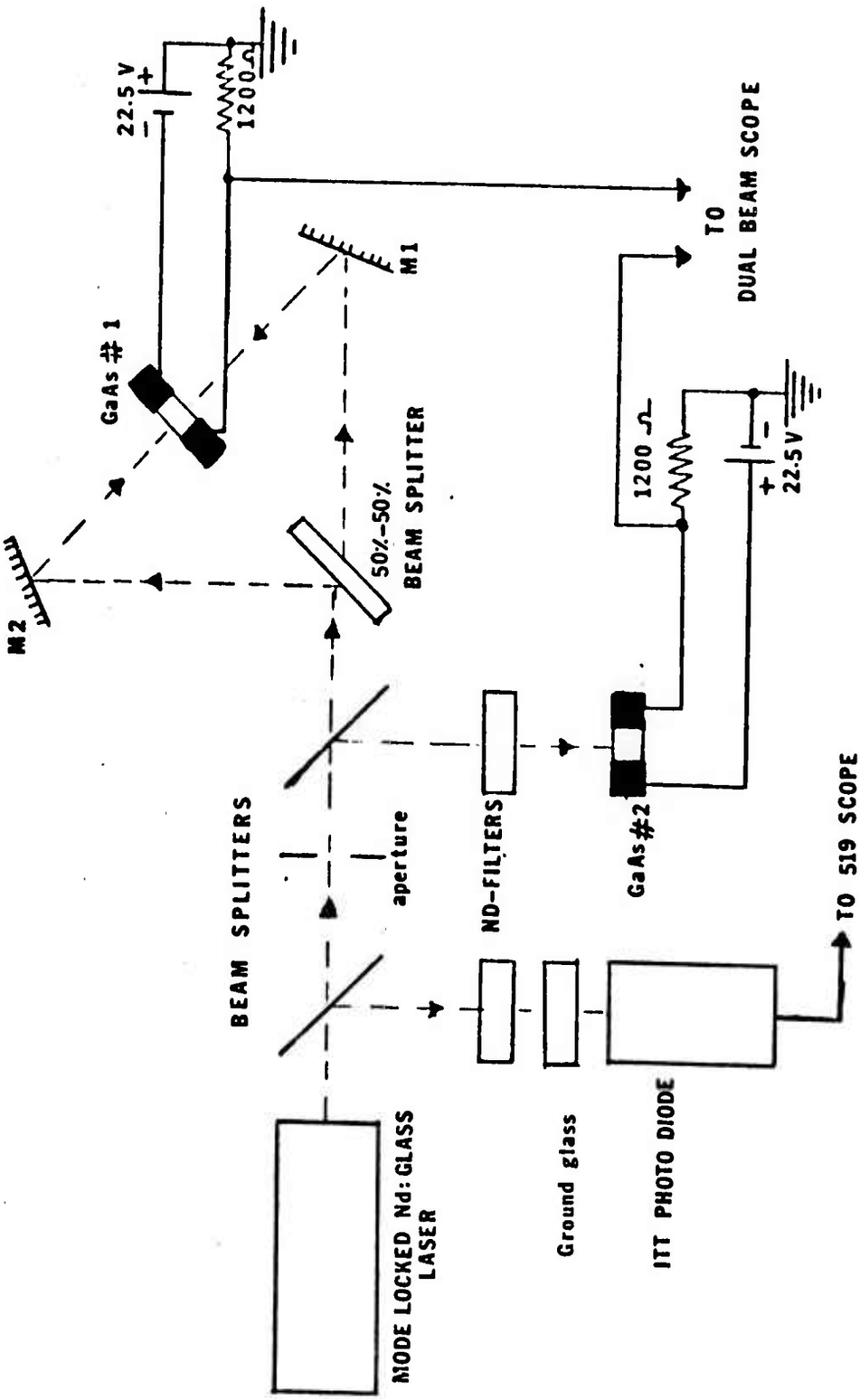
22.5 V
1200Ω
TO
DUAL BEAM SCOPE
M1
GaAs # 1
50%-50%
BEAM SPLITTER
M2
1200 Ω
22.5 V
BEAM SPLITTERS
aperture
ND-FILTERS
GaAs#2
TO 519 SCOPE
MODE LOCKED Nd:GLASS
LASER
Ground glass
ITT PHOTO DIODE

FIGURE 17

connected in series with a 1200Ω resistor through a 22.5 volts battery. The voltage developed across the resistance was monitored in a dual beam oscilloscope.

The mode-locked pulses were monitored on a 519 scope. Almost 80% of the shots gave a single neat pulse train, probably due to the contact dye cell used in the experiment. First, the slope two region of the two GaAs samples were confirmed. The ND filters were adjusted to keep the GaAs samples well inside the slope 2 region. The photoconductivity was calculated from the voltage 'υ' across the resistor R (1200Ω).

$$\Delta G = \frac{\upsilon}{V-\upsilon} \quad X \quad \frac{1}{R} \qquad , \qquad V = 22.5 \text{ volts}$$

In the slope two region, υ was of the order of 0.02 volts. Since $\upsilon \ll V$, ΔG is proportional to υ and so the voltage measured on the oscilloscope can be taken as a measure of the two-photon conductivity (TPC) . The crystal GaAs #1 monitored the photoconductivity produced by the overlap of the pulse with itself while the crystal GaAs #2 monitored the photo-conductivity due to a single passage of the short pulses, thereby providing the usual reference signal. The TPC pattern was scanned by moving the crystal #1 along the direction M_1 to M_2 and plotting the ratio of the pulse height from sample #1 to that from sample #2 as a function of distance. The result is shown in figure 18. Ratios obtained have been normalised to unity in the wings to conform with units defined reference (38) where the TPC yield due to a single pass was assigned a value of $\frac{1}{2}$. Only data points for which a single

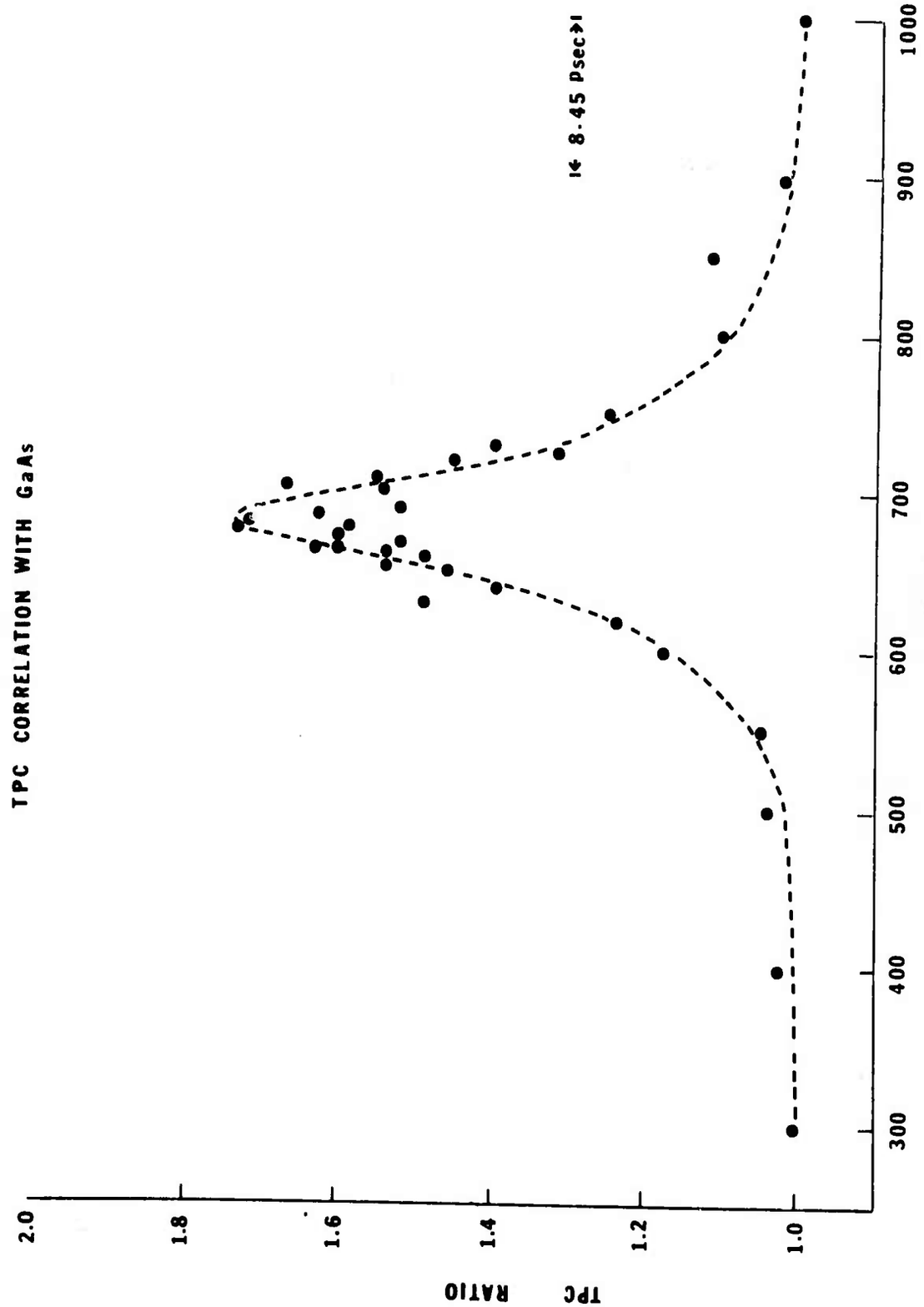
TPC CORRELATION WITH GaAs
8.45 Psec
TPC RATIO
2.0
1.8
1.6
1.4
1.2
1.0
300
400
500
600
700
800
900
1000
MILS

FIGURE 18

neat mode-locked pulse train was monitored on the 519 scope were plotted on the graph. Each data point was an average of 8 to 10 shots.

The contrast ratio for two-photon conductivity was shown to be 3 in chapter 2 . As we see in figure 18 , we get a contrast ratio of 1.8 only. This is because of the limited resolution of the crystal and partly because of the narrow slope two region of the samples. The thickness of the crystal is 0.33 mms and this corresponds to a resolution of $\sim$ 4 psecs ($\frac{t}{c} \times n$, $n = 3.4$, $c = 3 \times 10^{10}$ cm/sec). The half width of the curve approximately gives 8-10 psecs for the width of the pulse.

To effect a comparison with the Two-Photon Fluorescence (TPF) measurement, the TPF contrast ratio as obtained by Duguay et al.[34,39] for a mode-locked and a free running or a Q-switched laser is shown along with our measurement in figure 19. As seen in figure 19, the experimental points more or less follow the TPF curve for a mode-locked laser, not that of a free running or Q-switched laser. If we sample and integrate Duguay's curve over 4psecs at various points of the curve, we would expect the TPC or TPF curve with approximately 1.8 contrast ratio. Normally an ideal TPF for Nd:glass laser mode-locked pulses exhibits a peak contrast ratio 3 and a value of the contrast ratio 2 at the shoulder. The shoulder is broader compared to the peak portion. This structure is understood to have been caused by a model for

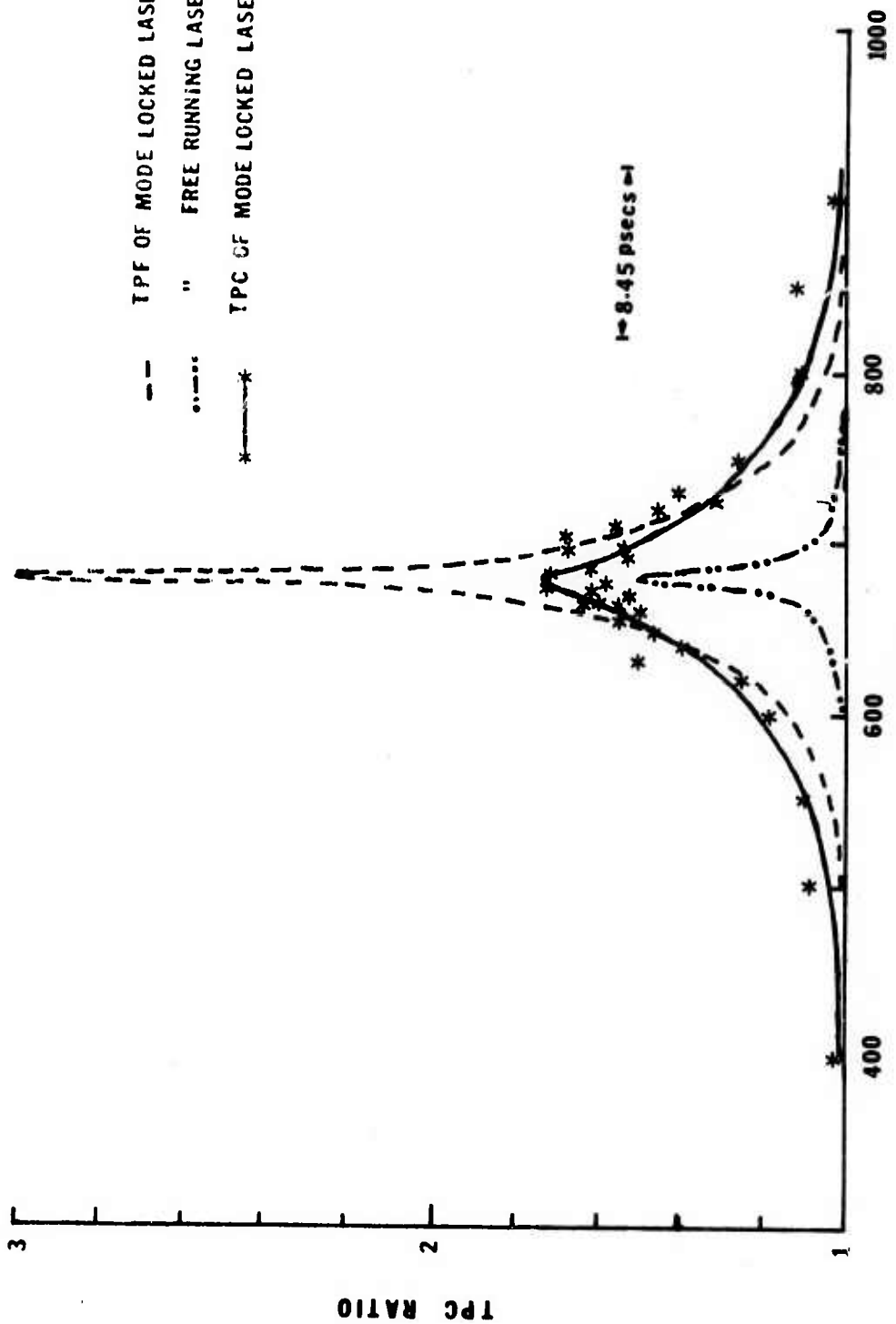
TPF OF MODE LOCKED LASER
" FREE RUNNING LASER
TPC OF MODE LOCKED LASER
8.45 psecs
TPC RATIO
3
2
1
400
600
800
1000
MILS

FIGURE 19

for the picosecond pulses in the form of a smooth Gaussian ensemble (giving rise to the broad shoulder in the correlation curve) with fluctuating substructure with a spectral content of about 100 cm^{-1} and amplitude fluctuations in a time scale corresponding to the inverse of the oscillating bandwidth. So we may miss the narrow region from shoulder to peak when we use a crystal of limited resolution.

Thus we show in principle that the two-photon conductivity can be used to measure the width of the picosecond pulses. We measured the autocorrelation of the pulse intensity using two-photon conductivity in GaAs which yielded the same shape of the curve as got by Duguay[39] but with a reduced contrast ratio of $\sim$ 1.8 because of limited resolution of the detector.

D. Two-Photon Conductivity in $CdS_{.5}$-$Se_{.5}$:

$CdS_{.5}$-$Se_{.5}$ is a II-VI semiconductor and has a forbidden energy gap of 2.0 ev[18] at room temperature. With a Nd:glass laser, the photon energy is 1.17 ev and so it is possible to excite electrons from the valence band to the conduction band by simultaneous absorption of two photons. Two-photon induced photoconductivity was indeed observed in CdS_x-Se_{1-x} crystals by V.S.Dneprovskii et al.[10] using a Q-switched ruby laser. M.S.Brodin et al.[18] measured the two-photon absorption coefficient in CdS_x-Se_{1-x} for various 'x' values using a Q-switched ruby laser. None of these experiments was done with Nd:glass laser. The mode-locked pulse train from Nd:glass laser consisted of shorter picosecond pulses with higher peak intensity and so should get absorbed in a two-photon process. The photoconductivity due to such a process was not studied before. We saw in the earlier section that GaAs had a higher two-photon absorption coefficient and so for a given thickness, saturation sets in at relatively low intensities. We were limited with a smaller square law region and this was part of the reason for the lower TPC contrast ratio in the picosecond pulse width measurement. In the case of $CdS_{.5}$-$Se_{.5}$, we get a theoretical value of $\beta_2 \simeq 0.14$ cm/MW (see Appendix 3) and since this value was smaller than that of GaAs by approximately 50 times, we expected a better square law region, extending over more than two decades of excitation intensity which would facilitate

the measurement of picosecond pulse width. So we decided to investigate the two-photon conductivity in $CdS_{.5}$-$Se_{.5}$ using mode-locked Nd:glass laser pulses.

The particular crystal used in the present experiment was a single crystal high resistivity wafer of $CdS_{.5}$-$Se_{.5}$ made by Gould Inc. The crystal had a thickness of 0.23 mms. A small crystal of 3 mm x 1 mm area was chosen and ohmic contacts were made to the end faces by alloying with Indium. The experimental arrangement for the measurement of photoconductivity was the same as before (figure 6). The mode-locked pulse train consisted of picosecond pulses (5-9 psecs wide) spaced at 4.5 nsecs over 300 -600 nsecs. The intensity incident on the crystal was varied using calibrated ND glass filters. The photoconductivity was estimated as before from the change in voltage 'v' across a resistance 'R' (127 Ω) which was connected in series with the sample to a battery 'V', using the relation

$$\Delta G = \frac{v}{(V - v) \times R}$$

In figure 20, we see the oscilloscope traces of photovoltage 'v' and laser intensity from a photo diode. Figure 20 (a) shows the traces in the dual beam oscilloscope. One can see the photo voltage following the mode-locked laser pulse train. This is confirmed by the other two traces (b) and (c). So the photo-conductivity responded to the individual pulses in the mode-locked pulse train. We could only see the slight wiggling in the photo signal and this was partly due to the slow response of the detector circuit. So the photo voltage peak corresponded to the peak of the laser pulse in the dual beam scope.

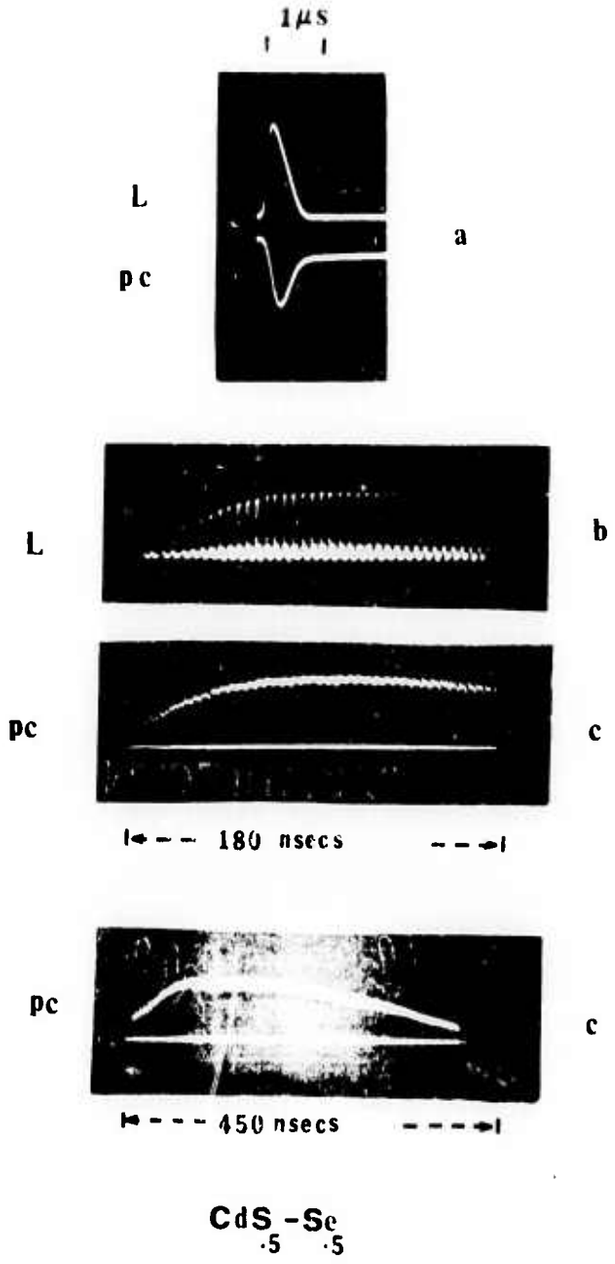

Figure: 20 - Oscilloscope traces of Photo voltage versus laser pulse

The photoconductivity ΔG in millimhos versus relative laser intensity is shown in figure 21. A least square fit was made and the slope was found to be 2.2. This indicated a power law of $\sim I_c^{2+0.2}$, characteristic of a two-photon process. We estimated the two-photon absorption coefficient from the measured photoconductivity. The two-photon conductivity for a transient process can be written as (see chapter 2 , Eq.(9)),

$$\Delta G^{(2)} = q \frac{a}{c} (\mu_e + \mu_h) \frac{t_i}{2\hbar\omega} \frac{\beta_2 I_o^2 L}{1+\beta_2 I_o L}$$

When $\beta_2 I_o L \ll 1$, we get $\Delta G^{(2)} \propto I_o^2$. This explains the square law observed in the experiment. To estimate β_2, we had to know the peak intensity of the pulse I_o, the pulse width t_i, the mobility and the geometric factor'a/c'. a/c was 1 in the present experiment. Since the crystals were of compensated high resistivity type, the mobility could not be measured accurately by the manufacturer and so the mean mobility in CdS and $CdS_{.5}$-$Se_{.5}$ of 400 cm^2/v-sec [62] was assumed. We measured the total energy of the laser pulse train by a calorimeter. The TPF photograph using 10^{-3} molar solution of Rhodamine 6G in ethanol gave a value of $t_i \sim 5$ psecs without measuring contrast ratio. From the pulse width and the energy of the peak pulse, the peak intensity I_o was determined. The thickness of the crystal 'L' was 0.023 cm. Approximately 0.3 GW/cm^2 corresponded to a value of $\Delta G^{(2)} \sim 80$ millimhos. From the expression for $\Delta G^{(2)}$, $\beta_2 I_o$ was estimated to be

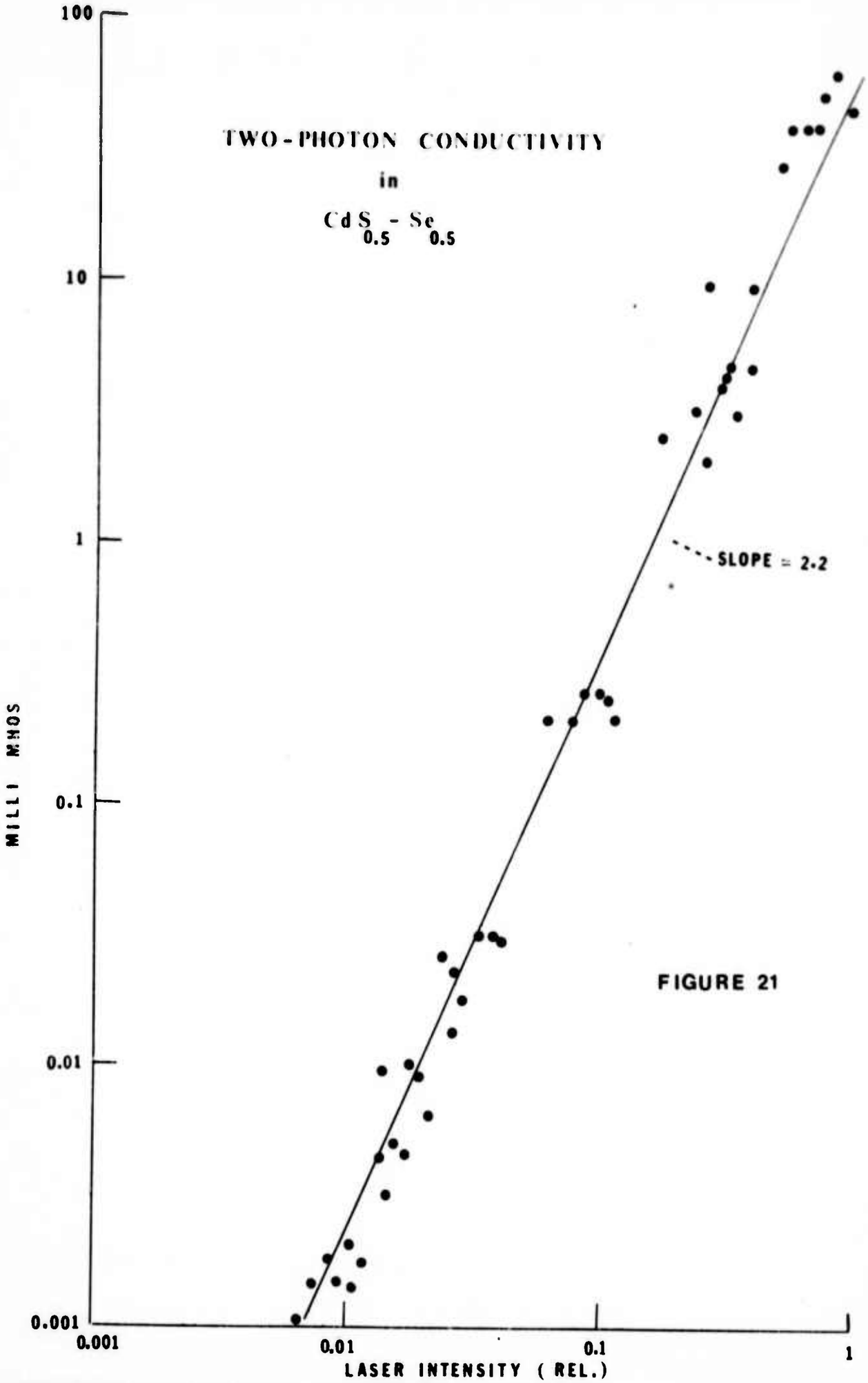
TWO-PHOTON CONDUCTIVITY
in
$CdS_{0.5}Se_{0.5}$
SLOPE = 2.2
MILLI MHOS
100
10
1
0.1
0.01
0.001
0.001
0.01
0.1
1
LASER INTENSITY (REL.)

FIGURE 21

20 cm^{-1}. For $I_0 = 300$ MW/cm^2, β was found to be 0.07 cm/MW. When we reduce the value of Brodin's[18] measurement for Nd:glass laser, they get a value of 0.15 cm/Mw for $CdS_{.53}$-$Se_{.47}$. The theoretical calculation for a single valence band to conduction was found to give (see appendix 3) 0. 4 cm/MW. Our experimental value thus agrees in order of magnitude with the theoretical value and the one measured by Brodin et al.[18]

A similar square law dependence could be obtained if second harmonic of the Nd:glass laser was generated in non-phase matched $CdS_{.5}$-$Se_{.5}$ and subsequently absorbed by single-photon absorption. We could calculate the absorption coefficient $\beta_{2\omega}$ in cm/MW for such a process. The conversion efficiency for second harmonic generation is given by (see Eq.(1) of the same chapter)

$$\eta_{SHG} = 2 \left(\frac{\mu_0}{\epsilon_0}\right)^{3/2} \frac{\omega^2 d^2 \ell^2}{n^3} \frac{\sin^2(\Delta k \cdot \ell/2)}{(\Delta k \cdot \ell/2)^2} I_0$$

$$\left(\frac{\mu_0}{\epsilon_0}\right)^{1/2} = 377\ \Omega$$

$$\ell = 0.00023 \text{ meters}$$

$$d = 1.5 \times 10^{-22} \text{ mks units}\ [41]$$

$$\hbar\omega = 1.17 \text{ ev}$$

$$n^3 = 27 \quad , n_{2\omega} - n_{\omega} = .329$$

$$\frac{\Delta k \cdot \ell}{2} = 430 \qquad -- \quad -$$

For $I_0 \simeq 100$ MW/cm^2, $\eta \approx 10^{-7}$, $\therefore$ $I_{2\omega} \approx 10^{-5}$ MW/cm^2.

$\alpha_{2\omega} = 10^5\ cm^{-1}$; From this we find $\beta_{2\omega} \approx 10^{-5}$ cm/MW . This value is negligible compared to the two-photon absorption coefficient observed in our experiment.

So in conclusion, we state that we observed two-photon conductivity in $CdS_{.5}$-$Se_{.5}$ using mode-locked Nd:glass laser pulses and found that the photoconductivity exhibited a square law dependence on intensity over a much wider range than in GaAs. The magnitude of the twophoton absorption coefficient agreed favourably with the theoretical and other experimental values. Measurement of picosecond pulse width using this square law region of $CdS_{.5}$-$Se_{.5}$ is described in the next section.

E. Measurement of Picosecond Pulse Width Using $CdS_{.5}$-$Se_{.5}$:

In section D , we saw that the photoconductivity of $CdS_{.5}$-$Se_{.5}$ when excited by mode-locked Nd:glass laser pulses, showed a power law $\Delta G^{(2)} \propto I^2$. Such a square law could be used to measure the second order intensity correlation function of the picosecond pulses and hence estimate the pulse width.

The experimental arrangement was similar to figure 17 where we used $CdS_{.5}$-$Se_{.5}$ samples instead of GaAs. The TPC pattern was scanned by moving the crystal #1 along the direction M_I to M_2 and plotting the ratio of pulse height from sample #1 to that from sample #2.as a function of distance. Here also $\Delta G^{(2)} = \frac{v}{(V-v)\cdot R}$; Since 'v' was much smaller than V, the change in voltage across R was taken to be a measure of photoconductivity. The TPC ratio at the wings was normalised to unity. The TPC ratio as a function of distance moved is shown in figure 22(a). Here the contrast ratio is ~ 2.4 . Comparing the results we obtained with GaAs, we see that $CdS_{.5}$-$Se_{.5}$ gives a better contrast ratio. This was partly because of the improved resolution (~ 2 psecs) of the detector and partly due to a very wide square law region. The half width of the TPC curve gives 8 - 10 psecs for the width of the pulse.

Figure 22(b) represents the above TPC curve along with Duguay's[39] TPF pattern when integrated over a 2 psecs detector. We see that the general pattern of the TPC curve agrees with Duguay's curve except we get a slightly broader base. This may be due to a broadened pulse in our laser.

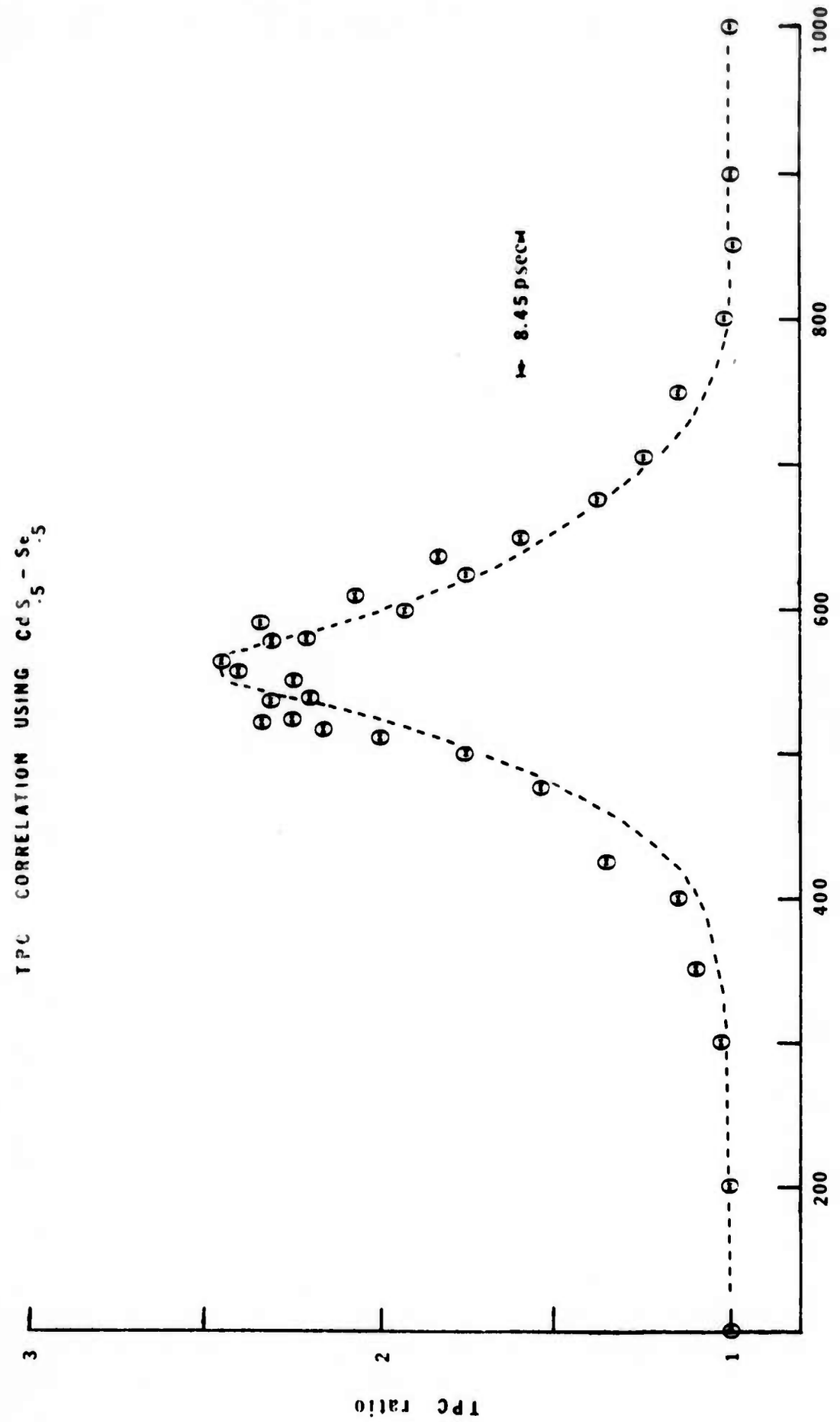
TPC CORRELATION USING CdS.5 - Se.5
8.45 psec
TPC ratio
3
2
1
200
400
600
800
1000
MILS

FIGURE 22 a.

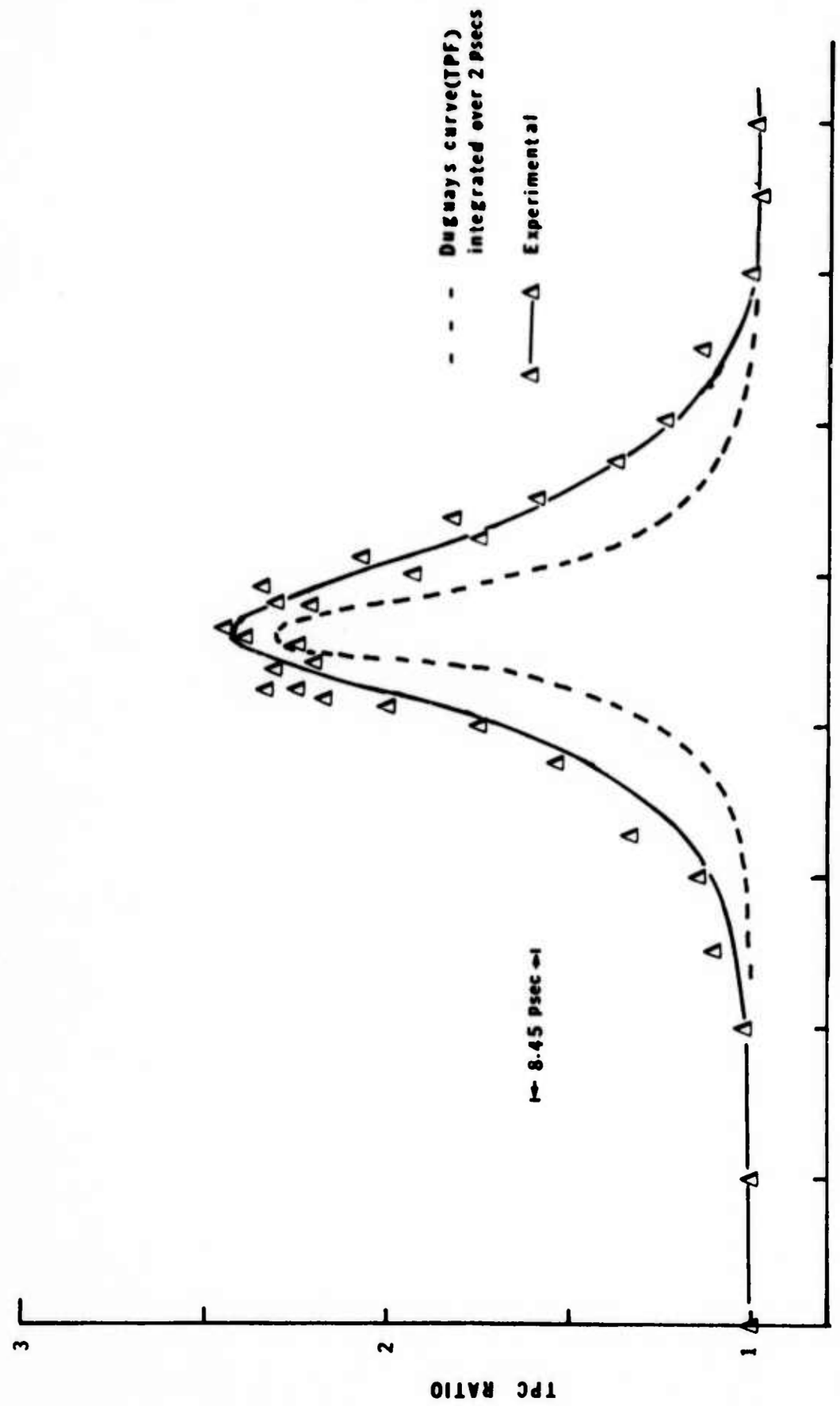
Dugways curve(TPF)
integrated over 2 μsecs
Experimental
8.45 μsec
TPC RATIO
MILS
1
2
3
200
400
600
800

FIGURE 22 b.

In conclusion, we state that two-photon conductivity can be used to measure the picosecond pulse width. Since $CdS_{.5}Se_{.5}$ exhibited a smaller absorption coefficient than GaAs, and consequently had a better square law region of conductivity, $CdS_{.5}Se_{.5}$ proved to be a better two-photon semiconductor for the measurement of second order intensity correlations of the picosecond pulses.

F. Three-Photon Conductivity in CdS:

CdS is a II-VI semiconductor with a forbidden energy gap of 2.42[62] ev at room temperature. With a Nd:glass laser of photon energy 1.17 ev, it is possible to measure three photon absorption. B.M.Ashkinadze et al.[22] detected the luminescence emitted by CdS at 77 K after three-photon absorption of a Q-switched Nd:glass laser. They observed the luminescence when the excitation intensity was varied between 20 and 100 MW/cm^2. Since they were using a Q-switched laser, they had to focus it to get higher intensities to observe this third order process. With the availability of mode-locked Nd:glass lasers, it is possible to produce upto a few GW/cm^2 without focussing. Further because of the high peak power, the higher order absorption processes could be easily observed in the case of picosecond pulse excitation. Another advantage of using picosecond pulses for the investigation of higher order non-linear optical effects is to raise the damage threshold because of the short time duration of the pulses. In the present section, we present an investigation of the three-photon conductivity in polycrystalline and single crystal CdS at room temperature using a mode-locked Nd:glass laser.

The polycrystalline CdS was a commercially available photoconductive cell (CL 902 type 2 CdS) made by the Clairex Corporation. The cell has a spectral peak at 5150° A (2.42 ev) The single crystal CdS is of high resitivity type made by

Gould Inc . Both the samples were alloyed with Indium at the end faces which served as ohmic contacts. Both the samples had a dark resistance of well over several megohms. We enclosed the samples in a box and cut off the light from the flash lamp and other sources using optical filters which cut off light other than 1.06 micron laser beam. This protection of shielding the sample from stray light was necessary since the CdS is sensitive to ordinary light. The CdS photoconductive sample was connected to a 22.5 volts battery through a 127Ω resistor. The voltage across this resistance was monitored and measured on a dual beam scope along with the laser pulse from an ITT photo diode. The mode-locking of the pulses was monitored on a 519 oscilloscope.

We used the same laser system as before. The output of the laser consisted of a train of equally spaced picosecond pulses separated by $\sim$ 4.5 nsecs, which was equal to the cavity round trip time. The pulse train lasted for 200 - 300 nsecs. The intensity of the beam was varied by inserting calibrated ND filters. The change in conductivity ΔG was computed as before using

$$\Delta G = \frac{\vartheta}{(V - \vartheta) R}$$

Since the electron life time and other recombination times are long compared to the excitation pulses, we are in fact measuring the integrated transient photoconductivity from the change in voltage. Both the laser pulse and the photoconductivity were displayed on the dual beam scope with the same

resolution. So the photoconductivity peak corresponded approximately to the peak of the laser pulse.

The photoconductivity ΔG in millimhos versus light intensity is shown in figures 23 and 24 for the polycrystalline and single crystal CdS respectively. A least square fit was made and the slope was found to be 3 ± 0.2 in both the cases. This indicated a power law of $\sim I^3$, characteristic of a three-photon process.

The generation of non-equilibrium carriers could be due to an absorption of a second harmonic generated in a non-phase matched CdS. Since the second harmonic is of 5300° A, it will be absorbed only as a result of a two-photon process. Hence the photoconductivity due to such a process is of fourth order and will be very weak compared to a three photon process. Therefore the observed photoconductivity is due to a three-photon absorption in CdS.

We made an order of magnitude estimate of the three-photon absorption coefficient from the measured photoconductivity. The three-photon conductivity $\Delta G^{(3)}$ can be written as (see Eq. (10) of chapter 2)

$$\Delta G^{(3)} = \eta V \frac{a}{c} (\mu_n + \mu_h) \frac{\tau_1}{3\hbar\omega} I_0 \left[1 - \frac{1}{(1 + 2\beta_3 I_0^2 L)^{1/2}} \right]$$

When $\beta_3 I_0^2 L \ll 1$, we get $\Delta G^{(3)} \propto I^3$. This explains the cubic law observed in the experiment. To make a quantitative estimate of the three-photon absorption coefficient, we should include

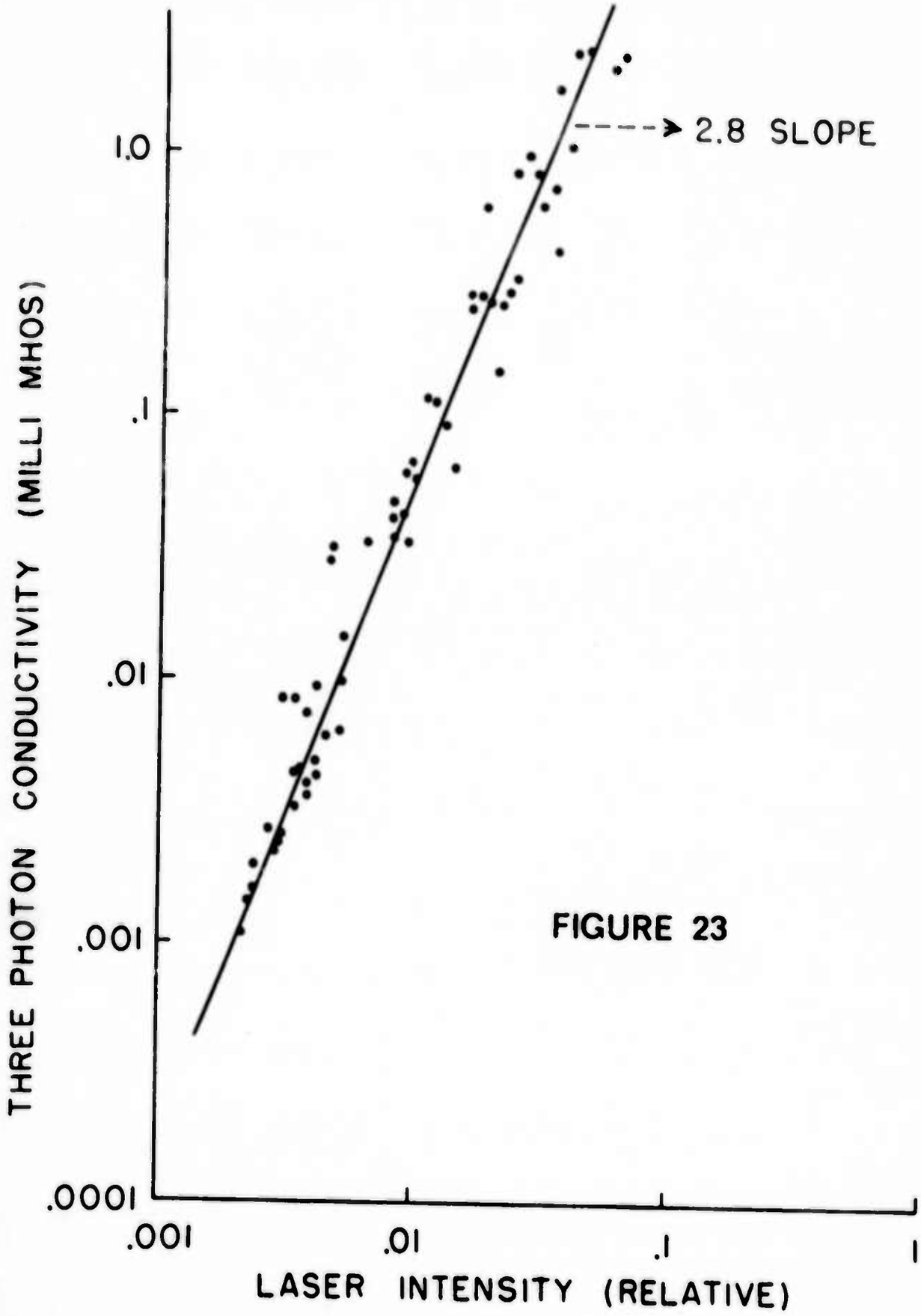
CdS POLY CRYSTAL
2.8 SLOPE
1.0
.1
.01
.001
.0001
THREE PHOTON CONDUCTIVITY (MILLI MHOS)
.001
.01
.1
1
LASER INTENSITY (RELATIVE)

FIGURE 23

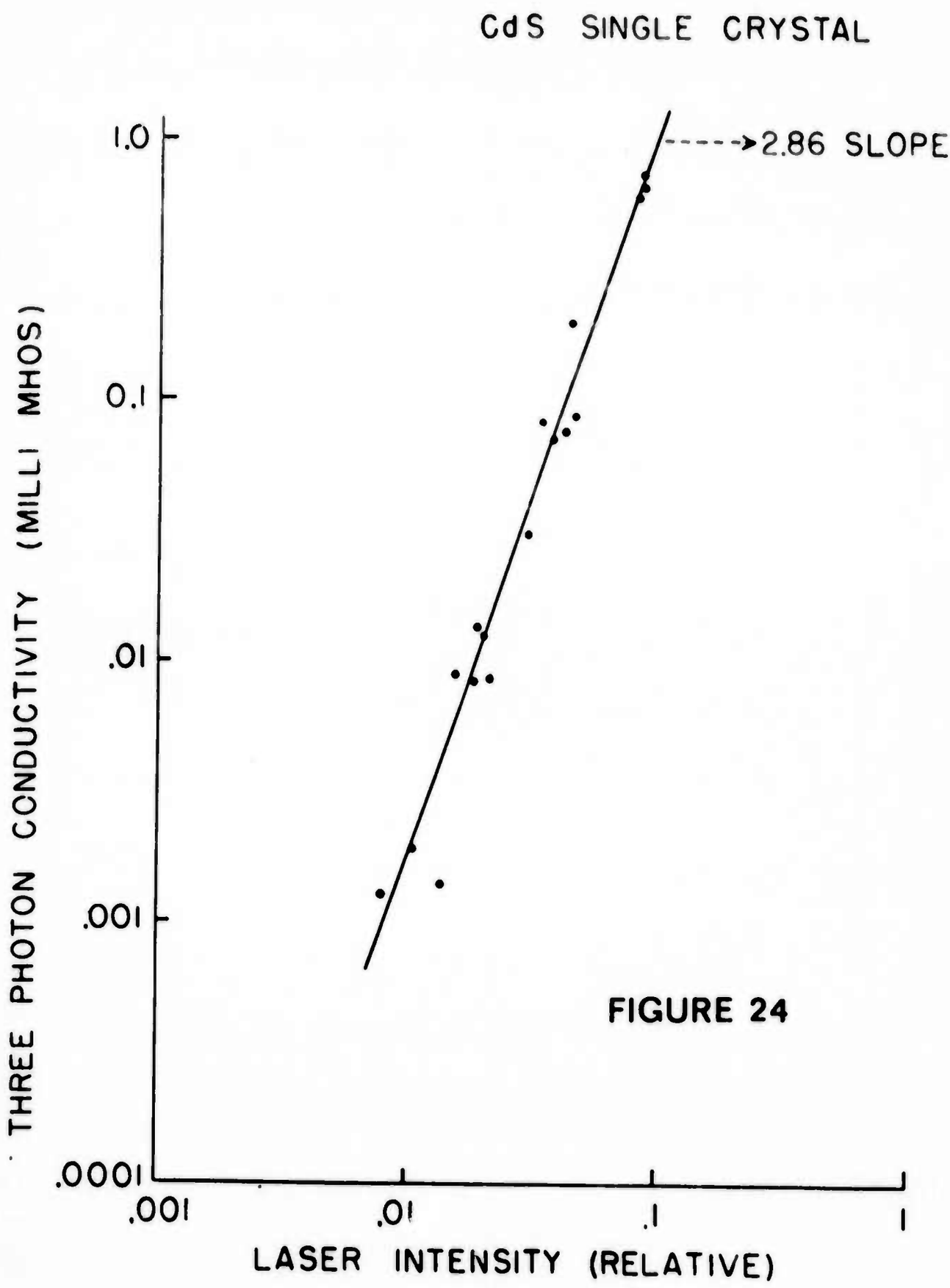
CdS SINGLE CRYSTAL
2.86 SLOPE
1.0
0.1
.01
.001
.0001
THREE PHOTON CONDUCTIVITY (MILLI MHOS)
.001
.01
.1
1
LASER INTENSITY (RELATIVE)

FIGURE 24

the integration factor in the photoconductivity expression. We multiply the above expression by the average number of pulses 'N' that take part effectively in contributing to the conductivity. The pulses towards the end of the train contribute negligibly towards the conductivity compared to the middle portion of the pulse train. 'N'was approximately taken as 10 . In addition, we had to know the peak intensity of the pulse I_o, the pulse width t_i, the mobility and the geometric factor a/c . a/c was 2.0 in the present experiment. Since the crystals were of compensated high resistivity type, the mobility could not be measured accurately by the manufacturer and so the normal mobility of 200 $cm^2/v\text{-}sec$ [15] was assumed. We measured the total energy of the beam by a calibrated thermopile detector. Under similar conditions, the TPF pattern was photographed and this gave a value of 5-9 psecs for the pulse width. From the pulse width (~9 psecs) and the energy per pulse, the peak intensity I_o was determined.

In the case of polycrystalline CdS, 0.5 GW/cm^2 gave a value of $\Delta G^{(3)} \approx 0.8$ millimhos. The thickness of the crystal was measured with a microscope and was found to be 0.2 mms . From the expression for $\Delta G^{(3)}$, $\beta_3 I_o^2$ was estimated to be 0.01 cm^{-1}. This corresponds to $\beta_3 \approx 0.04$ cm^3/GW^2.

For single crystal CdS , 0.66 GW/cm^2 gave $\Delta G^{(3)} \sim 1.0$ millimhos. The thickness of the crystal was 0.28 mms. β_3 was found to be 0.013 cm^3/GW^2. The theoretical estimation for CdS is shown in appendix 5 and we get a value of 0.2 cm^3/GW^2.

Azkinadze et al.[22] reported a value of 2.5 cm^3/GW^2 for β_3. Their experiment was done with a Q-switched laser beam and their intensity dependence of recombination radiation was $I_o^{3.4}$. Arsenev et al.[23] estimated using mode-locked pulses and they got a value of 0.02 cm^3/GW^2. Our experimental arrangement was similar to Arsenev's and so the order of magnitude agreement with the calculated value and Arsenev's experimental value gives one more evidence to the three-photon generation process in CdS. Table #I gives the comparison of the different values of β_3. The lower values got in the present experiment may be attributed to the uncertainty in the incident intensity, higher value of mobility used in the calculation and partly due to the inhomogeneity of the beam distribution.

CdS is an anisotropic semiconductor and so the effective masses are different in different directions. Recently, Jick H.Yee[27] has calculated the variation of the three-photon absorption coefficient with direction. The variation of the value of β_3 was less than 20%. In our experiment, we used a crystal of random orientation and general polarisation of the laser beam and so our experiment was rather insensitive to detect these changes as proposed by Jick H.Yee. More controlled experiments taking into account the crystal orientation and laser beam polarisation had to be done to verify the predictions made by Jick H.Yee.[27]

B.M.Ashkinadze et al.[22] observed a power law of $I_o^{3.4}$ in their experimental investigation of the recombination radiation

Table 1

	β_3 in cm^3/GW^2	
calculated value [27]	0.2	
Azkinadze [22]	2.5	
Arsenev [23]	0.02	
Polycrystal	0.04	present experiment
single crystal	0.013	present experiment

of the 5200°A band from CdS at 77°K after three-photon absorption of Q-switched Nd:glass radiation. Since they conducted the experiment at 77°K, they observed a large number of excitons. The excitons formed another recombination channel. They explained a power law of $I_o^{2.6}$ in the case of luminescence of CdS with two-photon excitation[13] by assuming two recombination channels and the pumping of carriers from one recombination channel to another. The power law of $I^{3.4}$ could be similarly explained. In the photoconductivity experiment at room temperature, B.M.Ashkinadze et al.[12] excited the CdS crystal with a Q-switched ruby laser and observed an intensity dependence of I^2. This could be explained as follows. There are very little excitons formed at room temperature and further excitons do not contribute to photoconductivity. Since the photoconductivity was a transient one, a measurement of photoconductivity corresponded to a measurement of the generated charge carriers which depended only on the timewidth of the pulse and the intensity. The present experiment is similar to their experiment except we are measuring the three-photon conductivity using mode-locked pulse train. Extrapolating the above arguments, the slope of 3.0 ± 0.2 in the log-log plot of ΔG versus I in both the crystals could be justified.

Figure 25 shows the oscilloscope display of laser pulse against the photoconductivity signal for both the crystals. In both the samples, the trap limited decay times are greater than the length of the laser pulse train. In the single crystal CdS,

CdS – Single Crystal

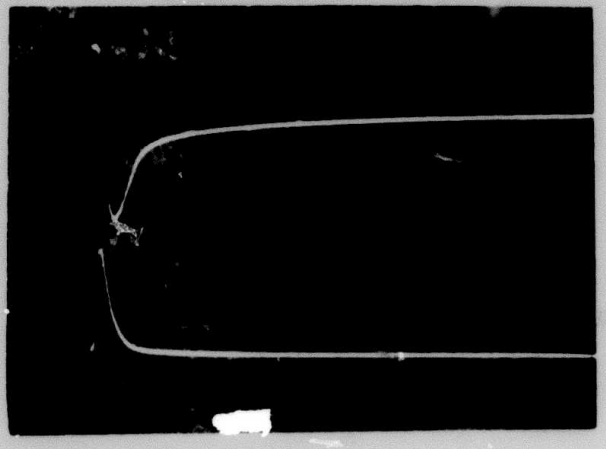

Photo current

laser

CdS – Poly Crystal

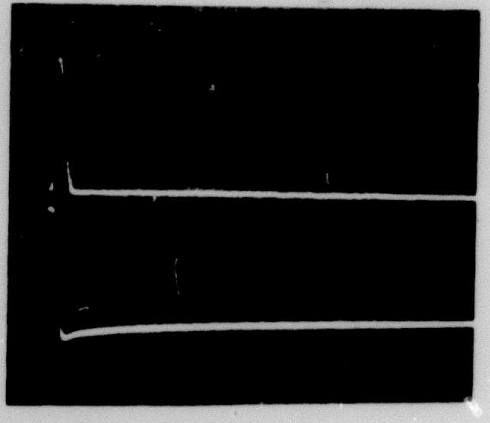

laser

Photo current

2 μsec

Figure 25

we observed three different time constants in qualitative agreement with the observations made by Nicholas and Woods.[64] In the three-photon conductivity using ultra short pulses, the rise time is determined by the pulse train. The individual pulses are of picosecond duration and the photoconductivity due to these excitations are somewhat integrated since the free elctron recombination time is of the order of 20 - 30 nsecs.[68] So the peak of the pulse occurs near the end of the laser pulse. After the end of the laser pulse, the decay time is modified by the kinetics of traps in CdS.

Nicholas and Woods[64] studied the steady state photoconductivity in single crystal CdS and they found, when suddenly stopping the exciting source, that the decay process consisted of three distinct parts:

I. Initial fast decay associated with free electron recombination occurred.
2. Then an intermediate region existed where electrons started to be released from traps and
3. finally, decay associated with emptying of trapping levels very close to the equilibrium Fermi level occurred.

In the present experiment, we measured the transient photoconductivity and we have to take into account the trap filling before trap-limited recombination occurs. The fast free electron recombination process could be explained in the integration of photoconductivity signal. The electrons in the

conduction band come to equilibrium with the traps and the decay thereafter is trap controlled. As we see in figure 29, the 200 - 300 nsecs (time constant) decay immediately after the end of the pulse is due to the trap filling and the free electron recombination and afterwards the whole decay is trap controlled and we can see the intermediate region associated with the electrons emptying from the traps. The dark conductivity of several megohms regained its value only after two to three minutes interval from the laser pulse, which could be observed on a volt-ohm-meter. For this reason, the experiments with the single crystal were conducted with successive laser shots at intervals of two minutes or more.

In the case of polycrystalline material, we did not observe the very slow decay, instead the dark conductivity regained its value in a couple of seconds. The free electron recombination time of several nanoseconds explains the integration of the signal. We barely observe the trap filling process. This confirms the absence of very slow decay in the case of polycrystalline CdS which can be explained by invoking low trap densities compared to single crystal CdS. That is why the trap controlled recombination sets in earlier. J.S.Skarman[65] studied extensively on the relationship between photo current decay time and trap distribution in CdS and found that the polycrystalline CdS contained less traps compared to single crystal CdS and as a result the photoconductivity decay time was shorter in the case of polycrystal CdS compared to single

crystal CdS.

In conclusion, we observed the three-photon conductivity in CdS at room temperature using mode-locked Nd:glass laser pulses. Third order processes like this could be observed easily with the use of picosecond pulses because of higher peak intensity. When Q-switched pulses of the same envelope density as that of the mode-locked pulse train were used to excite the CdS crystal. no observable signal was detected. This indicates the advantages of using picosecond pulses in the investigation of muti-photon absorption processes in semiconductors. The three-photon conductivity in CdS exhibited a power law dependence on excitation intensity as $I^{3\pm0.2}$. Such cubic power laws could be used to measure the third order intensity correlations of the picosecond pulses. The use of three-photon conductivity in picosecond pulse width measurement is demonstrated in the next section.

G. Picosecond Pulse Width Measurement Using Three-Photon Conductivity In CdS:

In the last section, we saw that the photoconductivity of CdS when excited by mode-locked Nd:glass laser pulses showed a power law $\Delta G^{(3)} \propto I^3$. Such a cubic law could be used to measure the intensity autocorrelation function in third order of the picosecond pulses.

We used two identical single crystalline CdS samples for this measurement. The experimental set up was something similar to figure 17 where we used CdS samples instead of GaAs. The sample #1 monitored the photoconductivity produced by the overlap of the pulse with itself while CdS #2 monitored the three-photon conductivity due to a single passage of the short pulses, thereby providing the usual reference signal. The three-photon conductivity (3PC) pattern was scanned by moving the crystal #1 along the direction M_1 to M_2 and plotting the ratio of the pulse height from sample #1 to that from sample #2 as a function of distance. Here also $\Delta G^{(3)} = \frac{v}{(V-v)R}$; Since 'v' was much smaller than V , the change in voltage across R was taken to be a measure of photoconductivity. The 3PC ratio at the wings was normalised to unity. The 3PC ratio as a function of distance moved is shown in figure 26.

The contrast ratio for 3PC measurement was shown to be 10 in chapter 2 . As we see in figure 26, we get a contrast ratio of 3.2 only. This is because of the limited resolution of the

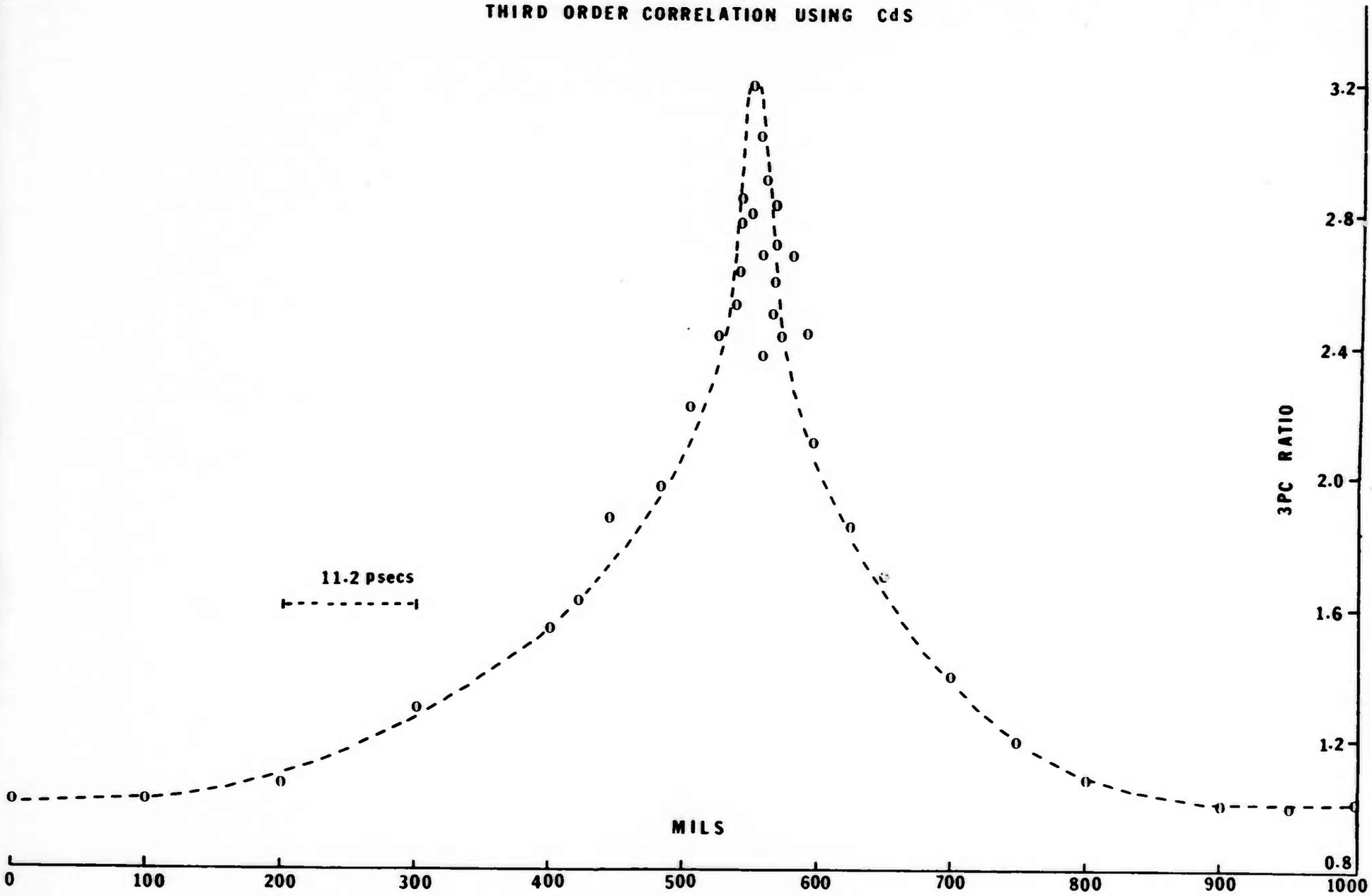
THIRD ORDER CORRELATION USING CdS
3PC RATIO
3.2
2.8
2.4
2.0
1.6
1.2
0.8
11.2 psecs
MILS
0
100
200
300
400
500
600
700
800
900
1000

FIGURE 26

crystal. The thickness of the crystal was 0.28 mms and this corresponded to a resolution of $\sim$3 psecs. The half width of the curve approximately gives 10 psecs for the width of the pulse.

Eckardt and Lee[68] measured the same autocorrelation function of the picosecond pulses using third harmonic generation. They utilised the unique polarisation properties of optical third harmonic generation in a phase matched dye solution. Consequently their method eliminated the background. Their signal ratio was directly proportional to $G^3(\tau)$. Because of the limited resolution of our detector, we missed the spike on the correlation curve observed by them. P.M.Rentzepis et al.[67] measured the three-photon fluorescence (3PF) pattern using BBOT and Dimethyl Popop in methyl cyclohexane and they obtained a contrast ratio of $\sim$9. We got a contrast ratio of 3.2 and this was because of the finite resolution of the crystal. Thinner crystals with resolution of the order of 0.1 psec should be used to get a better map of the third order correlation function.

Apart from the limitation in resolution, we show in principle that the three-photon conductivity effect can be used to measure the width of the picosecond pulses. We measured the autocorrelation function of the pulse intensity in third order using CdS which yielded the same form of the curve as got by Eckardt and Lee[68] but with a reduced contrast ratio of $\sim$3.2 because of limited resolution of the detector.

Hence, in effect, the multi-photon conductivity in semiconductors could be used to measure picosecond pulse width. Construction of an electronic multilayered thin film semiconductor detector seemed to be possible in the near future.

Chapter 5

Conclusion

The two-photon conductivity in GaAs and $CdS_{.5}$-$Se_{.5}$ and the three-photon conductivity in CdS were investigated with Q-switched and mode-locked Nd:glass laser pulses and these effects were subsequently utilised to measure the second and third order intensity auto correlation function of the picosecond pulses. In the Q-switched pulse excitation, photoconductivity of O_2-doped GaAs was measured in the intensity range 0.01 to 10 MW/cm^2. In the low intensity region below 1 MW/cm^2, single photon process was dominant and the slope of the log ΔG - log I line was ≈ 0.6 which could be understood by a continuous distribution of levels in the forbidden gap as proposed by A.Rose[45]. Above 1 MW/cm^2, the two-photon process dominated and the observed two-photon conductivity was in agreement with Jick Yee's[29] theoretical calculations (slopes ≈ 1.8). Mode-locked excitation of the photoconductivity displayed the two-photon nature over a wide range of intensities because of the short pulse excitation (picosecond pulses) with a higher intensity. The photoconductivity curve in the case of both O_2-doped GaAs and Cr-doped semi-insulating GaAs displayed a slope of 2 at lower intensities changing to unity slope at higher intensities. This slope change was expected since $\Delta G \propto \frac{\beta_2 I_0^2 L}{1+\beta_2 I_0 L}$; at lower intensities, $\Delta G \propto \beta_2 I_0^2 L$ since $\beta_2 I_0 L \ll 1$ and at higher intensities,

$\Delta G \propto I_o$ since $\beta_2 I_o L >> 1$. At very high intensities, the photoconductivity curve displayed a sub-linear region which was proved to be due to stimulated intra-band absorption of holes in GaAs. The magnitude of the absorption coefficient varied from 10 - 30 cm^{-1}, linearly with the intensity. This agreed approximately with the values reported in the references.[59,60] The effect of stimulated intra-band (valence) absorption on two-photon conductivity in InSb at 90° K using a Q-switched CO_2 laser was studied by A.M.Danishevskii et al.[70] Towards the end of the high intensity region, absorption which led to the generation of carriers was observed. This absorption coefficient was found to be proportional to the square of the light intensity indicating the generation of non-equilibrium electron-hole pairs in GaAs due to three-photon absorption. The calculated three-photon absorption coefficient agreed approximately with the experimentally observed values.

Two-photon conductivity in $CdS_{.5}$-$Se_{.5}$ with the use of mode-locked Nd:glass laser pulses was found to exhibit a square law over a more dynamic range of the incident laser intensity. The two-photon absorption coefficient estimated from the measured photoconductivity (0.07 cm/MW) agreed well within an order of magnitude with the theoretically computed values. The extended square law region in the case of $CdS_{.5}$-$Se_{.5}$ was consistent with the lower value of β_2 got from our measurement.

Finally, we conclude that two-photon conductivity in semiconductors need not necessarily depend on I^2 as discussed

by Jick H.Yee[31] and by Paul Kelly et al.[71]. Because of absorption of laser beam in a finite thickness of the sample and surface recombination, this dependence is modified. Picosecond pulse excitation in the present experiment excluded surface recombination and because of absorption of laser beam in the sample (GaAs), the two-photon conductivity was found to be proportional the first power of intensity at higher intensities. This was not observed in the case of $CdS_{.5}$-$Se_{.5}$ because $\beta_2 I_0 L < 1$ even at the highest intensity. Near to damage threshold, in GaAs, stimulated intra-band absorption and higher order processes modify the exponent in the present experiment. So care must be exercised in detecting two-photon absorption in semiconductors.

The square law regions in the ΔG - I curves of GaAs and $CdS_{.5}$-$Se_{.5}$ were then used to measure the second order intensity auto correlation of the picosecond pulses. The photoconductivity yield gave contrast ratios of $\sim$ 1.8 and 2.4 for GaAs and $CdS_{.5}$-$Se_{.5}$ respectively). The half width of the correlation curve gave a value of 8 - 10 psecs for the pulse width in both the cases. The higher contrast ratio we got when we used CdS-Se was evident from the difference in resolution (4 psecs for GaAs and 2 psecs for $CdS_{.5}$-$Se_{.5}$) and also from the extended square law region of $CdS_{.5}$-$Se_{.5}$ which facilitated the measurement of second order correlation.

We measured the three-photon conductivity in CdS at room temperature using a mode-locked Nd:glass laser and the three-photon

conductivity depended on excitation intensity as $I^{3.0\pm0.2}$. An order of magnitude estimate of the three-photon absorption coefficient was found to be in fair agreement with the theoretically calculated values. Third order processes like this could be easily observed with the use of picosecond pulses because of higher peak intensity. When Q-switched pulses of the same envelope density as that of the mode-locked pulse train were used to excite the CdS crystal no detectable signal was observed. This indicates the advantage of using picosecond pulses in the investigation of multi-photon processes in condensed media.

The cubic law of the three-photon conductivity in CdS was used to measure the auto correlation of the pulse intensity in third order. The 3PC yield gave a contrast ratio of ~ 3.2 and a pulse width of 9 - 12 psecs. This lower contrast ratio (compared to an ideal value of 10) was partly because of the limited resolution (3 psecs) of the CdS sample used in the experiment.

In conclusion, we state that the multi-photon conductivity in semiconductors could be studied with great ease with the use of mode-locked Nd:glass lasers. Such an independent investigation of these isolated fast optical non-linearities is useful in understanding the dynamics of light filaments where all higher order optical non-linearities compete.[72] Further, the multi-photon conductivity could be exploited to design an opto-electronic multi-channel detector consisting of a layered

semiconductor for the measurement of picosecond pulse width. Future experiments with thinner crystals (epitaxial layers) are suggested to extend the quadratic dependence of photo-conductivity to higher intensity regions in the case of GaAs and to improve the resolution in the picosecond pulse width measurement. Better quantitative estimates could be got if one uses single picosecond pulses. More careful experimentation with amplified single picosecond pulses will reveal the difference in the multi-photon absorption in CdS and $CdS_{.5}Se_{.5}$ due to the anisotropy of the valence bands in these crystals.

APPENDIX 1

Derivation of Two-photon absorption coefficient:

The Hamiltonian $\mathcal{H}$ for an electromagnetic field interacting with the valence electrons in a semiconductor is given by

$$\mathcal{H} = \frac{1}{2m}\left(\vec{p} + \frac{e\vec{A}}{c}\right)^2 + V(r)$$

where

m = electron rest mass

$\vec{p}$ = electron momentum operator

e = electronic charge

$\vec{A}$ = vector potential of e.m.field

V(r) = potential energy

$$\mathcal{H} = \underbrace{\frac{p^2}{2m} + V(r)}_{H_0} + \frac{e}{mc}\hat{p}\cdot\vec{A} + \frac{e^2}{2mc^2}\vec{A}\cdot\vec{A} \qquad \text{---- (1)}$$

$$= H_0 + H'$$

where H_0 is the unperturbed Hamiltonian in the absence of e.m.field and H' is the interaction Hamiltonian and can be considered as a perturbation. The second term in H' is of order e^2 and can be neglected compared to the first term. Further the term containing $\vec{A}.\vec{A}$ can be omitted, for the orthogonality of the wavefunctions causes its contribution to appear only when more than two photons are absorbed. Therefore,

$$H' = \frac{e}{mc}\vec{p}\cdot\vec{A}$$

where $\vec{A} = A\,\vec{\alpha}$, $\vec{\alpha}$ is the polarisation vector. Since ($h\omega < E_g$) the photon energy is less than the forbidden gap of the semiconductor, the first order calculation gives no contribution and so the transition

rate is to be calculated from the second order terms. The following derivation of the two-photon transition rate was first given by N.G.Basov et al.[8]

Two-photon transition rate:

According to the well known Fermi's Golden Rule, the transition probability for two-photon absorption between an initial state 'i' and a final state 'f' can be written as follows:

$$W'_{if} = \frac{2\pi}{\hbar} |\langle i|H|f\rangle|^2 \delta(E_f - E_i - 2\hbar\omega) \quad \text{---(2)}$$

From second order perturbation theory, the matrix element

$$\langle i|H|f\rangle_{2^{nd}\,order} = \sum_n \frac{\langle i|H'|n\rangle\langle n|H'|f\rangle}{E_n - (E_i + \hbar\omega)}$$

where $|n\rangle$ is the virtual intermediate state.
The total transition probability W_{if} can be got by summing over all the initial and final states. Thus,

$$W_{if} = \frac{2\pi}{\hbar} \iint_{f\ i} d^3k_f\, d^3k_i \left[\sum_n \frac{H_{fn} H_{ni}}{E_n - (E_i + \hbar\omega)}\right]^2 \delta(E_f - E_i - 2\hbar\omega) \quad \text{---(3)}$$

where

$H_{fn} = \langle f|H'|n\rangle$

$H_{ni} = \langle n|H'|i\rangle$

H' = is the interaction Hamiltonian.

k_i = wavenumber for initial states

k_f = wavenumber for final states.

First take the sum of the states over a unit cell of the crystal and then perform over all the cells in the crystal of volume V. Thus we replace

$$H_{ni} = (H_{ni})_{cell}\ \delta^3(k_n - k_i)$$

$$H_{fn} = (H_{fn})_{cell}\ \delta^3(k_f - k_n)$$

$$\therefore\quad W_{if} = \frac{2\pi}{\hbar}\iint d^3k_f\, d^3k_i \left[\int d^3k_n \sum_{\substack{n \\ \text{over cell}}} \frac{(H_{fn})_{cell}\,(H_{ni})_{cell}}{E_n - (E_i + \hbar\omega)}\right.$$

$$\left. \times\, \delta^3(k_f - k_n)\,\delta^3(k_n - k_i)\right]^2 \delta(E_f - E_i - 2\hbar\omega)$$

$$= \frac{2\pi}{\hbar}\iint d^3k_f\, d^3k_i \left[\sum_{\substack{n \\ cell}} \frac{(H_{fn})_{cell}(H_{ni})_{cell}}{E_n - (E_i + \hbar\omega)}\right]^2 \left[\delta^3(k_f - k_i)\right]^2 \delta(E_f - E_i - 2\hbar\omega)$$

Now

$$\left[\delta^3(k_f - k_i)\right]^2 = \delta^3(k_f - k_i)\,\delta^3(0) = \delta^3(k_f - k_i)\,\frac{V}{(2\pi)^3}$$

since $\quad V = \int d^3x\, e^{i(k_f - k_i)x} = (2\pi)^3\,\delta(0)$

$$W_{if} = \frac{2\pi}{\hbar}\frac{V}{(2\pi)^3}\iint d^3k_f\, d^3k_i\, \delta^3(k_f - k_i)\left[\sum_n \frac{H_{fn}\,H_{ni}}{E_n - (E_i + \hbar\omega)}\right]^2 \delta(E_f - E_i - 2\hbar\omega) \quad \text{---(4)}$$

Integrating over k_i and putting $k = k_i = k_n = k_f$, the transition rate per unit volume is given by

$$\frac{W}{V} = \frac{2\pi}{\hbar}\frac{1}{(2\pi)^3}\int d^3k \left[\sum_n \frac{H_{fn}\,H_{ni}}{E_n-(E_i+\hbar\omega)}\right]^2 \delta(E_f-E_i-2\hbar\omega) \quad ----(5)$$

Basov considered the initial valence band and the final conduction band as the intermediate states. The points in the valence and conduction bands away from k=0 are represented by mixed parity states and the dipole matrix elements are non-vanishing. The higher conduction bands and the deeper valence bands are far away and consequently the square of the energy denominator makes them negligible. Taking the transitions from υ to C we get the energy denominators as $\pm\hbar\omega$. The quantity $\hbar\omega$ is the smallest of all possible values of denominators. Thus these terms dominate over the rest.

$$\therefore W_i = \frac{2\pi}{\hbar}\frac{1}{(2\pi)^3}\int d^3k \left(\frac{H_{cc}\,H_{c\upsilon}}{\hbar\omega} + \frac{H_{c\upsilon}H_{\upsilon\upsilon}}{-\hbar\omega}\right)^2 \delta(E_c-E_\upsilon-2\hbar\omega)$$

$$= \frac{2\pi}{\hbar}\left(\frac{1}{2\pi}\right)^3\frac{1}{(\hbar\omega)^2}\int d^3k \left(H_{cc}H_{c\upsilon}-H_{c\upsilon}H_{\upsilon\upsilon}\right)^2 \delta(E_c-E_\upsilon-2\hbar\omega) \quad ---(6)$$

where $i = 1,2,3$ for three valence bands, $E_c - E_\upsilon = 2\hbar\omega$

Using the Bloch wave functions,

$$\psi_{c,k} = \frac{1}{(2\pi)^{3/2}}\,u_{ck}(r)\,e^{ik\cdot r} \qquad \text{-- Conduction electron}$$

$$\psi_{\upsilon,k} = \frac{1}{(2\pi)^{3/2}}\,u_{ck}(r)\,e^{ik\cdot r} \qquad \text{-- Valence electron}$$

and assuming the photon momentum to be small compared with the electron momentum, we can write the matrix elements as follows:

$$H_{c\upsilon} = \frac{eA}{mc}\,(\hat{p}\cdot\vec{\alpha})_{c\upsilon}\,\delta(\vec{k}_c-k_\upsilon)$$

$$H_{cc} = \frac{eA}{m_c^* C} (\hbar \vec{k}_c \cdot \vec{\alpha}) \; \delta(\vec{k}_c - \vec{k}_{c'})$$

$$H_{vv} = -\frac{eA}{m_v^* C} (\hbar \vec{k}_v \cdot \vec{\alpha}) \; \delta(\vec{k}_v - \vec{k}_{v'})$$

The -ve sign in the last expression is as a result of negative effective mass.

$$\therefore W_i = \frac{2\pi}{\hbar} \left(\frac{1}{2\pi}\right)^3 \left(\frac{1}{\hbar w}\right)^2 \int d^3k \; \frac{e^4 A^4}{m^2 C^4} \times$$

$$\left[\frac{\hbar k_c \alpha}{m_c^*} (\hat{p} \cdot \vec{\alpha})_{cv} \; \delta(\vec{k}_c - \vec{k}_v) \; \delta(\vec{k}_c - \vec{k}_{c'}) + \frac{\hbar k_v \alpha}{m_v^*} (\hat{p} \cdot \vec{\alpha})_{cv} \right.$$

$$\left. \delta(\vec{k}_c - \vec{k}_v) \; \delta(\vec{k}_v - \vec{k}_{v'}) \right]^2 \delta(E_c - E_v - 2\hbar w)$$

$$= \frac{2\pi}{\hbar} \left(\frac{1}{2\pi}\right)^3 \left(\frac{1}{\hbar w}\right)^2 \frac{e^4 A^4}{m^2 C^4} \; \hbar^2 \alpha^2 (\hat{p} \cdot \hat{\alpha})_{cv}^2 \left[\frac{1}{m_c^{*2}} + \frac{2}{m_c^* m_v^*} + \frac{1}{m_v^{*2}} \right]$$

$$\int d^3k \; k^2 \; \delta(E_c - E_v - 2\hbar w) \qquad \text{-----(7)}$$

Let $\frac{1}{m^*_{cv_i}} = \frac{1}{m_c^*} + \frac{1}{m^*_{v_i}}$; $E_c - E_v = E_g + \frac{\hbar^2 k^2}{2 m^*_{cv_i}}$

We know

$$\delta\{f(x)\} = \frac{\delta(x - x_0)}{\left|\frac{\partial f(x)}{\partial x}\right|} \qquad (74)$$

where $f(x_0) = 0$

$$\delta(E_c - E_v - 2\hbar\omega) = \delta(P(k))$$

$$= \frac{\delta(k-k')}{\hbar^2 k'/m^*_{cv_i}}$$

$$\therefore \int d^3k\, k^2\, \delta(E_c - E_v - 2\hbar\omega) = \int d^3k'\, k'^2\, \delta(k-k')\, \frac{m^*_{cv_i}}{\hbar^2 k'}$$

$$= \int k'^3\, \frac{4\pi\, m^*_{cv_i}}{\hbar^2}\, \delta(k-k')\, dk' \qquad \text{since } d^3k' = 4\pi k'^2 dk'$$

$$= \frac{4\pi m^*_{cv_i}}{\hbar^2} \cdot k^3$$

$$= \frac{m^*_{cv_i}}{\hbar^2} \cdot \frac{4\pi \cdot 2^{3/2} m^{*3/2}_{cv_i}}{\hbar^3} (2\hbar\omega - E_g)^{3/2} \quad \text{since } \frac{\hbar^2 k^2}{2 m^*_{cv_i}} = (2\hbar\omega - E_g)$$

$$\therefore W_i = \frac{2\pi}{\hbar} \left(\frac{1}{2\pi}\right)^3 \left(\frac{1}{\hbar\omega}\right)^2 \frac{e^4 A^4}{m^2 c^4}\, \hbar^2 \alpha^2 \left(\hat{p}\cdot\hat{\alpha}\right)^2_{cv_i}\, \frac{1}{m^{*2}_{cv_i}} \times$$

$$\frac{m^*_{cv_i}}{\hbar^2}\, 4\pi\, 2^{3/2}\, \frac{m^{*3/2}_{cv_i}}{\hbar^3}\, (2\hbar\omega - E_g)^{3/2}$$

now, Intensity $I = v\, N \hbar\omega$ $\qquad v$ = velocity

$$= v\, \frac{\epsilon E_i^2}{8\pi} = \frac{\omega^2 \epsilon^{1/2} A^2}{8\pi c} \quad \because E = \frac{\omega}{c} A$$

$$\alpha^2 = 1$$

$$\therefore W_i = \frac{2^{15/2} \pi e^4}{\epsilon c^2 (\hbar\omega)^6}\, \frac{|(\hat{\alpha}\cdot\hat{p})_{cv_i}|^2}{m^2}\, m^{*1/2}_{cv_i}\, (2\hbar\omega - E_g)^{3/2}\, I^2 \qquad \text{---(8)}$$

Taking into account the spin degeneracy, there will be an extra factor of 2. Now the two-photon absorption coefficient $K_i^{(2)}$ is defined as

$$K_i^{(2)} = \frac{2\hbar\omega \cdot W_i}{I}$$

$$\therefore \quad K_i^{(2)} = \frac{2^{19/2}\pi e^4}{\epsilon c^2 (\hbar\omega)^5} \frac{\left|(\hat{\alpha}\cdot\hat{p})_{cv_i}\right|^2}{m^2} m^{*1/2}_{cv_i} (2\hbar\omega - E_g)^{3/2} I \quad ---(9)$$

where i = 1,2,3 for three valence bands.

APPENDIX 2

Calculation of Two-photon Absorption Coefficient in GaAs:-

$$K_i^{(2)} = \frac{2^{19/2}\pi e^4}{\epsilon c^2 (\hbar\omega)^5} \frac{|(\hat{\alpha}\cdot\hat{P})_{c v_i}|^2}{m^2} m_{c v_i}^{*1/2} (2\hbar\omega - E_g)^{3/2} I$$

Taking into account the transitions from the valence bands v_1, v_2 and v_3 to the conduction band 'C' (the band structure of GaAs is shown in Fig.1) , the total two-photon absorption coefficient

$$K^{(2)} = K_1^{(2)} + K_2^{(2)} + K_3^{(2)}$$

$e = 4.8 \times 10^{-10}$ esu

$\epsilon = 11.8$

$c = 3 \times 10^{10}$ cm/sec

$\hbar\omega = 1.17$ ev

$E_g = 1.41$ ev (For v_3 to C transition $E_g = 1.74$ ev)

$m = 9.11 \times 10^{-28}$ gms

$$\frac{1}{m^*_{c v_i}} = \frac{1}{m^*_c} + \frac{1}{m^*_{v_i}}$$

$m_c^* = 0.072$ m

$m_{v_1}^* = 0.68$ m

$m_{v_2}^* = 0.085$ m

$m_{v_3}^* = 0.25$ m

$$\frac{|(\hat{\alpha}\cdot\hat{P})_{c v_i}|^2}{m^2} = \frac{3}{4}\frac{E_g}{m_c^*} \qquad (73)$$

Substituting all these values in the above expression, and expressing the intensity 'I' in MW/cm^2,

$$K^{(2)} = K_1^{(2)} + K_2^{(2)} + K_3^{(2)}$$

$$= 1.575 \times I + 1.22 \times I + 0.89 \times I \quad cm^{-1}$$

$$= 3.7 \times I \ cm^{-1}$$

$$K^{(2)} = \beta_2 \times I$$

$$\beta_2 = 3.7 \ cm/MW$$

APPENDIX 2

Calculation of Two-Photon Absorption Coefficient in $CdS_{.5}$-$Se_{.5}$:

$$K^{(2)} = \frac{2^{19/2}\pi e^4}{\epsilon c^2 (\hbar\omega)^5} \frac{|(\alpha \cdot P)_{cv}|^2}{m^2} m_{cv}^{*1/2} (2\hbar\omega - E_g)^{3/2} I$$

In the case of $CdS_{.5}$-$Se_{.5}$, We estimated $K^{(2)}$ taking into account only transitions from heavy hole valence band to the conduction band. This is because of the relatively unknown band parameters of the mixed crystals. Some of the values we use the average CdS and CdSe.

ϵ = 9.0

E_g = 2.0 ev [18]

m_c^* = 0.14 m

m_v^* = 0.5 m

m = free electron rest mass $\approx 9.1 \times 10^{-28}$ gms

All other values are the same as in appendix 2.

We get

$$K^{(2)} = \beta_2 I \quad , \quad \underline{\beta_2 = 0.4 \text{ cm/MW.}}$$

APPENDIX 4

Three-photon Absorption Coefficient:

The Hamiltonian 'H' for an electromagnetic field interacting with the valence electrons in a semiconductor is given by,

$$H = H_o + H' + H'' \qquad \text{------(1)}$$

where $H_o = \frac{p^2}{2m} + V(r)$

$$H' = \frac{e}{mc}\,\vec{p}\cdot\vec{A}$$

$$H'' = \frac{e^2}{2mc}\,\vec{A}\cdot\vec{A}$$

According to Fermi's Golden Rule, the total transition probability for three-photon absorption between a group of initial states 'i' and a group of final states 'f' can be written as follows:

$$W_t = \frac{2\pi}{\hbar}\sum_f\sum_i \left|\sum_n \frac{H'_{fn}H''_{ni}}{E_{ni}-2\hbar\omega} + \sum_n \frac{H''_{fn}H'_{ni}}{E_{ni}-\hbar\omega} + \sum_n\sum_m \frac{H'_{fn}H'_{nm}H'_{mi}}{(E_{ni}-2\hbar\omega)(E_{mi}-\hbar\omega)}\right|^2 \times \delta(E_f-E_i-3\hbar\omega) \qquad \text{----(2)}$$

where $H'_{fn} = \langle f|H'|n\rangle$

$$H''_{fn} = \langle f|H''|n\rangle$$

As shown in appendix 1, the transition rate per unit volume is given by

$$\frac{W_t}{V} = \frac{2\pi}{\hbar}\frac{1}{(2\pi)^3}\int d^3k \left| \sum_n \frac{H'_{fn} H''_{ni}}{E_{ni} - 2\hbar\omega} + \sum_n \frac{H''_{fn} H'_{ni}}{E_{ni} - \hbar\omega} \right.$$

$$\left. + \sum_n \sum_m \frac{H'_{fn} H'_{nm} H'_{mi}}{(E_{ni} - 2\hbar\omega)(E_{mi} - \hbar\omega)} \right|^2 \delta(E_f - E_i - 3\hbar\omega) \quad ----(3)$$

In the two band approximation as before (one conduction band and one valence band), using Bloch functions we can write the matrix elements as

$$H'_{cv} = \frac{eA}{mc} (\hat{p}\cdot\alpha)_{cv}\, \delta(k_c - k_v)$$

$$H'_{cc'} = \frac{eA}{m_c^* c} (\hbar k_c \cdot \alpha)\, \delta(k_c - k_{c'})$$

$$H'_{vv'} = -\frac{eA}{m_v^* c} (\hbar k_v \cdot \alpha)\, \delta(k_v - k_{v'})$$

$$H''_{(c_n, k_s)(c_m, k_t)} \approx \delta_{(\vec{k}_s + 2\vec{q}, k_t)}\, \delta_{c_n c_m} \left[\frac{1}{2m} \left(\frac{e}{c}\right)^2 \vec{A}\cdot\vec{A} \right]$$

In these matrix elements, the photon momentum can be neglected. As before, only the final conduction band and the initial valence band are considered as intermediate states. Then,

$$\frac{W_t}{V} = \frac{2\pi}{\hbar}\frac{1}{(2\pi)^3}\int d^3k\, \delta(E_c - E_v - 3\hbar\omega) \left| W_{cv} \right|^2 \quad ----(4)$$

where

$$W_{cv} = \sum_n \frac{H'_{cn} H''_{nv}}{(E_{nv} - 2\hbar\omega)} + \sum_n \frac{H''_{cn} H'_{nv}}{(E_{nv} - \hbar\omega)} + \sum_n \sum_m \frac{H'_{cn} H'_{nm} H'_{mv}}{(E_{nv} - 2\hbar\omega)(E_{mv} - \hbar\omega)}$$

$$W_{cv} = \frac{H'_{cv}\, H''_{vv}}{-2\hbar\omega} + \frac{H''_{cc}\, H'_{cv}}{2\hbar\omega}$$

$$+ \frac{H'_{cv}\, H'_{cc}\, H'_{cv}}{(E_{cv}-2\hbar\omega)(E_{cv}-\hbar\omega)} + \frac{H'_{cv}\, H'_{vv}\, H'_{vv}}{(-2\hbar\omega)\,(-\hbar\omega)}$$

$$+ \frac{H'_{cv}\, H'_{vc}\, H'_{cv}}{(-2\hbar\omega)\,(E_{cv}-\hbar\omega)} + \frac{H'_{cc}\, H'_{cv}\, H'_{vv}}{(E_{cv}-2\hbar\omega)\,(-\hbar\omega)}$$

The first two second order terms coming from the $\vec{A}.\vec{A}$ term cancel out to zero and we are left with the four 3rd order terms containing the dipole matrix elements. The Feynmann diagrams corresponding to the four third order terms are as shown below.

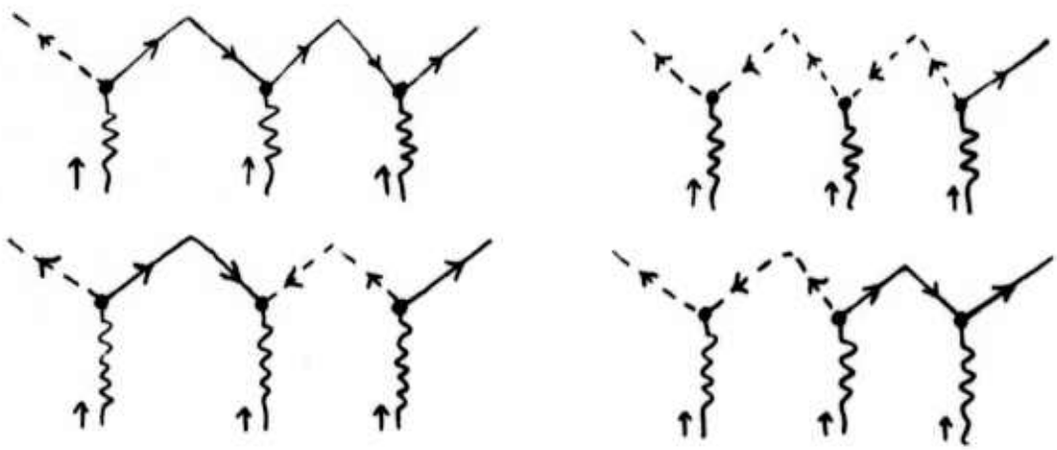

The continuous, dashed, wavy lines represent electrons, holes, and photons respectively. Lines which leave the vortex correspond to creation of a particle and lines which enter the vortex correspond to annihilation.

$$E_{cv} = 3\hbar\omega$$

Substituting the matrix element into W_{cv}, we get

$$\frac{W_t}{V} = \frac{2\pi}{\hbar}\frac{1}{(2\pi)^3}\int d^3k\ \delta(E_c - E_v - 3\hbar\omega)\ \times$$

$$\left[\frac{e^2A^2}{m_c^{*2}c^2}\hbar^2(k\cdot\hat{\alpha})^2\frac{eA}{mc}\frac{B_o}{2\hbar^2\omega^2} + \frac{e^2A^2}{m_v^{*2}c^2}\hbar^2(k\cdot\alpha)^2\frac{eA}{mc}\frac{B_o}{2\hbar^2\omega^2}\right.$$

$$\left. + \frac{e^2A^2}{m_c^* m_v^* c^2}\hbar^2(k\cdot\hat{\alpha})^2\frac{eA}{mc}\frac{B_o}{\hbar^2\omega^2} - \frac{e^3A^3}{m^3c^3}\frac{B_o^3}{4\hbar^2\omega^2}\right]^2 \qquad \text{--- (5)}$$

where $B_o = \langle\hat{p}\cdot\vec{\alpha}\rangle_{cv}$ and $\alpha^2 = 1$

$$= \frac{2\pi}{\hbar}\frac{1}{(2\pi)^3}\frac{e^6A^6}{c^6}\frac{B_o^2}{m^2}\frac{1}{4(\hbar^2\omega^2)^2}\int d^3k\ \delta(E_c - E_v - 3\hbar\omega)\ \times$$

$$\left[\frac{\hbar^2k^2}{m_c^{*2}} + \frac{\hbar^2k^2}{m_v^{*2}} + \frac{2\hbar^2k^2}{m_c^* m_v^*} - \frac{B_o^2}{2m^2}\right]^2$$

$$= \frac{2\pi}{\hbar}\frac{1}{(2\pi)^3}\frac{e^6A^6}{c^6}\frac{B_o^2}{m^2}\frac{1}{4(\hbar\omega)^4}\int d^3k\ \delta(E_c - E_v - 3\hbar\omega)\ \times$$

$$\left[\hbar^2k^2\left(\frac{1}{m_c^*} + \frac{1}{m_v^*}\right)^2 - \frac{B_o^2}{2m^2}\right]^2$$

Let $$\frac{1}{\mu} = \frac{1}{m_c^*} + \frac{1}{m_v^*}$$

$$\frac{W_t}{V} = \frac{2\pi}{\hbar}\frac{1}{(2\pi)^3}\frac{e^6A^6}{c^6}\frac{B_o^2}{m^2}\frac{1}{4(\hbar\omega)^4}\int d^3k\ \delta(E_c - E_v - 3\hbar\omega)\ \times$$

$$\left[\frac{\hbar^2k^2}{\mu^2} - \frac{B_o^2}{2m^2}\right]^2 \qquad \text{--- (6)}$$

Taking the polarisation direction to be the Z-axis

$$k = (\vec{k}\cdot\hat{\alpha}) = k_r \cos\theta$$

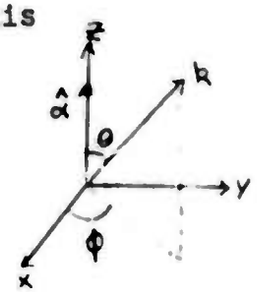

$$\therefore \int d^3k\, \delta(E_c - E_v - 3\hbar\omega)\left[\frac{\hbar^4 k^4}{\mu^4} - \frac{\hbar^2 k^2 B_0^2}{m^2\mu^2} + \frac{B_0^4}{4m^4}\right]$$

$$= \iiint k_r^2\, dk_r \sin\theta\, d\theta\, d\phi\ \frac{\delta(k_r' - k_r)}{\frac{\hbar^2 k_r}{\mu}}\left[\frac{\hbar^4 k_r^4 \cos^4\theta}{\mu^4} - \frac{\hbar^2 k_r^2 \cos^2\theta B_0^2}{m^2\mu^2} + \frac{B_0^4}{4m^4}\right]$$

We used the relation $E_c - E_v - 3\hbar\omega = f(k_r) = E_g + \frac{\hbar^2 k_r^2}{2\mu} - 3\hbar\omega$

and $\delta(f(k_r)) = \dfrac{\delta(k_r - k_r')}{\left|\frac{\partial f}{\partial k_r}\right|}$ where $f(k_r') = 0$

and also $k = k_r \cos\theta = (\vec{k}\cdot\hat{\alpha})$

Performing the integration, we get

$$\frac{W_t}{V} = \frac{2\pi}{\hbar}\ \frac{1}{(2\pi)^3}\ \frac{e^6 A^6}{c^6}\ \frac{B_0^2}{m^2}\ \frac{1}{4(\hbar\omega)^4}\cdot\frac{4\pi\mu}{\hbar^2}\times$$

$$\left[\frac{\hbar^4 k_r'^5}{5\mu^4} - \frac{\hbar^2 k_r'^3 B_0^2}{3m^2\mu^2} + \frac{B_0^4 k_r'}{4m^4}\right] \quad ----(7)$$

Now $\dfrac{\hbar^2 k_r'^2}{2\mu} = 3\hbar\omega - E_g$

We get,

$$\frac{W_t}{V} = \frac{2\pi}{\hbar}\ \frac{1}{(2\pi)^3}\ \frac{e^6 A^6}{c^6}\ \frac{B_0^2}{m^2}\ \frac{1}{4(\hbar\omega)^4}\ \frac{4\pi\mu}{\hbar^2}\cdot\frac{1}{\hbar}\times$$

$$\left[\frac{2^{5/2}(3\hbar\omega - E_g)^{5/2}\mu^{5/2}}{5\mu^4} - \frac{B_0^2 2^{3/2}\mu^{3/2}(3\hbar\omega - E_g)^{3/2}}{3m^2\mu^2} + \frac{B_0^4 2^{1/2}\mu^{1/2}(3\hbar\omega - E_g)^{1/2}}{4m^4}\right]$$

$$\frac{W_t}{V} = \frac{2\pi}{\hbar}\frac{1}{(2\pi)^3}\frac{e^6}{c^6}\frac{B_0^2}{m^2}\frac{1}{4(\hbar\omega)^4}\cdot\frac{4\pi\mu}{\hbar^2}\cdot\frac{1}{\hbar}\cdot A^6\cdot\sqrt{2}\cdot\frac{1}{\mu^{3/2}}\times$$

$$\left[\frac{4}{5}(3\hbar\omega-E_g)^{5/2}-\frac{2}{3}\frac{B_0^2}{m^2}\mu(3\hbar\omega-E_g)^{3/2}+\frac{1}{4}\frac{B_0^4}{m^4}\mu^2(3\hbar\omega-E_g)^{1/2}\right]$$

The intensity I is related to the vector potential A as

$$I = \frac{\omega^2\epsilon^{1/2}A^2}{8\pi c}$$

$$\therefore \frac{W_t}{V} = 2^{15/2}\pi^2\hbar^2\frac{1}{(\hbar\omega)^{10}}\left(\frac{e^2}{c\epsilon^{1/2}}\right)^3\left(\frac{1}{\mu}\right)^{1/2}\frac{B_0^2}{m^2}\ I^3$$

$$\times\left[\frac{4}{5}(3\hbar\omega-E_g)^{5/2}-\frac{2}{3}\frac{B_0^2}{m^2}\mu(3\hbar\omega-E_g)^{3/2}+\frac{1}{4}\frac{B_0^4}{m^4}\mu^2(3\hbar\omega-E_g)^{1/2}\right] \quad ---(8)$$

Taking into account spin degeneracy and the definition of three-photon absorption coefficient $K^{(3)} = \frac{3\hbar\omega\, W_t/V}{I}$, we get

$$K^{(3)} = 3\times 2^{17/2}\pi^2\hbar^2\frac{1}{(\hbar\omega)^9}\left(\frac{e^2}{c\epsilon^{1/2}}\right)^3\left(\frac{1}{\mu}\right)^{1/2}\frac{B_0^2}{m^2}\ I^2$$

$$\left[\frac{4}{5}(3\hbar\omega-E_g)^{5/2}-\frac{2}{3}\frac{B_0^2}{m^2}\mu(3\hbar\omega-E_g)^{3/2}+\frac{1}{4}\frac{B_0^4}{m^4}\mu^2(3\hbar\omega-E_g)^{1/2}\right] \quad ---(9)$$

This agrees with the formula given by A.I.Bobrysheva and J.H.Yee.

APPENDIX 5

Calculation of $K^{(3)}$ in CdS:

$$K^{(3)} = 3 \times 2^{17/2} \pi^2 \hbar^2 \frac{1}{(\hbar\omega)^9} \left(\frac{e^2}{c\epsilon^{1/2}}\right)^3 \left(\frac{1}{\mu}\right)^{1/2} \frac{B_0^2}{m_0^2} I^2$$

$$\times \left[\frac{4}{5}(3\hbar\omega - E_g)^{5/2} - \frac{2}{3}\frac{B_0^2}{m^2}\mu(3\hbar\omega - E_g)^{3/2} + \frac{1}{4}\frac{B_0^4}{m^4}\mu^2(3\hbar\omega - E_g)^{1/2}\right]$$

$$K^{(3)} = \beta_3 I^2$$

Using the band structure of CdS[62] as shown in figure 28, we can evaluate the three-photon absorption coefficient for each of the three valence bands and find the total absorption coefficient. CdS is anisotropic and we could calculate $K^{(3)\parallel^l}$ and $K^{(3)\perp^r}$ for the two directions. The momentum matrix element is given by

$$\frac{B_0^2}{m^2} = \frac{3}{4}\frac{E_g}{m^*c}$$ [73]

$e = 4.8 \times 10^{-10}$ esu

$m = 9.11 \times 10^{-28}$ gms

$c = 3 \times 10^{10}$ cm/sec

$\epsilon = 8.4$

$\hbar\omega = 1.17$ ev

The values of the effective masses and the forbidden gap are shown in figure 28. We get an estimate of $K^{(3)}$ as shown in Table #2.

For a random direction, we could take the calculated

CdS BAND STRUCTURE

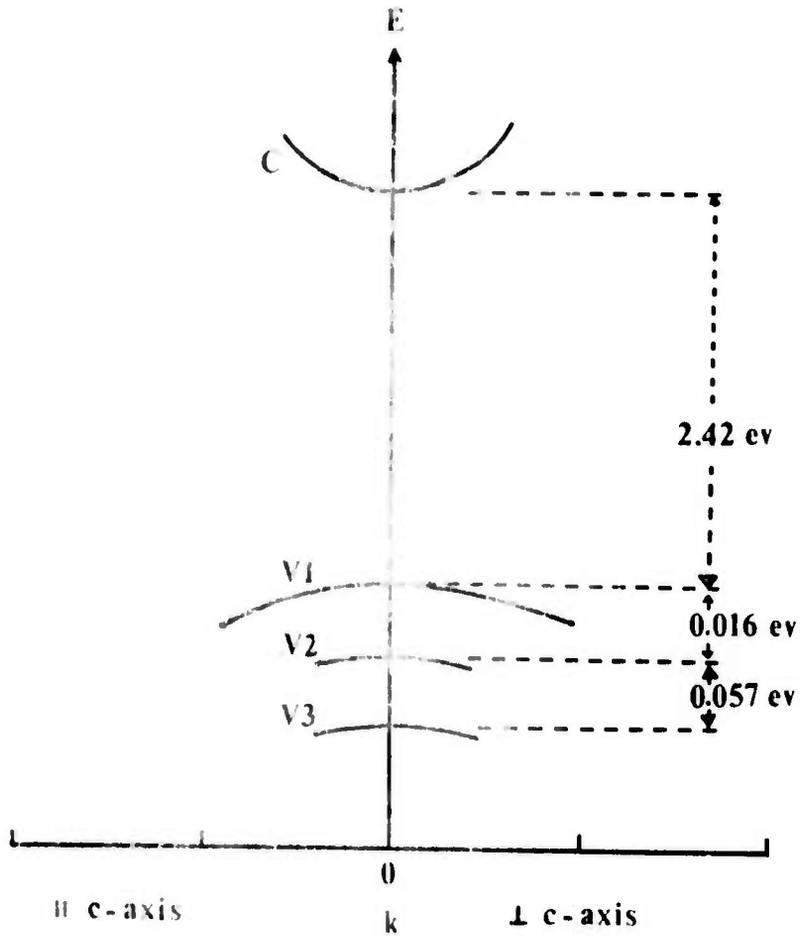

C -- CONDUCTION BAND
V1,V2,V3 -- VALENCE BANDS

EFFECTIVE MASS	∥	⊥
m^{v1}	5 m_o	0.56 m_o
m^{v2}	0.24 m_o	1.2 m_o
m^{v3}	0.77 m_o	0.43 m_o
m^{c}	0.16 m_o	

m_o -- FREE ELECTRON MASS

FIGURE 27

Table #2

$K^{(3)}$ in cm^{-1} (x 10^{-8})

	II^{l}_{caxis}	I^{r}_{caxis}
c - v_I	3.06 I^2	4.22 I^2
c - v_2	I2.65 I^2	9.20 I^2
c-- v_3	9.55 I^2	7.50 I^2
Total	25.26 I^2	20.92 I^2

value as $K^{(3)} = 20.0 \times 10^{-8} I^2 \text{ cm}^{-1}$ where I is in MW/cm^2. We get a value for β_3 as

$$\beta_3 = 0.2 \text{ cm}^3/GW^2 .$$

This value agrees with Jick H.Yee's[27] calculated value.

APPENDIX 6

Calculation Of Multi-Photon Conductivity In Semiconductors:[29,30,31]

Let us consider a semiconductor as shown in figure . When it is illuminated by a laser beam of intensity I_o, electrons and holes are created in the semiconductor. Some of the free carriers will recombine inside the crystal with the volume life time τ and some will diffuse to the surface and recombine at the surface with surface recombination velocity V_s'.

Let us assume that the photon energy is less than the forbidden gap of the semiconductor. So non-equilibrium charge carriers are produced by multi-photon absorption. If $(n-1)\hbar\omega$ is less than the fobidden gap and if $n\hbar\omega > E_g$, then there will be n-photon absorption.

Let F(x) be the generation rate of carriers at a distance x from the surface of the semiconductor. In the case of steady state conditions, the concentration of the generated carriers can be obtained from the following diffusion equation

$$D_p \frac{\partial^2 p}{\partial x^2} - \frac{p}{\tau} = -F(x)$$

Where p is the concentration of non-equilibrium electron-hole pairs and D_p is the diffusion constant. $\lambda = (D_p \tau)^{-\frac{1}{2}}$ is the inverse diffusion length. The equation becomes

$$\frac{\partial^2 p}{\partial x^2} - \lambda^2 p = -\frac{F(x)}{D_p} \qquad ---- (1)$$

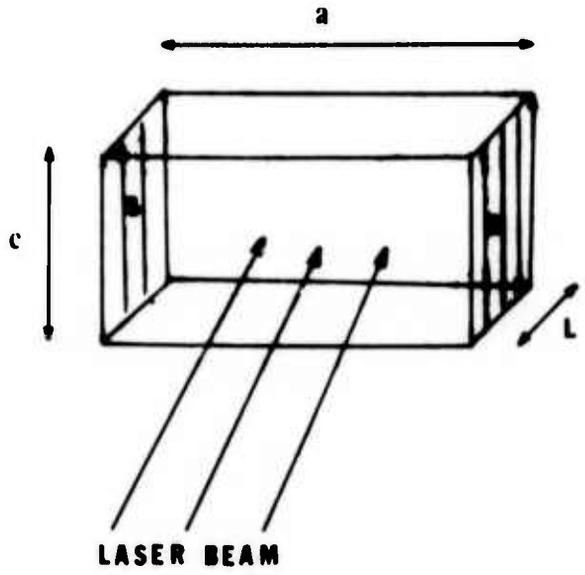

S - OHMIC CONTACTS

FIGURE 28: PHOTO CONDUCTOR

The solution of this equation $p(x)$ can be obtained using the method of variation of parameters as follows:

$$\frac{\partial^2 p}{\partial x^2} - \lambda^2 p = 0$$

This equation gives the general solution as

$$p(x) = A e^{-\lambda x} + B e^{\lambda x}$$

Let the particular solution be

$$p(x) = u_1(x)\, e^{-\lambda x} + u_2(x)\, e^{\lambda x}$$

$$\frac{\partial p}{\partial x} = p' = -\lambda u_1(x)\, e^{-\lambda x} + u_1' e^{-\lambda x} + \lambda u_2 e^{\lambda x} + u_2' e^{\lambda x}$$

If $u_1' e^{-\lambda x} + u_2' e^{\lambda x} = 0$ ------- (2)

Then $p' = -\lambda u_1 e^{-\lambda x} + \lambda u_2 e^{\lambda x}$

$$p'' = \lambda^2 u_1 e^{-\lambda x} - \lambda u_1' e^{-\lambda x} + \lambda u_2' e^{\lambda x} + \lambda^2 u_2 e^{\lambda x}$$

Substituting in (I), we get

$$-\lambda u_1' e^{-\lambda x} + \lambda u_2' e^{\lambda x} = -\frac{F(x)}{D_p} \quad \text{----------(3)}$$

Solving (2) and (3) for u_1' and u_2' and integrating we get,

$$u_1(x) = \int_0^x \frac{F(x')\, e^{\lambda x'}}{2\lambda D_p}\, dx'$$

$$u_2(x) = \int_0^x \frac{F(x')\, e^{-\lambda x'}}{2\lambda D_p}\, dx'$$

The complete solution is given by

$$p(x) = A e^{-\lambda x} + B e^{\lambda x} + \frac{1}{2D_p\lambda}\left[e^{-\lambda x}\int_0^x e^{\lambda x'} F(x')\, dx' - e^{\lambda x}\int_0^x e^{-\lambda x'} F(x')\, dx'\right] \quad \text{---(4)}$$

The constants A and B are to be determined from the boundary conditions at the two surfaces of the crystal. Recombination

occurs at each surface of the crystal at a rate which may be represented by a recombination current $I_s = \pm V_s' p_s$ where p_s is the density of the carriers at the surface.

At the first surface,

$$I_s(0) = V_s' p_s\Big|_{x=0} = D_p \frac{\partial p}{\partial x}\Big|_{x=0} \qquad \text{----(5)}$$

At the rear surface

$$I_s(L) = -V_s' p_s\Big|_{x=L} = D_p \frac{\partial p}{\partial x}\Big|_{x=L} \qquad \text{----(6)}$$

where L is the thickness of the photoconductor.

From (4),

$$p_s(0) = A + B$$

$$p_s(L) = A e^{-\lambda L} + B e^{\lambda L} + \frac{1}{2D_p\lambda}\left[e^{-\lambda L}\int_0^L e^{\lambda x'} F(x')\,dx' - e^{\lambda L}\int_0^L e^{-\lambda x'} F(x')\,dx'\right]$$

$$\frac{\partial p}{\partial x}\Big|_{x=0} = -\lambda A + \lambda B$$

(5) gives $(A + B) V_s = -\lambda A + \lambda B$ where $\frac{V_s'}{D_p} = V_s$

$$A(V_s + \lambda) + B(V_s - \lambda) = 0 \qquad \text{-------(7)}$$

Let $f_1(x) = \frac{1}{2D\lambda}\, e^{-\lambda x} \int_0^x F(x')\, e^{\lambda x'}\, dx'$

$$f_2(x) = -\frac{1}{2D\lambda}\, e^{\lambda x} \int_0^x F(x')\, e^{-\lambda x'}\, dx'$$

$$p_s(x) = A e^{-\lambda x} + B e^{\lambda x} + f_1(x) + f_2(x)$$

$$p_s(L) = A e^{-\lambda L} + B e^{\lambda L} + f_1(L) + f_2(L)$$

$$p_s'(L) = -\lambda A e^{-\lambda L} + \lambda B e^{\lambda L} + f_1'(L) + f_2'(L)$$

Using (6) we can get

$$(V_S - \lambda) A e^{-\lambda L} + (V_S + \lambda) B e^{\lambda L} = -V_S [f_1(L) + f_2(L)] - [f_1'(L) + f_2'(L)] \quad ----(8)$$

Solving (7) and (8), we get A and B as

$$A = \frac{(\lambda - V_S)\, e^{-\lambda L}}{(\lambda + V_S)^2 - (\lambda - V_S)^2 e^{-2\lambda L}} \left[- V_S f_1(L) - V_S f_2(L) - f_1'(L) - f_2'(L) \right]$$

$$B = \frac{(\lambda + V_S)\, e^{-\lambda L}}{(\lambda + V_S)^2 - (\lambda - V_S)^2 e^{-2\lambda L}} \left[- V_S f_1(L) - V_S f_2(L) - f_1'(L) - f_2'(L) \right]$$

$$f_1'(x) = -\lambda f_1(x) + \frac{F(x)}{2D\lambda}$$

$$f_2'(x) = +\lambda f_2(x) - \frac{F(x)}{2D\lambda}$$

$$f_1'(L) = -\lambda f_1(L) + \frac{F(L)}{2D\lambda}$$

$$f_2'(L) = \lambda f_2(L) - \frac{F(L)}{2D\lambda}$$

Substituting the values of A and B in (4) we get after simplification

$$p(x) = \frac{1}{2D\lambda} \left[e^{-\lambda L} (\lambda - V_S) \int_0^L F(x') e^{\lambda x'} dx' + e^{\lambda L} (\lambda + V_S) \int_0^L F(x') e^{-\lambda x'} dx' \right]$$

$$\times \left[\frac{(\lambda - V_S)\, e^{-\lambda(x+L)} + (\lambda + V_S)\, e^{\lambda(x-L)}}{(\lambda + V_S)^2 - (\lambda - V_S)^2 e^{-2\lambda L}} \right]$$

$$+ \frac{1}{2D\lambda} \left[e^{-\lambda x} \int_0^x e^{\lambda x'} F(x')\, dx' - e^{\lambda x} \int_0^x e^{-\lambda x'} F(x')\, dx' \right] \quad ----(9)$$

The conductivity is defined as[75]

$$\Delta G = \int_0^L \int_0^{a/c} q\nu\,(\mu_h p + \mu_e n)\, dy\, dx \qquad \text{------} \quad (10)$$

where q is the electronic charge and μ_h, μ_e = mobility of holes, electrons. The charge neutrality condition holds good for a multi-photon process.

$$n = p$$

$$\therefore \quad \Delta G = q\nu \frac{a}{c} (\mu_e + \mu_h) \int_0^L p(x)\, dx$$

$$= \alpha \int_0^L p(x)\, dx \qquad \text{---} \quad (11)$$

Substituting for p(x) from (9), we get

$$\Delta G = \frac{\alpha}{2D\lambda^2} \frac{(1 - e^{-\lambda L})}{(\lambda + V_S) - (\lambda - V_S) e^{-\lambda L}} \left[(\lambda - V_S) e^{-\lambda L} \int_0^L F(x') e^{\lambda x'} dx' \right.$$

$$\left. + (\lambda + V_S) e^{\lambda L} \int_0^L F(x') e^{-\lambda x'} dx' \right]$$

$$+ \frac{\alpha}{2D\lambda} \left[\underbrace{\int_0^L e^{-\lambda x} dx \int_0^x e^{\lambda x'} F(x') dx'}_{\Theta} - \underbrace{\int_0^L e^{\lambda x} dx \int_0^x e^{-\lambda x'} F(x') dx'}_{\Psi} \right] \qquad \text{---} \quad (12)$$

The two double integrals Θ and Ψ can be simplified as follows:

$$\Theta = \int_0^L e^{-\lambda x} dx \int_0^x e^{\lambda x'} F(x')\, dx'$$

$$= \int_0^L e^{-\lambda x}\, dx \int_0^L e^{\lambda x'} F(x') dx' - \int_0^L e^{-\lambda x} dx \int_x^L e^{\lambda x'} F(x') dx'$$

Now,

$$\int_0^L e^{-\lambda x}\, dx \int_x^L e^{\lambda x'} F(x')\, dx'$$

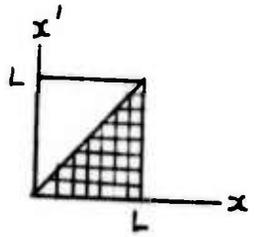

$$= \int_0^L e^{-\lambda x'} dx' \int_{x'}^L e^{\lambda x} F(x)\, dx$$

The elements are summed from x = x' to x = L and then from x'= 0 to x'=L. We can sum up alternatively (as is evident from the figure) from x'= 0 to x'= x and then from x = 0 to x = L and the above integral becomes,

$$= \int_0^L e^{\lambda x} F(x) dx \int_0^x e^{-\lambda x'} dx'$$

$$\Theta = \int_0^L e^{-\lambda x} dx \int_0^L e^{\lambda x'} F(x') dx' - \int_0^L e^{\lambda x} dx \int_0^x F(x)\, e^{-\lambda x'} dx'$$

After partial integration, the above integral becomes

$$\Theta = -\frac{e^{-\lambda L}}{\lambda} \int_0^L e^{\lambda x'} F(x') dx' + \frac{1}{\lambda} \int_0^L F(x) dx$$

Similarly,

$$\Psi = \frac{e^{\lambda L}}{\lambda} \int_0^L e^{-\lambda x'} F(x')\, dx' - \frac{1}{\lambda} \int_0^L F(x)\, dx$$

Substituting these expressions for Θ and Ψ back in (12) and after a simple algebraic simplification, we get

$$\Delta G = \frac{\alpha}{D\lambda^2}\int_0^L F(x)\,dx - \frac{2V_S\alpha}{D\lambda^2}\,\frac{e^{-\lambda L/2}\int_0^L \cosh\lambda\left(\frac{L}{2}-x\right)F(x)\,dx}{\left[(\lambda+V_S)-(\lambda-V_S)\,e^{-\lambda L}\right]} \quad \text{---(13)}$$

The generation rate of non-equilibrium charge carriers is given by (Eq.(4) of chapter 2)

$$F(x) = \frac{\beta_n}{n\hbar\omega}\cdot\frac{I_o^{\,n}}{\left[1+(n-1)\beta_n I_o^{\,n-1}x\right]^{\frac{n}{n-1}}} \quad \text{---(14)}$$

Substituting (14) in (13) and performing the integration, we get the final expression for the muti-photon conductivity $\Delta G^{(n)}$ as,

$$\Delta G^{(n)} = \alpha\tau\,\frac{I_o}{n\hbar\omega}\left[1-\frac{1}{\left[1+(n-1)\beta_n I_o^{\,n-1}L\right]^{\frac{1}{n-1}}}\right]$$

$$-\frac{\alpha\tau\beta_n I_o^{\,n}}{n\hbar\omega}\cdot\frac{V_S\,e^{-\frac{\lambda L}{2}}}{\left[(\lambda+V_S)-(\lambda-V_S)e^{-\lambda L}\right]}\int_0^L\frac{\cosh\lambda\left(\frac{L}{2}-x\right)}{\left[1+(n-1)\beta_n I_o^{\,n-1}x\right]^{\frac{n}{n-1}}}\,dx \quad \text{---(15)}$$

where $\alpha = q\,\frac{a}{c}\,(\mu_e+\mu_h)$ and $D_p\lambda^2 = \frac{1}{\tau}$.

APPENDIX 7

Model to account for $\Delta G \propto I^{\alpha}$ where $\frac{1}{2} < \alpha < 1$ (13) :

The model in Fig.29(a) is for an unilluminated crystal. 'v' is the filled valence band.and 'c' is the empty conduction band. N_r is the filled recombination center . N_t correponds to the trapping center. p_r is the active recombination center. Note that the p_r states are negligible or absent at zero light intensity. The N_t states have an exponential distribution of energy such that

$$N_t(E) = A \exp\left(-|E_c - E_t|/kT_1\right)$$

The temperature T_1, is a formal parameter that can be adjusted to make the density of states vary more or less rapidly with energy. Let $T_1 \geq T$, where T is the ambient temperature. Let

$$N_r > \int_{E_f}^{E_c} N_t(E)\, dE$$

We also take the capture cross section 'S_n' for electrons to be much less than the capture cross section 'S_p' for holes so that the density of the photo-excited electrons is much larger than that of photo-excited holes (ie) $n \gg p$. Also assume for simplicity the capture cross section of the N_t states to be the same as those for the N_r states.

Fig29b shows the conditions at some intermediate light intensity. E_{fn} is the steady state Fermi level defined by the electron density 'n'.

Now exponents less than unity can be accounted for by a simple physical picture. As the light intensity is increased,

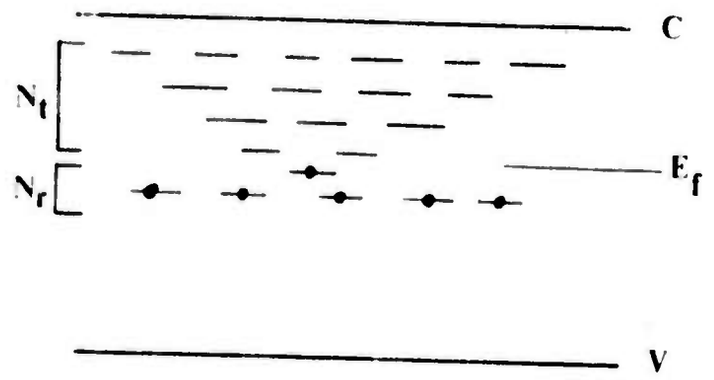

a

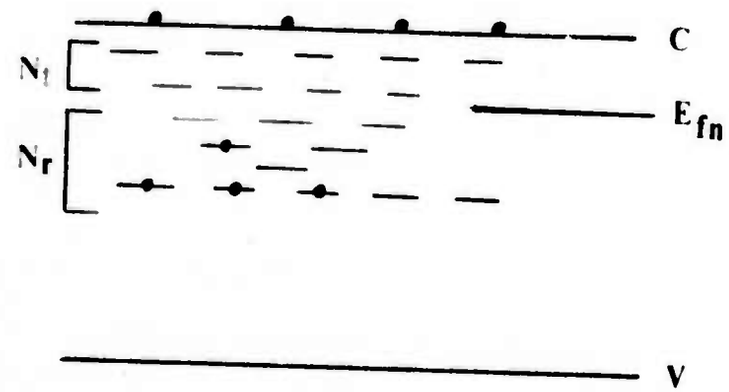

b

FIGURE 29 : RECOMBINATION CENTERS IN Ga As

more and more of the N_t states are converted from trapping to recombination states. This conversion takes place as the steady state fermi level E_{fn} sweeps through the N_t states towards the conduction band. As p_r, the density of recombination states for electrons, increases, the electron life time decreases. This is what is meant by an exponent less than unity.

To a good approximation, the density of empty states p_r is given by the number of N_t states lying between the original Fermi level E_f and the steady state Fermi level E_{fn}.

$$p_r = \int_{E_f}^{E_{fn}} N_t(E)\, dE$$

$$= \int_{E_f}^{E_{fn}} A \exp\left[-|E_c - E_t| / kT_1\right] dE$$

$$\approx kT_1\, N_t(E_{fn})$$

Now $n = f \tau_n$, f = photons absorbed / cm^3

n = electron density (steady state)

$$\tau_n = \frac{1}{p_r \upsilon S_n} = \text{life time}$$

υ = velocity , S_n = capture cross section

$$n = \frac{1}{kT_1\, A \exp\left[-|E_c - E_{fn}|/kT_1\right] \upsilon S_n} \quad \text{--- (I)}$$

By definition

$$n = N_C \exp\left[-|E_c - E_{fn}| / kT\right]$$

where N_c = effective density of states in the conduction band

$$N_C \propto 2\left(\frac{2\pi m^* kT}{h^2}\right)^{3/2}$$, m^* = electron effective mass.

$$n = N_c \exp\left(-\frac{|E_c - E_{fn}|\, T_1}{k\, T_1\, T}\right) \qquad (2)$$

Eliminating the exponential term in (I) and (2), we get

$$n = \left[\frac{f\, N_c^{\,T/T_1}}{k T_1 A \upsilon S_n}\right]^{\frac{T_1}{T+T_1}}$$

The conductivity change ΔG is proportional to 'n', and 'f' is proportional to I for a single photon process. So we get

$$\Delta G \propto I^{\frac{T_1}{T+T_1}}$$

Since $T_1 \geqslant T$, the exponent $\frac{T_1}{T+T_1}$ lies between 0.5 and unity.

From this discussion, we see that an exponent lying between 0.5 and I requires a distribution states in the forbidden gap. The odd exponents lying between 0.5 and unity has been observed in the case of GaAs by Bube[47] and Blinov[46].

REFERENCES

I. M.Goppert-Mayer, Ann. Physik (Paris), 9, 273(I93I).

2. W.Kaiser and C.B.Garret, Phys. Rev. Letters, 7, 229(I96I).

3. I.D.Abella, Phys. Rev. Letters, 9, 453(I962).

4. K.Hasegawa and S.Yoshimura, J. Phys. Soc. Japan, 20, 460(I965).
ibid 2I,2626(I966).

5. R.Braunstein, Phys. Rev., I25, 475(I962).

6. R.Braunstein and N.Ockmann, Phys. Rev., I34, A499(I964).

7. N.G.Basov et al., Proc. of the International Conference on The Physics of Semiconductors, Phys. Soc. of Japan, 277(I966).

8. N G.Basov et al., Sov. Phys.-JETP, 23, 366(I966).

9. S.Wang and C.C.Chang, Appl. Phys. Letters, I2, I93(I968).

I0. V.S.Dneprovskii et al., Sov. Phys.-Semiconductors, 3, 4II(I969).

II. B.V.Zubov et al., Sov. Phys.-JETP Letters, 9, I30(I969).

I2. B.M.Azkinadze et al., Sov. Phys.-Solid State, 9, 46I(I967).

I3. N.A.Goryunova et al., Phys. Stat. Solidi(a), I, KI6I(I970).

I4. A.Cingolani et al., IL Nuova Cimento, 4B, 2I7(I97I).

I5. S.Rafi Ahmad and D.Walsh, J.Phys. D: Appl.Phys., 4,I820(I97I).

I6. G.B.Abdullaev et al., Sov.Phys.-Semiconductors, 4, II89(I970).

I7. ---- --- --- , 4, II87(I970).

I8. M.S.Brodin et al., Sov. Phys.-Solid State, I3, I328(I97I).

I9. J.M.Ralstron and R.K.Chang, Appl.Phys.Letters, I5, I64(I969).

20. J.M.Ralstron and R.K.Chang, Opto-Electronics, I, I82(I969).

2I. L.M.Lisitzyn, Sov. Phys.-JETP Letters, 9, I65(I969).

22. B.M.Azkinadze et al., Sov.Phys.-Semiconductors, 2, I285(I969).

23. V.V.Arsenev et al., Sov. Phys.-JETP, 33, 64(I97I).

24. G.I.Aseev et al., Sov. Phys.-JETP Letters, 8, I03(I968).

25. I.M.Catalano et al., Phys. Rev., B5, I629(I972).

26. E.O.Kane, J. Phys. Chem. Solids, I, 249(I957).

27. Jick H.Yee, Phys. Rev., B5, 449(I972).

28. A.I.Bobrysheva et al., Sov.Phys.-Semiconductors, 3,I347(I970).

29. Jick H.Yee, Appl. Phys. Letters, I4, 23I(I969).

30. Jick H.Yee, Appl. Phys. Letters, I5, 43I(I969).

3I. Jick H.Yee, Phys. Rev., I86, 778(I969).

32. H.P.Weber and R.Dandliker, IEEE J.Q.E., QE-4, I009(I968).

33. J.A.Giordmaine et al., Appl. Phys. Letters, II, 2I6(I967).

34. S.L.Shapiro et al., Phys. Letters, 28A, 698(I969).

35. A.Gold, in 'Quantum Optics', Enrico Fermi International School of Physics, Course XLII, edited by R.J.Glauber, Academic Press, New York,(I969).

36. J.A.Armstrong, Appl. Phys. Letters, I0, I6(I967).

37. R.J.Glauber, Phys. Rev., I30, 2529(I963).

38. J.R.Klauder et al., Appl. Phys. Letters, I3, I74(I968).

39. M.A.Duguay et al., IEEE J.Q.E., QE-6, 725 (I970).

40. D.H.Austen, IEEE J.Q.E., QE-7, 465(I97I).

4I. A.Yariv, 'Introduction to Optical Electronics ', HWR Inc., New York, II4(I97I).

42. A.J.DeMaria et al., Proc. IEEE, 57, I(I969).

43. A.J.DeMaria, Progress in Optics, 9, 33(I97I).

44. S.M.Ryvkin, ' Photoelectric Effects in Semiconductors ', Consultants Bureau, New York,(I964).

45. A.Rose, ' Concepts in Photoconductivity and Allied Problems ', Interscience, 38(I963).

46. L.M.Blinov et al , Sov. Phys.-Semiconductors, I, II24(I967).

47. R.H.Bube, J. Appl. Phys., 3I, 3I5(I960).

48. S.S.Li and C.I.Huang, J. Appl. Phys., 43, I757(I972).

49. R.Cronin and R.W.Haisty, J. Electrochem. Soc., III,874(I964).

50. A.A.Patrin et al., Sov. Phys.-Semiconductors, 3, 383 (I969).

5I. S.M.Sze, ' Physics of Semiconductor Devices', Wiley(I969).

52. F.J.Morin,and J.P.Maita, Phys. Rev., 94, I525(I954).

53. T.S.Mass and T.D.F.Hawkins, Infrared Phys., I, III(I96I).

54. E.M.Belenov and I.A.Poluektov, Sov.Phys.-JETP, 29, 754(I969).

55. T.L.Gvardzhaladze et al., Sov. Phys.-JETP Letters,I3,III(I97I).

56. S.L.McCall and E.L.Hahn, Phys. Rev. Letters, I8, 908(I967).

57. T.L.Gvardzhaladze et al., Preprint (I972).

58. O.Madelung, ' Physics of III-V Compounds ', Wiley(I964).

59. R.Braunstein, J. Phys. Chem. Solids, 8, 280(I959).

60. R.Braunstein and E.O.Kane, J. Phys. Chem. Solids, 23,I423(I962).

6I. V.A.Babenko et al., Sov. Phys.-JETP, 34, I2I6(I972).

62. Brian Ray, ' II-VI Compounds ', Pergamon Press, 54(I969).

63. B.M.Azkinadze and I.D.Yaroshetskii, Sov. Phys.-Semiconductors, I, I4I3(I968).

64. K.H.Nicholas and J.Woods, Brit. J. Appl. Phys., I5,783(I964).

65. J.S.Skarman, Solid State Electronics, 8, I7(I965).

66. A.Hordvik, IEEE J. Q. E., QE-6, I99(I970).

67. P.M.Rentzepis et al., Appl. Phys. Letters, I7, I22(I970).

68. R.C.Eckardt and C.H.Lee, Appl. Phys. Letters, I5, 425(I969).

69. V.V.Arsene'v et al., Kvantovaya Electronica, 7, 82(I972).

70. A.M.Danishevskii et al., Sov. Phys.-JETP, 29, 781(1969).

71. P.Kelley and P.Braunlich, Phys. Rev., B3, 2090(1971).

72. A.L.Dyshko et al., Sov. Phys.-JETP, 34, 1235(1972).

73. L.V.Keldysh, Sov. Phys.-JETP, 18, 253(1964).

74. J.D.Jackson, ' Classical Electrodynamics ', John Wiley and Sons, Inc., 4(1962).

75. S.Wang, ' Solid State Electronics ', McGraw Hill Book Co., New York, (1966).

--------******--------